UNIVERSITY OF MODENA AND REGGIO EMILIA

Department of Biomedical, Metabolic, and Neural Sciences

International Ph.D. Program in Clinical and Experimental Medicine

CEM Curriculum: Translational Medicine

XXXIV cycle

LncRNA *BlackMamba*-DNA helicase HELLS axis drives ALK$^-$ALCL proliferation by orchestrating a complex oncogenic transcriptional program

Ph.D. candidate: Dr. Tameni Annalisa

Supervisor: Dr. Alessia Ciarrocchi

Coordinator of the Ph.D. program: Prof. Giuseppe Biagini

INDEX……...3

ABBREVIATION INDEX……5

SUMMARY (English Version) …….....7

SUMMARY (Italian Version) ……..8

INTRODUCTION……....9

Peripheral T-cell lymphoma (PTCL) ……9

1. Anaplastic large cell lymphoma (ALCL) ……11

1.1 ALCLs genetic characteristics……14

1.1.2 ALK signaling……...14

1.1.3 JAK/STAT3 signaling……..17

1.2 ALK+ALCL: Systemic ALK Positive Anaplastic Large Cell Lymphoma……..18

1.2.1 Clinical and epidemiological features……...18

1.2.2 Morphological features and immunophenotype……19

1.3 ALK-ALCL: Systemic ALK Negative Anaplastic Large Cell Lymphoma……..21

1.3.1 Clinical and epidemiological features……...21

1.3.2 Morphological features and immunophenotype……....21

1.4 BIA-ALCL: Breast-Implanted Associated Anaplastic Large Cell Lymphoma….22

1.4.1 Clinical, epidemiological and genetic features……...22

1.4.2 Immunophenotype……..23

1.5 Therapeutic strategies and new experimental approaches……25

Chromatin remodeling…….28

2. Description and functions……..28

2.1 The role of chromatin remodeling in T cell biology and PTCLs……31

3. The role of Rho-GTPases in T cell biology and PTCLs……..34

4. PRELIMINARY RESULTS…….39

5. AIMS OF THE PROJECT……..47

6. MATERIALS AND METHODS……..48

7. RESULTS……..61

8. MOLECULAR MODEL……...78

9. DISCUSSION……...79

10. RECENT OBSERVATIONS AND FUTURE PERSPECTIVES……..84

BIBLIOGRAPHY……..86

PUBLICATIONS……...99

ACKNOWLEDGEMENTS……100

Abbreviation Index:

PTCL: peripheral T cell lymphoma

PTCL-NOS: peripheral T cell lymphoma not otherwise specified

ALCL: anaplastic large cell lymphoma

WHO: World Health Organization

AITL: angioimmunoblastic T cell lymphoma

ALK: anaplastic lymphoma kinase

ATLL: adult T cell leukemia/lymphoma

CNV: copy number variant

CTCL: cutaneous T cell lymphoma

CTLA4: cytotoxic T lymphocyte-associated protein 4

EATL: enteropathy-associated T cell lymphoma

EBV: Epstein–Barr virus

ENKTCL: extranodal natural killer cell/T cell lymphoma

GEP: gene expression profiling

HTLV-1: Human T cell lymphotropic virus type 1

ITK: IL-2-inducible T cell kinase

JAK: Janus kinase

MEITL: monomorphic epitheliotropic intestinal T cell lymphoma

NF-Kb: nuclear factor-κB

STAT: signal transducer and activator of transcription

SYK: spleen-associated tyrosine kinase

TAM: tumor-associated macrophage

TCR: T cell receptor

TRC: transcription-replication conflict

TFH cell: T follicular helper cell

TFH PTCL: peripheral T cell lymphoma with T follicular helper cell phenotype

Treg cell: regulatory T cell

LncRNAs: long noncoding RNAs

KD: knockdown

shRNA: short hairpin RNA

siRNA: short interference RNA

DOX: doxycycline

CTR: control

RNA-Seq: RNA sequencing

GO: Gene ontology

H3K4me3: trimethylation of lysine 4 on histone H3

H3K27me3: trimethylation of lysine 27 on histone H3

FDR: fold discovery rate

WB: Western blot

qRT-PCR: quantitative real-time polymerase chain reaction

Co-IP: protein co-immunoprecipitation

ChIP: chromatin immunoprecipitation

RIP: RNA immunoprecipitation

TF: transcriptional factor

RNAPII: RNA polymerase II

Summary (English version)

Although important steps forward have been made in the discovery of genomic alterations, the molecular mechanisms leading to the transformation of anaplastic lymphoma kinase negative (ALK^-) anaplastic large cell lymphoma (ALCL) have been only in part elucidated. To identify new culprits which promote and drive ALCL, we performed a high coverage and directional RNA sequencing of 21 ALK^+ALCL and 16 ALK^-ALCL primary samples, also including normal T-lymphocytes (corresponding to different stages of differentiation) and 10 ALCL cell lines (4 ALK^+ALCL, 6 ALK^-ALCL), and identified 1208 previously unknown intergenic long noncoding RNAs (lncRNAs), of which 18 lncRNAs preferentially expressed in ALCL. We selected for molecular and functional studies an unknown lncRNA, *BlackMamba*, which we found overexpressed only in ALK^-ALCL patients. Knockdown experiments demonstrated that *BlackMamba* regulates cell growth and cell morphology of ALK^-ALCL cells. Mechanistically, *BlackMamba* interacts with the DNA helicase HELLS controlling its expression and its recruitment to the promoter regions of the cytoskeleton and cytokinesis-related genes, fostering their expression. Since HELLS acts also as chromatin modifiers and they are emerging as new vulnerabilities of different cancer settings, we assessed in detail its function by performing RNA-sequencing profiling coupled with bioinformatic prediction to identify HELLS targets and transcriptional cooperators. We demonstrated that HELLS, together with the transcription factor YY1, contributes to appropriate cytokinesis via the transcriptional regulation of genes involved in cleavage furrow structure and regulation. Binding target promoters, HELLS primes YY1 recruitment and transcriptional activation of cytoskeleton genes including the small GTPases *RHOA* and *RHOU* and their effector kinase *PAK2.* Single or multiple knockdowns of these genes revealed that RhoA and RhoU proteins mediate HELLS effects on cell proliferation and cell division of ALK^-ALCL cells. Collectively, our work demonstrates the key role of the *BlackMamba*-HELLS axis in orchestrating a complex transcriptional program specific of neoplastic T cells, sustaining ALK^-ALCL proliferation and progression, contributing to its pathogenesis.

Summary (Italian version)

Nonostante siano stati fatti grandi progressi nella scoperta delle alterazioni genomiche, i meccanismi molecolari alla base della trasformazione del sottotipo di linfoma T anaplastico a grandi cellule ALK$^-$ sono stati chiariti solo in parte. Al fine di identificare nuovi driver molecolari in grado di promuovere la progressione dei linfomi anaplastici a grandi cellule (ALCL), è stato messo a punto un sequenziamento dell'RNA di 21 campioni di pazienti ALK$^+$ALCL e 16 campioni di ALK$^-$ALCL, di linfociti T sani (corrispondenti ai diversi stadi di differenziamento) e di 10 linee cellulari (4 ALK$^+$ALCL,6 ALK$^-$ALCL) che ci ha permesso di identificare 1208 nuovi RNA non codificanti intergenici, includendone tra questi 18 principalmente espressi negli ALCL. Per i successivi studi molecolari e funzionali la nostra attenzione si è concentrata su *BlackMamba*, un nuovo RNA non codificante che abbiamo dimostrato essere iperespresso solo nei pazienti ALK$^-$ALCL. Esperimenti di silenziamento hanno dimostrato che *BlackMamba* regola la crescita, la formazione di colonie e la morfologia delle cellule T di linfoma ALK$^-$ALCL. Dal punto di vista del meccanismo molecolare*, BlackMamba* interagisce fisicamente con la DNA elicasi HELLS controllando la sua espressione genica ed il suo reclutamento alle regioni promotoriali/regolatorie dei geni coinvolti nel controllo dell'organizzazione del citoscheletro e del processo di citocinesi. Dato che le DNA elicasi agiscono anche come fattori di rimodellamento della cromatina e stanno emergendo come nuove vulnerabilità di diversi contesti tumorali, abbiamo valutato nel dettaglio la funzione di HELLS utilizzando una strategia che accoppia il sequenziamento dell'RNA all'utilizzo di programmi di predizione bioinformatica per identificare i target e i cooperatori trascrizionali di HELLS. Abbiamo dimostrato che HELLS insieme al fattore trascrizionale YY1, contribuisce ad un corretto processo di citocinesi attraverso la regolazione trascrizionale dei geni coinvolti nella regolazione della struttura e funzione del solco di scissione delle cellule in divisione. Legandosi ai promotori dei geni target, HELLS innesca il reclutamento di YY1 e l'attivazione trascrizionale dei geni coinvolti nell'organizzazione citoscheletrica come le RhO-GTPasi *RHOA, RHOU* e il loro effettore *PAK2*. Esperimenti di silenziamento di questi geni, dimostrano che le proteine RhoA e RhoU mediano gli effetti di HELLS sulla proliferazione e divisione delle cellule ALK$^-$ALCL. Nel complesso, il nostro lavoro dimostra il ruolo chiave di *BlackMamba* ed HELLS nel dirigere un complesso programma trascrizionale specifico delle cellule T neoplastiche che sostiene la proliferazione e la progressione del sottotipo ALK$^-$ALCL, contribuendo in questo modo alla sua patogenesi.

INTRODUCTION

Peripheral T-cell lymphoma (PTCL)

Peripheral T-cell lymphomas are a group of composite and heterogeneous malignancies derived from the transformation of post-thymic T-cell and natural killer cell lineages[1]. The classification of hematological and lymphoid neoplasms was revised in 2017 and the World Health Organization now recognizes 30 established and provisional entities[2] of mature post-thymic T cell non-Hodgkin lymphomas. PTCLs include several different subtypes consisting of extranodal, nodal, cutaneous, and leukemic forms **(Figure 1)**. The most common subtypes are PTCL not otherwise specified (PTCL-NOS) that represent ~30% of PTCLs that are mostly extranodal neoplasms, angioimmunoblastic T cell lymphoma (AITL) that constitute about 15–30% of PTCLs, anaplastic large cell lymphoma (ALCL) that correspond to ~15% of PTCLs. ALCL represent 3% of Non-Hodking Lymphoma (NHLs) in adult and 10-20% of high-grade lymphoma in children[3]. Next, the 10% of PTCLs is represented by extranodal natural killer (NK) cell/T cell lymphoma (ENKTCL) and 5-6% of them include intestinal T cell lymphomas, encompassing enteropathy-associated T cell lymphoma (EATL) and monomorphic epitheliotropic intestinal T cell lymphoma (MEITL; 10–20% of intestinal T cell lymphomas[4]). Instead, hepatosplenic T cell lymphoma (HSTL; 2.1% of PTCLs), sporadic subcutaneous panniculitis-like T cell lymphoma (SPTCL; 1.7% of PTCLs), and γδ T cell lymphoma (0.9% of PTCLs) have a low frequency[5].

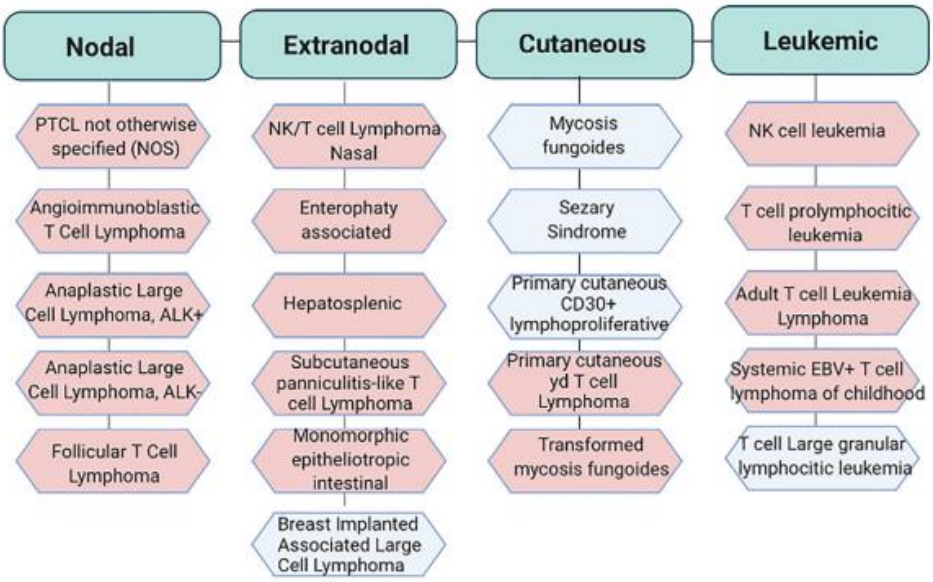

Figure 1. Classification of the most recurrent T cell lymphoproliferative disorders. World Health Organization (WHO) classification of PTCLs. In light blu aggressive subtypes and in light pink indolent subtypes. Adapted from Swerdlow S.H. et al. WHO Classification of Haematopoietic and Lymphoid Tissue. Revised 4th edition. Ed. Lyon:2017. EBV, Epstein Barr virus. *(Fragliasso V, Tameni A, Cytoskeleton Dynamics*

in Peripheral T Cell Lymphomas: An Intricate Network Sustaining Lymphomagenesis, Frontiers in Oncology,2021, doi.org/10.3389/fonc.2021.643620).

Due to their expansion and proliferation rate, peripheral T-lymphocytes are prone to accumulate error and transformation[6]. The accumulation of different genomic rearrangements and deregulated signaling pathways **(Table 1)**, the lack of knowledge and experimental models, have impaired clinical success making PTCLs a heterogeneous group of orphan neoplasms that generally have a poor clinical outcome. In almost 50% of cases, this complexity makes it hard to assign the tumor to a specific classification.

Table 1 | Pathogenic mechanisms relevant to the most frequent PTCL entities *(Fiore D, Peripheral T cell lymphomas: from the bench to the clinic, Nat Rev Cancer,2020, DOI: 10.1038/s41568-020-0247-0)(Reproduced with permission, license number: 5218170409893).*

Lymphoma type	Dysregulated pathways	Associated molecular events	Microenvironmental modulation	Virus-mediated oncogenesis
AITL and T_{FH} PTCL	TCR	Mutations: *CD28*, *VAV1*, *PLCG1*, *CTNNB1*, *GTF2I*, PI3K pathway components	Reduced immunogenicity (*B2M* mutations); increased response to co-stimulatory signals (*CD28* mutation); altered response to proapoptotic signals; cytokine, T_{reg} cell-mediated and endothelial cell-mediated immunomodulation; immune checkpoint regulation	EBV^+ B cells, the pathogenetic role of which remains unclear (lymphokine mediated signals, antigen-driven stimulation?)
	RHOA	Mutations: *RHOA*; fusion protein: VAV1–STAP2		
	Epigenetic modifiers	Mutations: *TET2*, *IDH2*, *DNMT3A*		
PTCL-NOS	TCR and NF-κB	Mutations and/or CNVs: *CD28*, *PLCG1*, *CARD11*, *FYN*, *VAV1*, *TNFAIP3*, *PTPRC*; fusion protein: ITK–SYK	Reduced immunogenicity; altered cell–cell interactions (*CD58* and *LFA1* mutations); altered response to proapoptotic signals and immunoregulation; cytokine-mediated, T_{reg} cell-mediated and TAM-mediated immunomodulation; immune checkpoint regulation	Putative pathogenic role for EBV in a minority of cases
	T cell trafficking	Mutations: *CCR4*, *CCR7*		
	JAK–STAT	Pathway mutations and/or CNVs; fusion protein: PCM1–JAK2		
	Notch	Mutations and/or CNVs: *NOTCH1*; gene loss: *LEF1*, *TCF1*		
	RHOA	Mutations: *RHOA*; fusion proteins: VAV1–THAP4, VAV1–MYO, VAV1–S100A7		
	PI3K–AKT	Pathway mutations and/or CNVs; hyperactivation (GEP signatures)		
	Transcriptional regulation	Mutations and/or CNVs: *IKZF2*, *PRDM1*, *ETV6*, *FOXP1*, *TBL1XR1*, *IRF2BP2*, *YTHDF2*, *DDX3X*		
	Epigenetic modifiers	Mutations and/or CNVs: *TET2*, *DNMT3A*, *KMT2C*, *KMT2D*, *SETD1B*, *SETD2*, *CREBBP*, *EP300*, *ARID1A*, *KDM6A*		
	Tumour suppressors	Mutations and/or CNVs: *TP53*, *CDKN2A* (non-T_{FH} cell PTCL-NOS), *ATM*		
ALK^+ ALCL	TCR and CD30	Activation by ALK fusion proteins	Altered response to proapoptotic signals; T_{reg} cell-mediated and TAM-mediated immunoregulation; immune checkpoint regulation	No pathogenic role
	JAK–STAT	Gene loss: phosphatases		
	Notch	Activation by ALK fusion proteins		
	PI3K–AKT	Activation by ALK fusion proteins		
	AP-1	Hyperactivation		
ALK^- ALCL	TCR and CD30	Fusion proteins: DUSP22–FRA7H, TP63–TBL1XR1	Altered response to proapoptotic signals; T_{reg} cell-mediated and TAM-mediated immunoregulation; immune checkpoint regulation	No pathogenic role
	JAK–STAT	Mutations: *JAK1*, *STAT3*; fusion proteins: NCOR2–ROS1, NFKB2–ROS1, PABCA2–TYK2, NFKB2–TYK2; gene losses: phosphatases		
	Notch	Constitutive activation		
	Epigenetic modifiers	Mutations: *TET2*		
	Tumour suppressors	Mutation/deletion: *TP53*, *PRDM1*		

CTCL	TCR	Possible activation by superantigens	Increased response to co-stimulatory signals (high expression of CD28 and CD80); reduced response to proapoptotic signals; cytokine-mediated and TAM-mediated immunomodulation; immune checkpoint regulation	No pathogenic role
	JAK–STAT	Gene loss: phosphatases; rare mutations: *JAK3*		
	AP-1	Increased activation or expression: *JUNB*, *JUND*		
	Epigenetic modifiers	Mutations: *NCOR1*, *EP300*, *SETD1A*		
	Genomic instability	Mutations: *TP53*		
ENKTCL	JAK–STAT	Mutations: *JAK3*, *STAT3*, *STAT5B*	T_{reg} cell-mediated and TAM-mediated immunoregulation; immune checkpoint regulation	EBV infection plays key pathogenic roles
	Epigenetic modifiers	Mutations: *MLL2*, *ARID1A*, *EP300*, *ASXL1*		
EATL and MEITL	TCR (EATL)	Possible activation by gluten protein	Reduced immunogenicity	No pathogenic role
	JAK–STAT (MEITL)	Mutations: *STAT5B*		
	Epigenetic modifiers	Mutations: *TET2*, *SETD2* (specifically in MEITL)		
ATLL	TCR	Activation by CTLA4 and CD28 fusions	Hyperactive TCR signalling; cytoskeleton abnormality; reduced response to proapoptotic signals; immune checkpoint regulation; immunoescape	HTLV-1 infection plays key pathogenic roles
	JAK–STAT	Mutations: *JAK1*, *JAK3*, *STAT3*		
	Notch	Mutations: *NOTCH1*, *FBXW7*		
	RHOA	Mutations: *RHOA*, *VAV1*		
	PI3K–AKT	Mutations: *CCR4*		
	AP-1	Hyperactivation		
	Epigenetic modifiers	Mutations: *EP300*, *TET2*, *EZH2*, *MED12*, *PBRM1*, *DNMT3A*, *KMT2A*, *HIST1H1E*, *SPEN*, *IDH1*, *SMARCB1*, *ASXL1*		
	Immunosurveillance	Mutations: *HLA-A*, *HLA-B*, *CD58*, *FAS*		

1. Anaplastic large cell lymphoma (ALCL)

Anaplastic Large Cell Lymphomas (ALCLs) are aggressive, CD30+, non-Hodking lymphomas arising from the transformation of mature T-cell with or without extranodal involvement[7,8]***.*** Based on different clinical aspects and molecular features, the World Health Organization (WHO) in 2017 revised this classification and now recognizes four different entities: systemic ALK-positive ALCL (ALK^+ALCL), systemic ALK-negative ALCL (ALK^- ALCL), primary cutaneous ALCL (PC-ALCL), and breast implant-associated ALCL (BIA-ALCL), the last one included as a provisional entity[9]. ALCLs are also classified in systemic (ALK^+ALCL, ALK^-ALCL, BIA-ALCL) and cutaneous (cALCL) whose are indolent neoplasms with good prognoses. In addition, systemic ALCLs are categorized as de novo and secondary lesions, being the latest anaplastic transformation of pre-existing lymphoma[10]***.*** Among systemic ALCLs, the presence of translocations of *anaplastic lymphoma kinase (ALK)* stratifies ALCLs in two distinct tumor subtypes with different clinical behavior and prognosis[11,12]. ALK^-ALCL is known to be the most heterogeneous, complex, and aggressive subtype of ALCLs. The life expectancy of ALK^-ALCL patients is significantly reduced by the lack of effective therapies, while ALK^+ALCL patients are characterized by a favorable prognosis[13] **(Figure 2)**. BIA-ALCL shares with ALK^-ALCL some genetic alterations, even if the onset of this systemic ALCL subtype is mainly related to textured breast implants that, inducing a chronic inflammation, act as a stimulus of tumorigenesis. By contrast, BIA-ALCL

patients have a good prognosis and their outcomes are generally excellent after the removal of breast prosthesis.

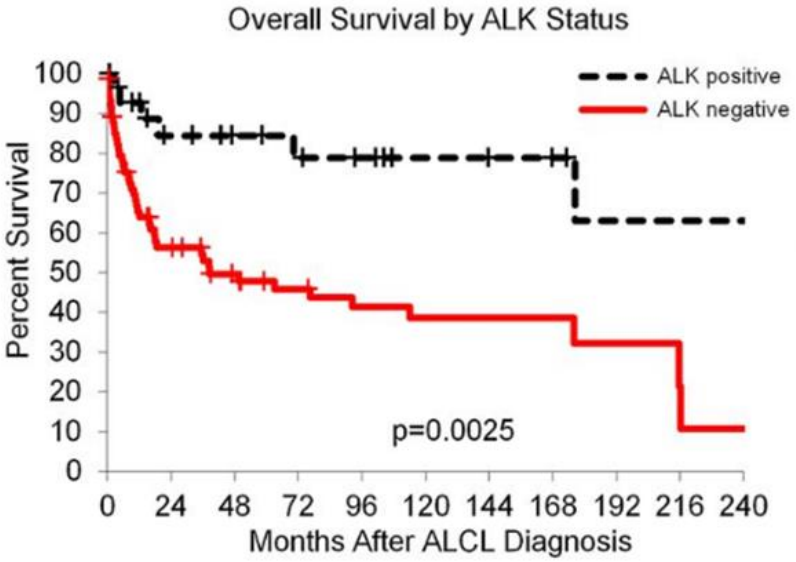

Figure 2. Outcome in patients with ALCL based on the genetic subtype. OS rates in patients with ALCL, stratified by ALK status only (ALK positive, N = 29; ALK negative, N = 67). *(Parilla Castellar E, ALK-negative anaplastic large cell lymphoma is a genetically heterogeneous disease with widely disparate clinical outcomes,* Blood *(2014) 124 (9): 1473–1480; DOI:10.1182/blood-2014-04-571091)(Reproduced with permission, license number: 5218171205885).*

The overall frequency of the ALK$^+$ and ALK$^-$ largely varies with age. ALK$^+$ALCL tumors are commonly seen in children and young adults while ALK$^-$ALCL neoplasms more frequently occur in older adults[14]**.** The majority of ALCL shows an important variability in molecular, cytogenetics, biological and clinical characteristics[15]. From the morphological point of view, ALCLs are sub-divided into five variants: common, giant cell-rich, lymphohistiocytic, small-cell type, and Hodgkin-like. Each subgroup is characterized by a peculiar proportion of "hallmarks cells", which are large lymphocytes with abundant cytoplasm and "kidney-shaped" morphology or lobed nuclei[16]. ALCLs are characterized by the strong expression of CD30 antigen (CD30+ immunophenotype) which is a cytokine receptor of the tumor necrosis factor (TNF) receptor superfamily **(Figure 3)**. CD30 receptor and its ligand CD30L display a restricted expression in activated subgroups of B and T cells in non-pathologic conditions, while in heterogeneous hematological neoplasms CD30 is upregulated. Instead, the neoplastic cells derived from T-cells, lack many T-cell markers but they also express cytotoxic molecules as a granzyme B, perforin, and TIA1(T-cell restricted intracellular antigen-1)[3]**.** In most cases of ALK$^+$ and ALK$^-$ALCL, tissue architecture is altered by a solid agglomerate of neoplastic cells with frequent lymph nodes infiltration, and ALK$^-$ is indistinguishable from ALK$^+$ in terms of morphological and clinical features[17]. The molecular

bases, the mechanisms of transformation, and progression of ALK$^-$ALCL remain largely unknown as a consequence of the biological complexity and rarity of this neoplasm that limit the possibility of extensive and deep genomic profiling[18,19]. The characterization of the molecular events that drive ALK$^-$ALCL development and progression is crucial to define the molecular vulnerabilities underlying carcinogenesis. The integration of genomic, functional, and clinical data is necessary to develop efficient patient genomic-based stratifications, more effective risk assessment, target-personalized therapies, and immunological approaches[3,5].

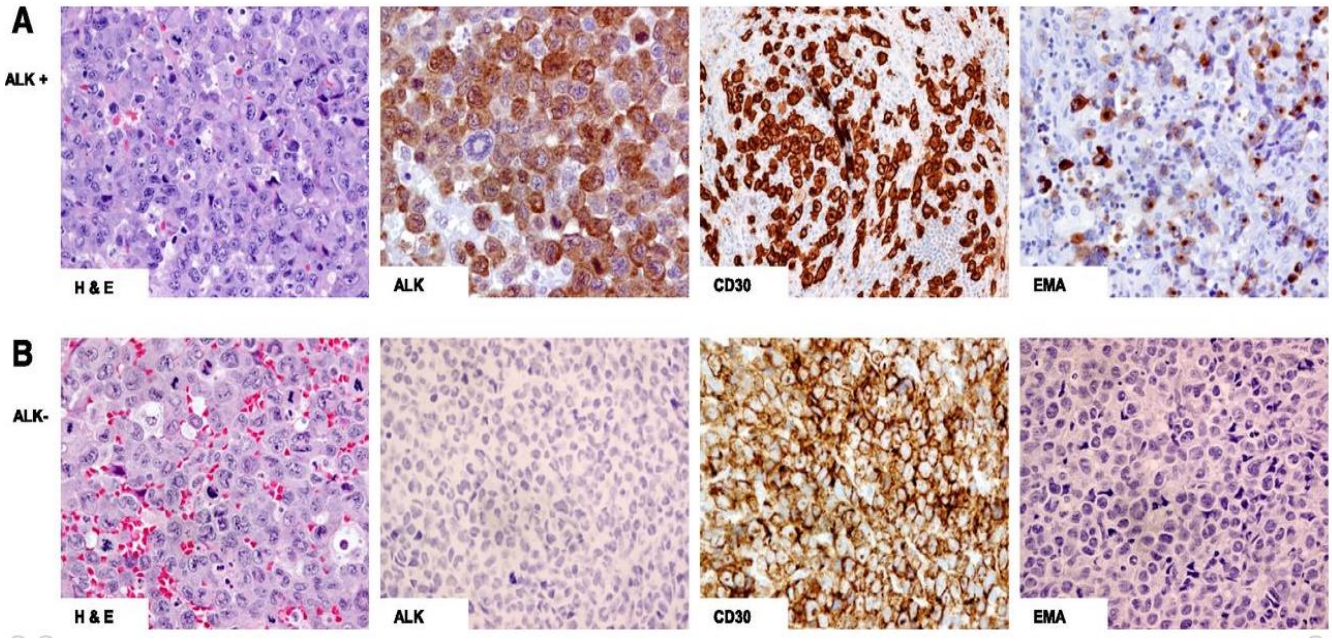

Figure 3. Hematoxylin and eosin (H&E) and immunohistochemical staining of ALCL. (A) ALK+: Hallmark cells demonstrated by H&E staining and tumor cells positive for ALK, CD30, and epithelial membrane antigen (EMA); **(B)** ALK−: Hallmark cells demonstrated by H&E staining and tumor cells positive for CD30 but negative for ALK and EMA staining *(Hapgood G, Savage K, The biology and management of systemic anaplastic large cell lymphoma, Blood 2015, doi.org/10.1182/blood-2014-10-567461) (Reproduced with permission, license number: 5218171498386).*

.

1.1 ALCLs genetic characteristics

The discovery of *Nucleophosmin (NPM)-ALK* fusion in many systemic ALCL has established the basis for the characterization of various subtypes among all ALCL patients, leading to the improvement of diagnostic techniques and a possible precise diagnosis. The anaplastic Lymphoma (ALK) tyrosine kinase receptor (TRK) belongs to the insulin receptor superfamily and is correlated to the leukocyte receptor tyrosine kinase (LTK). LTK is different from ALK kinase as it lacks a sequence corresponding to the amino-terminal half of the ALK extracellular domain[20,21]. The extracellular domain and protein kinase domain of LTK possess 50% and 78% amino acid identity, respectively, to the corresponding regions of ALK and these two kinases comprise a new subfamily of the insulin receptor family. ALK structure comprises an extracellular ligand-binding domain, a hydrophobic single-pass transmembrane region, and an intracellular kinase domain. Particularly, the ALK tyrosine kinase domain shows a high degree of homology in many species indicating its crucial role during evolution[22]**.** More than 80% of ALK^{+}ALCLs present genetic rearrangements involving the *ALK* gene. These rearrangements are mainly chromosomal translocations in which the intracytoplasmic region of ALK is fused with other protein domains leading to the aberrant expression and the uncontrolled function of ALK in lymphoid cells[23].

The most common (80%) translocation is the t(2;5;p23;q35) that leads to the formation of Nucleophosmin (NPM1)-ALK fusion protein[23]. Other and alternative translocations involve other partners as *IRF4, DUSP22, TFG*[24]*, TPM*[25]*, ATIC*[26]*, TSPYL2*[27]*, MSN*[28]*, VCL*[29]*, MYH9*[30]*, KIFB5*[31,32]*, ALO17* while other new translocations of *ALK* have been discovered in many human cancers[3]. Instead, the ALK^{-}ALCL subtype displays a heterogeneous genomic prolife different from the ALK^{+}ALCL subtype. About 70% of ALK^{-}ALCL genetic defects is represented by clonal rearrangement of TCR genes[33], 30% of *DUSP22/IRF4* translocation, 8% of *TP63* translocation, loss/translocation of *TP53/Blimp-1, PRDM1/ Blimp-1*, *NCOR2-ROS1, NFkB2-ROS1,* and *NFkB2-TYK2* involving chimeras combining transcriptional factor and tyrosine kinase, and finally 38% of activating mutations of *JAK1-STAT3*[18].

1.1.2 ALK signaling

ALK^{+}ALCL subtype is characterized by the constitutive activation of the ALK-mediated signaling pathway. The most common translocation displays the ALK kinase domain in fusion with the cytoplasmic domain of NMP1. NMP1 is a nucleus-cytoplasm shuttling phosphoprotein that is involved in several biological processes as ribosome biogenesis,

centrosome duplication, protein chaperoning, histone assembly, cell proliferation, and regulation of tumor suppressor *p53/TP53*. The N-terminus region of NPM1 homodimerization leads to the juxtaposition of the ALK kinase domains and this event triggers ALK auto-phosphorylation and the activation of ALK-downstream signaling pathways many of which affect cell transformation supporting ALK^+ neoplastic phenotype[23]. The interacting molecules of NPM-ALK protein belonging to key molecular pathways and involved in the development of this lymphoma subtype, include: RAS/Erk, PLC-γ, PI3K, JAK-STAT and Src that control and regulate the survival, proliferation, differentiation, apoptosis balances, and cytoskeletal modifications. Ras/Erk pathway activation drives ALK^+ ALCL cells growth. Indeed, ALK-dependent Ras activation leads, via MAPK, ERK1, and ERK2, to the deregulation of the AP-1 transcription factor known to be involved in ALCL neoplastic phenotype and regulation of cytotoxic molecule expression[34–36].

JAK-STAT3 pathway can be activated by NPM-ALK or other ALK chimera in ALK^+ALCL, sustaining ALK^+ cell cycle progression.

c-SRC is a proto-oncogene that can be activated by NPM-ALK. C-SRC is implicated in ALCL cell migration, proliferation, and growth by phosphorylating specific tyrosine residues in target proteins[37]. It takes part in Cdc42 signaling that regulates cell homeostasis, particularly cell shape and growth[38].

Many molecular adaptors have been shown to mediate the interaction of Src-homology 2 (SH2) or phosphotyrosine binding (PTB) domain with NPM-ALK fusion protein triggering the activation of this pathway. Despite some adaptors as Src Homology 2 Domain-Containing (SHC), Insulin Receptor Substrate 1 (IRS1), and Growth Factor Receptor Bound Protein 2 (Grb2) bind NPM-ALK, the loss of their docking site is not able to preclude cell transformation. GRB2, IRS-1, and SHC are molecular adaptors that mediate the regulation of p21/Ras signaling and control the downstream effector molecules by tyrosine kinase receptors through the formation of stable signaling complexes. In ALCL, Grb2 binds mainly Tyr (152-156), Tyr (567), and proline-rich region Pro (415-417) in different sites of NPM-ALK playing, through the regulation of phosphorylation, a key role in ALCL cell growth[39,40]. In addition, docking of NPM-ALK to PLC-γ at Y664 leads to the hydrolysis of phosphatidylinositol (PIP2) into inositol triphosphate (IP3) and diacylglycerol (DAG), molecules able to regulate the intra-extracellular balance of Ca^{2+} and activate the specific serine/threonine kinase C (PKC). PKC family members phosphorylate a series of protein targets, known to be involved in several pathways including cell adhesion, transformation,

and cell cycle regulation[41]. NPM-ALK also interacts directly and indirectly with the subunit p110 of PI3K. This interaction causes PKB/AKT activation and the subsequent involvement of all the downstream interactors. These events promote survival, growth, proliferation, and migration[41]. Understanding the ALK signaling and the mechanisms driven by its deregulation is important to define how ALK and other co-signaling kinases are involved in hemopoietic cells transformation and is necessary to discover new targeted therapies[3] **(Figure 4)**.

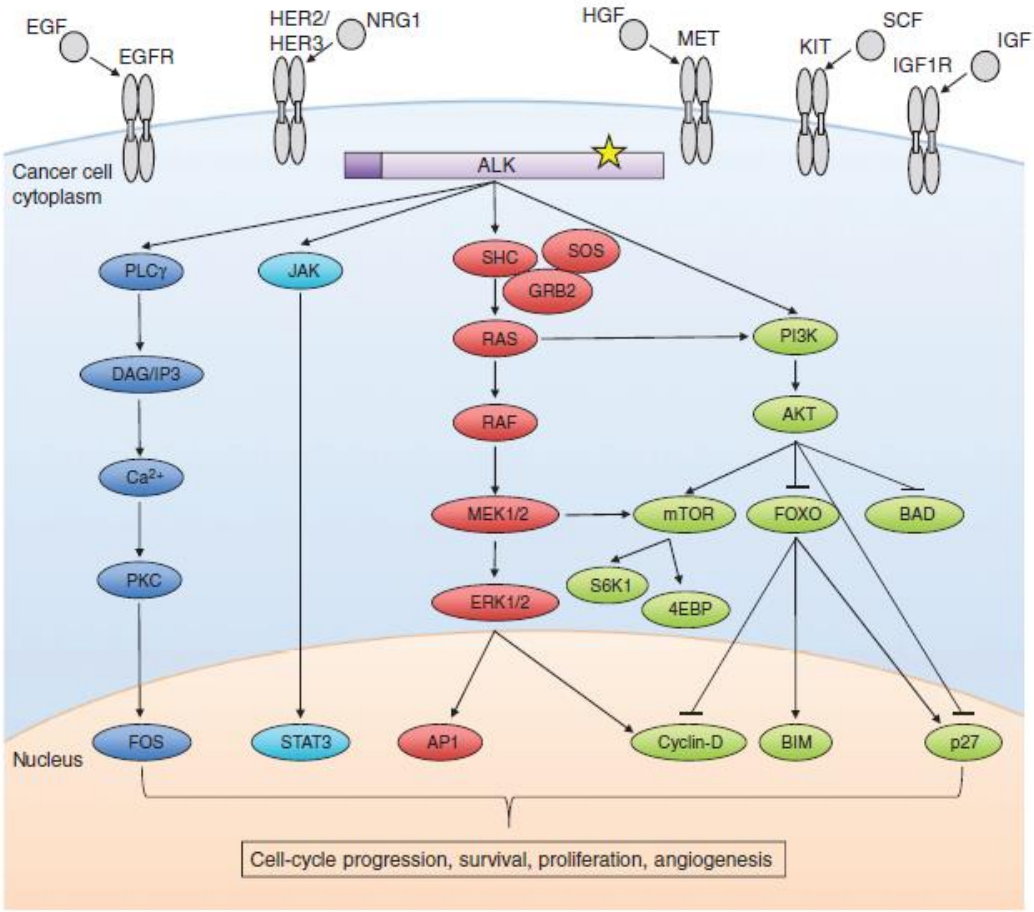

Figure 4. Oncogenic ALK signaling. The ALK fusion protein is constitutively active and signals *via* phospholipase C(PLC), JAK-STAT, RAS–RAF–MEK–ERK, and PI3K–AKT–mTOR pathways. This signaling results in the aberrant regulation of a number of genes (some of which are represented here),ultimately driving cell-cycle progression, survival, proliferation, and angiogenesis. Secondary mutations in the ALK kinase domain (starred) cause acquired resistance to ALK TKIs. Several of the bypass signaling tracks implicated in ALK TKI resistance are also shown here—EGFR, HER2/HER3, MET, KIT, and IGF1R with their respective ligands. *(Lin J, Targeting ALK: Precision Medicine Takes on Drug Resistance, Cancer Discovery,2017, DOI: 10.1158/2159-8290.CD-16-1123) (Reproduced with permission, license number: 5218180354389).*

1.1.3 JAK/STAT3 signaling

Signaling transducers and activators of transcription proteins (STAT) are a family of transcription factors that participate to cellular responses via cytokines and growth factors stimuli. STATs functions are regulated by post-translational modification at specific tyrosine phosphorylation sites that controls change conformations, dimerization, and nuclear localization[42]. Janus Kinase 1 (JAK1) is a protein tyrosine kinase characterized by the presence of a second phosphotransferase-related domain immediately N-terminal to the PTK domain, able to phosphorylate STAT3 which transcriptionally activates a signature of genes involved in inflammation and immune response. The JAK1/STAT3 pathway plays an essential role in regulating the balance of cell survival, proliferation and apoptosis and due to its importance is frequently mutated and functionally altered in solid tumors and hematological malignancies. The constitutive activation of RTK receptors-mediated signaling, the uncontrolled activity of G proteins coupled receptors (GCPR) converge on the aberrant activation of the JAK1/STAT3 signaling that assumes an oncological behavior. Similarly, the hyperactivation of STAT3 in stromal or host immune cells contest makes this transcription factor the main protagonist of inflammation-induced cancer[18]. Furthermore, the conditions necessary to activate the oncological potential of STAT3 are cell-dependent and/or restricted to a specific lineage. Several alternative mechanisms, independently from ALK, can constitutively activate the JAK/STAT3 pathway such as NFkB2-ROS1, NFkB2-TYK2, and NCOR2-ROS1 fusion proteins. Oncogenic mutations of *JAK1* and *STAT3* represent 38% of ALK^{-}ALCL genetic defects and are associated with hyperactive p-STAT3 that promotes oncogenesis **(Figure 5)**. These are mainly deletions, missense mutations, and translocations in chromosomal hot spots[18]. Finally, the absolute request for the activation of STAT3 protein in ALCLs makes it an ideal target for the discovery of advanced treatments against these subtypes of lymphomas, mostly in the context of mutated chimera and resistant forms of ALK[18,43].

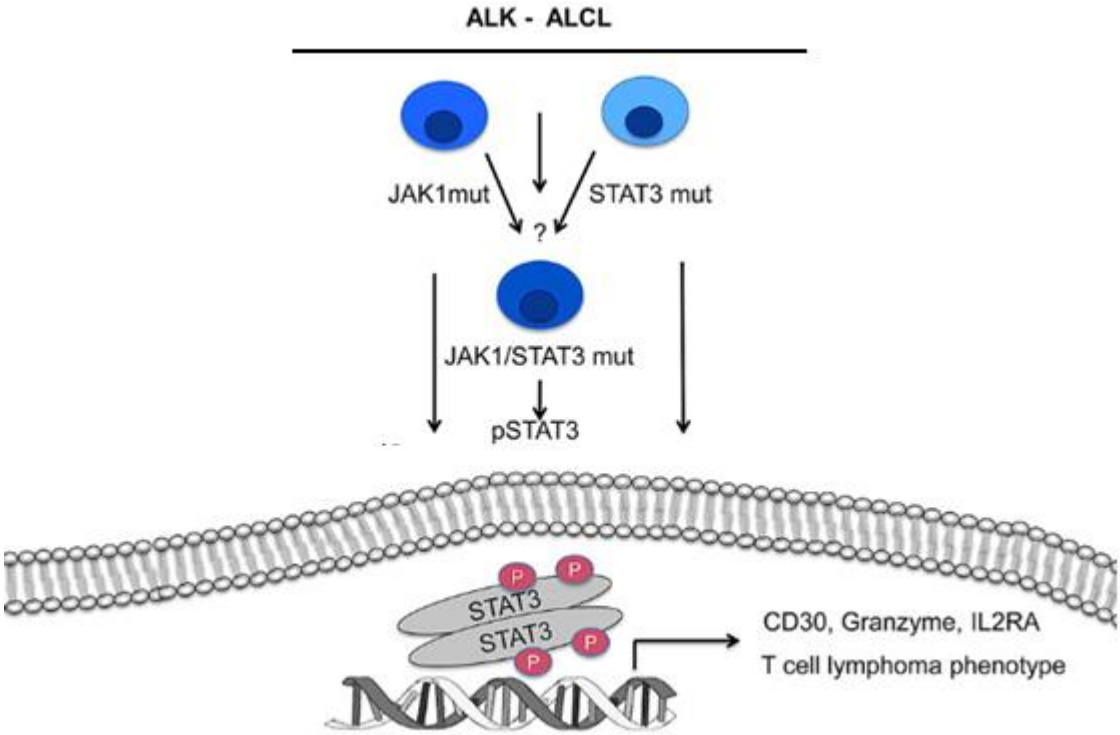

Figure 5. Activation of JAK1/STAT3 pathway. Oncogenic *JAK1-STAT3* mutations lead to the aberrant and constitutive hyperactivation of p-STAT3 that sustains T-cell lymphoma neoplastic features. (*Modified from Crescenzo R, Convergent mutations and kinase fusions lead to oncogenic STAT3 activation in anaplastic large cell lymphoma, Cell, 2015, doi.org/10.1016/j.ccell.2015.03.006) (Reproduced with permission, license number: 5218180874701).*

1.2 ALK$^+$ALCL: Systemic ALK$^+$ Positive Anaplastic Large Cell Lymphoma

1.2.1 Clinical and epidemiological features

ALK$^+$ALCL is an aggressive subtype of PTCLs with systemic symptoms and extranodal involvement (liver, lungs, skin, bone, soft tissues, and rarely gut and central nervous system) commonly seen in children and young adults, with male predominance. Bone marrow is involved approximately in 10-25% of cases and the small cell variant of ALK$^+$ may have leukemic traits with peripheral blood involvement[2]**.** Clinically, the majority of patients (70%) in the late phase of the disease present peripheral and/or abdominal lymphadenopathy, often associated with bone marrow impairment and extranodal infiltrates. ALK$^+$ subtype presents often B symptoms (54-75%) and high fever. The good prognosis and favorable clinical outcome of ALK$^+$ALCL are related to the age of onset and to the type of mutation, in particular *ALK* fusion[2,9].

1.2.2 Morphological features and immunophenotype

Morphologically, ALK$^+$ALCL presents a great variety of morphological features. Five morphologic patterns can be observed[2]: the “common pattern” (60-70%), the “wreath-like pattern”, the “lymphohistiocytic pattern”, the “small cell pattern” and the “Hodgkin-like pattern”. In the “common pattern”, tumor cells have abundant basophilic or eosinophilic cytoplasm, with the possibility of invasion of the lymph node sinuses with perivascular distribution. The “wreath-like pattern” (15%) is characterized by the presence of multi-nucleated cells and basophilic nucleoli. Where is still visible the lymph node architecture, the tumor grows within the sinus, resembling a metastatic invading tumor[2,9]. In the “lymphohistiocytic pattern” (10%) tumor cells are mixed with a large number of reactive histiocytes that mask the malignant cells and exhibit signs of erythrophagocytosis. These tumor cells cluster around blood vessels and by immunostaining are positive for CD30 and/or ALK[2]. The “small cell pattern” (5-10%) shows predominantly small, medium-size tumor cells with pale cytoplasms and centrally located irregular nuclei. In this case, hallmark cells are often clustered around blood vessels[2]. The “Hodgkin-like pattern” (3%) is characterized by morphological traits similar to Nodular Sclerosis Classical Hodgkin Lymphoma (NSCHL). This subtype shows tumor nodules surrounded by a fibrous band. Tumor cells can be highlighted by ALK staining indicating the presence of the translocation and the NPM-ALK fusion protein[2]. Immunophenotypically, ALK$^+$ALCL shows homogenous and strong expression of CD30 even if this receptor is also present in B and T activated cells and solid tumors[44–46]**(Figure 6)**.

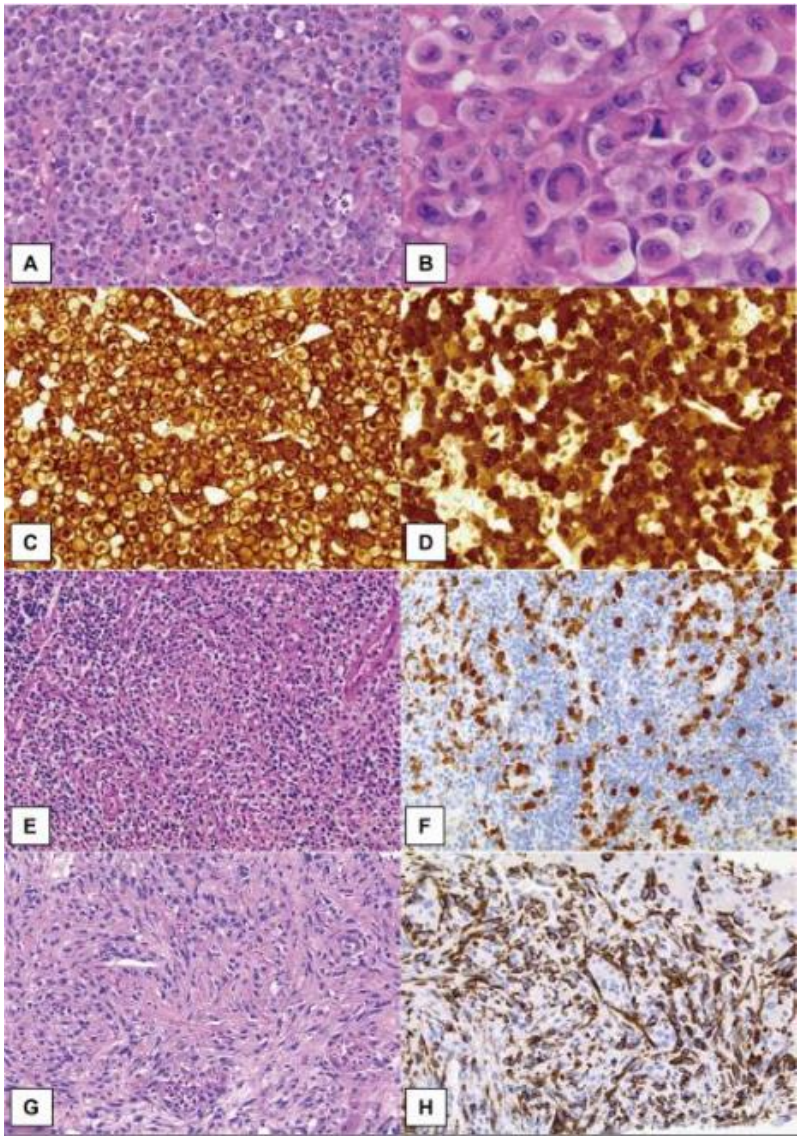

Figure 6. Morphological patterns and immunostaining of ALK-positive ALCL. The common pattern of ALK-positive ALCL comprises sheets of large, "hallmark" cell proliferation. Neoplastic cells exhibit variably shaped nuclei; invaginated, horseshoe- or kidney-shaped, donut-like, or Reed-Sternberg-like nuclei with abundant cytoplasm **(*A, B*)**. Strong immunoreactivity for CD30 is generally observed both on the membrane and in the Golgi regions **(*C*)**. In cases of ALCL with the t(2;5) translocation, as shown in this figure, the ALK protein has both nucleolar and cytoplasmic staining patterns **(*E, F*)**. The lymphohistiocytic pattern of ALCL shows conspicuous infiltration of small lymphocytes and histiocytes with pale cytoplasm. Morphologically, neoplastic cells are not clear but are highlighted by ALK immunostaining **(*F*)**. The sarcomatoid pattern of ALCL is characterized by atypical spindle-shaped cell proliferation with fascicular arrangement, simulating soft tissue sarcomas. Neoplastic cells are positive for CD30 **(*H*)** and ALK antigen expression **(*G, H*)**. *(Kengo Takeuchi, Anaplastic large cell lymphoma: pathology, genetics, and clinical aspects, J Clin Exp Hematop. 2017, DOI: 10.3960/jslrt.17023)(Free Access, Reproduced with permission, license from The Japanese Society for Lymphoreticular Tissue Research).*

1.3 ALK$^-$ALCL: Systemic ALK-Negative Anaplastic Large Cell Lymphoma

1.3.1 Clinical and epidemiological features

ALK negative (ALK$^-$) ALCL is the most aggressive, complex, and heterogeneous subtype of systemic ALCLs, that lacks *ALK* genetic alterations. This type of neoplasm represents 15-50% of all systemic ALCLs. From an epidemiological point of view, ALK$^-$ALCL is typical of adults (50-65 years) and shows a thin male preponderance. Clinically, ALK$^-$ALCL includes lymph nodes at diagnosis (49%) and extranodal tissues (20%) as skin, bone, and soft tissues causing systemic symptoms. The majority of patients in the late phase of the disease present peripheral and/or abdominal lymphadenopathy with B symptoms[14]**.** Unfortunately, this neoplasm lacks effective therapies and 70% of ALK$^-$ALCL patients have high morbidity and mortality[18].

1.3.2 Morphological features and immunophenotype

From the morphological point of view, ALK$^-$ALCL induces the destruction of the node or other tissues structures by cohesive and compact sheets of neoplastic cells. These cells tend to grow and proliferate in T-cell areas and diffuse through sinuses showing a metastatic behavior, similar to carcinoma[2]. Morphologically, the neoplastic ALK$^-$ cells are similar to ALK+ although the “small cell variant” is not identified. The ALK$^-$ cells tend to be larger and more pleomorphic, to have a higher nuclear: cytoplasmic ratio than the ALK$^+$ subtype[9,14]. ALK$^-$ALCL cells are strongly positive for CD30 and the staining shows the same intensity at the cell membrane and in the Golgi apparatus[2]. This feature is important to distinguish ALK$^-$ALCL from PTCLs in which CD30 staining is heterogeneous and the intensity very low. T-cell antigens such as CD2 (about 45%) and CD3 (about 65%) are more commonly expressed in ALK$^-$ than in ALK$^+$ALCL cells, while CD5 is often not expressed. In neoplastic settings, CD8+ cells are rare while CD4+ cells are more frequent. Although the neoplastic cells show a T-helper phenotype, cytotoxic markers such as TIA-1, granzyme B, and perforin are present, except cases with *DUSP22* rearrangement **(Figure 7)**[12,47].

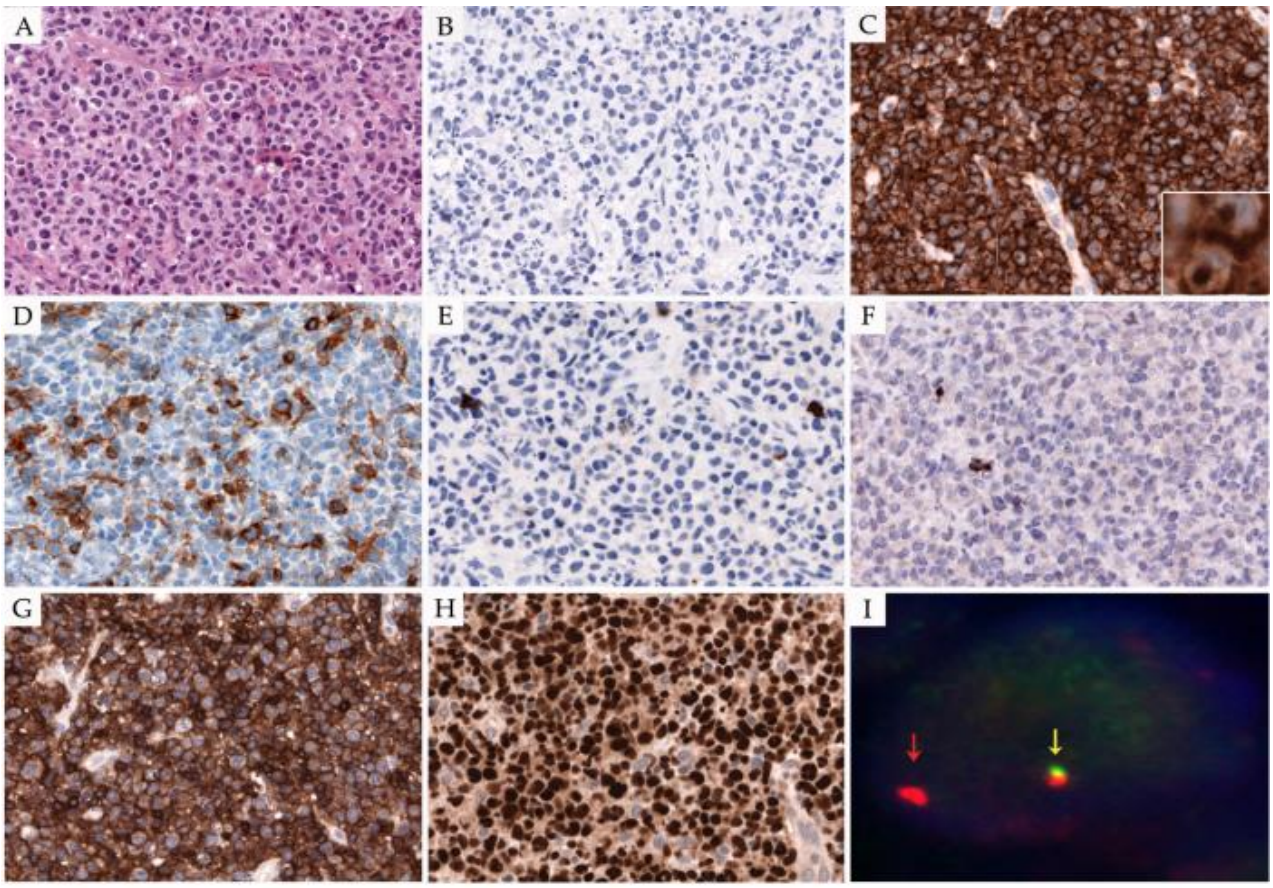

Figure 7. ALK− ALCL with DUSP-22 rearrangement. (A) Classic ALCL morphology is displayed; cells are relatively monomorphic (H&E stain, 400×); **(B)** Neoplastic cells lack ALK expression; **(C)** CD30 staining is strong and homogenous, showing a membranous and Golgi zone pattern (immunohistochemistry 400× and insert 630×); **(D)** CD4; **(E**) CD8, and **(F)** TIA-1 are negative in the neoplastic cells, exhibiting a triple-negative phenotype; **(G)** Neoplastic cells stained positive for TCR alpha-beta (beta F1), demonstrating the T-cell origin; **(H)** IRF4/MUM1 reveals nuclear expression in all neoplastic cells **(B, D–H)**; immunohistochemistry, 400×); **(I)** Fluorescent in situ hybridization (FISH) using a break-apart probe to the *IRF4-DUSP22* locus on 6p25.3 shows one normal fusion signal (yellow arrow), one red signal (red arrow), and loss of one green signal, indicative of a *IRF4-DUSP22* rearrangement. Abbreviations: H&E: hematoxylin and eosin *(*Montes-Mojarro, I.A.; Steinhilber, J.; Bonzheim, I.; Quintanilla-Martinez, L.; Fend, F. The Pathological Spectrum of Systemic Anaplastic Large Cell Lymphoma (ALCL). *Cancers* **2018**, *10*, 107. https://doi.org/10.3390/cancers10040107*). (Reproduced with permission, Creative Commons Attribution 4.0 International Public License ("Public License-CC-BY 4.0"), unmodified material).*

1.4 BIA-ALCL: Breast-Implanted Associated Anaplastic Large Cell Lymphoma

1.4.1 Clinical, epidemiological and genetic features

BIA-ALCL is an uncommon CD30+/ALK-, T-cell non-Hodgkin lymphoma. Due to BIA-ALCL s uncommon occurrence, it is difficult to determine the exact prevalence. Since the onset of primary lymphoma of the breast is very rare (0.12-0.53% of all malignant breast neoplasms), there has been increasing doubt about an etiologic link between breast implants and the

development of ALCL[48]. All patients are women presenting breast mass and in 90% of cases, periprosthetic fluid, approximately 8-10 years after the implantation of the breast prosthesis[49]**.** BIA-ALCLs, due to their clinical features, comprise two subgroups: the first is the most common characterized by a fluid accumulation around the implant (called seroma), while the second clinical subgroup presents a palpable indolent tumor generally confined to the breast, but occasionally can be associated with systemic involvement[50–52]**(Figure 8 and 9)**. Indeed, BIA-ALCL development is a complex process that involves multiple factors, but it is mainly related to textured implants (silicone or saline) that act as a chronic stimulus to generate chronic inflammation which is proposed as a precursor of tumorigenesis. Although the pathogenesis of BIA-ALCL is not completely understood, a combination of textured breast implant, bacterial contamination, and genetic predisposition seems to be essential for BIA-ALCL onset and development. BIA-ALCL share with ALK^{-}ALCL some genetic alterations such as *JAK1-STAT3* activating mutations (followed by the hyperactivation of p-STAT3) and deregulation of chromatin modifiers[53,54]**.** By contrast, translocations involving *ALK, DUSP22, and TP63* are absent[50,55]. Recent studies demonstrated that the increase of hypoxia signaling pathways and the activation of hypoxia-specific gene signature is a typical BIA-ALCL molecular feature able to sustain and drive tumor growth[56].

For this reason, the discovery of specific BIA-ALCL molecular defects could lead to the identification of new biomarkers to improve early detection, diagnosis, and follow-up. BIA-ALCL patients display an excellent outcome since generally, this subtype regresses after breast implant surgical removal (93% of patients complete remission) and disease re-occurrence is rare. Differently, patients with non-resectable neoplasm undergo chemotherapy.

1.4.2 Immunophenotype

BIA-ALCL cells are strongly and uniformly positive for CD30 antigen expression and negative for ALK even if some rare cases are reported to display ALK antigen expression and positivity[57,58]. CD4 expression is often present while CD3, CD5, and CD7 markers are absent. CD8 is negative, but cytotoxic markers (TIA-1, granzyme B, perforin) can be observed.

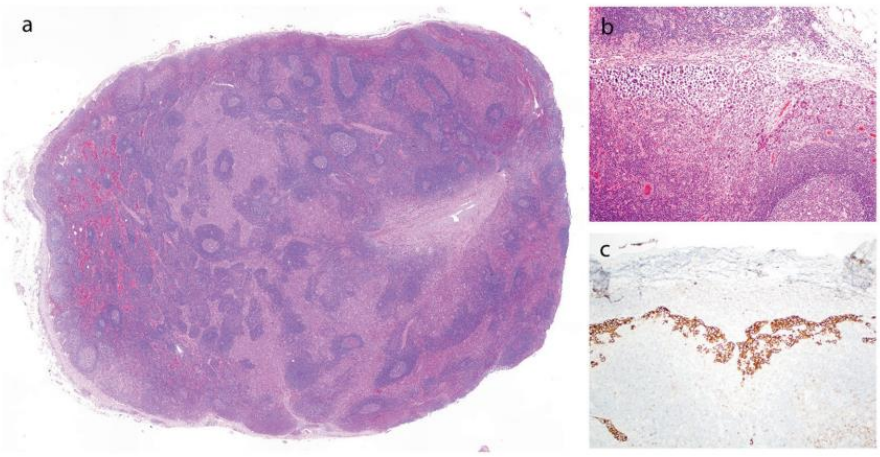

Figure 8. Lymph node involvement by breast implant ALCL. (A) Enlarged lymph node with partial architectural distortion due to involvement by breast implant ALCL in sinuses and interfollicular areas; H&E, 40×. **(B)** Higher magnification shows extensive sinusoidal involvement; H&E, 100×. **(C)** CD30 immunohistochemistry highlights the lymphoma cells within sinuses, 100×. *(Andrés E. Quesada, Breast implant-associated anaplastic large cell lymphoma: a review, Modern Pathology (2019), doi.org/10.1038/s41379-018-0134-3)(Reproduced with permission, license number: 5218180354389).*

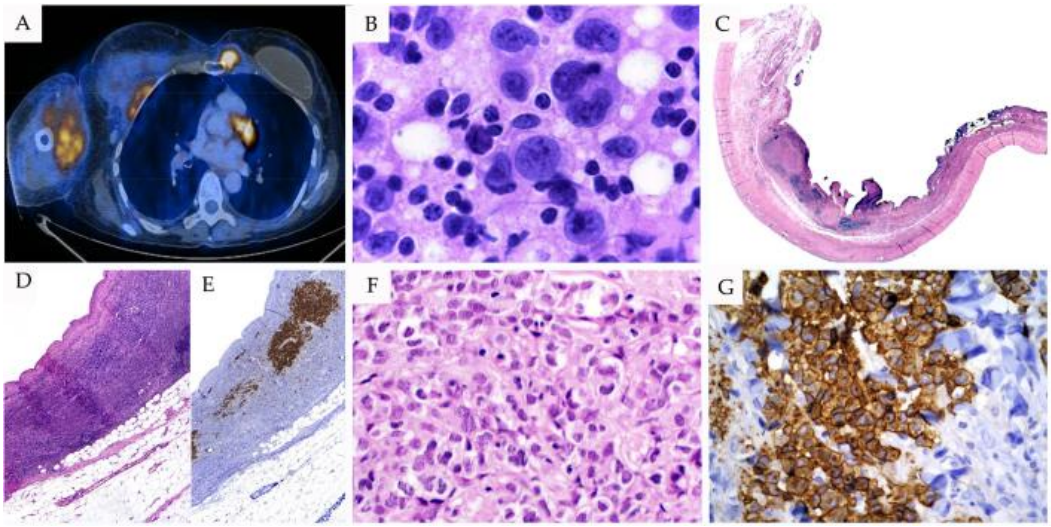

Figure 9. Breast implant-associated ALCL with systemic involvement. **(A)** 18 F-fluorodeoxyglucose positron emission/computerized tomography (FDG-PET/CT) scan demonstrating hypermetabolic activity in the anterior right thorax and upper arm soft tissues accompanied by muscle and cutaneous involvement, maximum standardized uptake value-6 (SUVmax-6). **(B)** Fine needle aspirate showing large neoplastic cells with abundant eosinophilic cytoplasm and eccentric horseshoe-shaped nuclei with multiple nucleoli (H&E stain, 630×). **(C)** Low-power view demonstrating capsule engrossment and extensive lymphoma infiltrate (H&E stain 25×). **(D, E)** Infiltration of the neoplastic cells to the surrounding soft tissue confirmed by CD30 immunostaining (H&E stain 50× and CD30 immunostaining 50×). **(F)** Sheets of large atypical neoplastic cells, as well as some occasional hallmark cells (H&E stain, 400×). **(G)** Neoplastic cells show strong and homogenous staining of CD30 (immunohistochemistry, 400×). Abbreviations: H&E: hematoxylin and eosin. *((*Montes-Mojarro, I.A.; Steinhilber, J.; Bonzheim, I.; Quintanilla-Martinez, L.; Fend, F. The Pathological Spectrum of Systemic Anaplastic Large Cell Lymphoma (ALCL). *Cancers* **2018**, *10*, 107. https://doi.org/10.3390/cancers10040107*). (Reproduced with permission, Creative Commons Attribution 4.0 International Public License ("Public License-CC-BY 4.0"), unmodified material).*

1.5 Therapeutic strategies and new experimental approaches

The discovery of a spectrum of genomic defects that drive T cells transformation and sustain PTCLs progression allowed to identify new genomic-based stratifications, which are being used to establish objective diagnostic criteria, more effective risk assessment, and target-based interventions[59,60]. The integration of genomic, functional, and clinical data has provided the basis for targeted therapies, immunological approaches, and combined strategies, that underlie individual tumor vulnerabilities and are expected to ameliorate clinical responses. Since the survival outcome of PTCLs is still very poor also after the first-line treatment, preclinical models are essential in testing novel therapeutic approaches that can be translated to the clinic for the design and planning of new trials.

Although ACVBP chemotherapy (doxorubicin, cyclophosphamide, vindesine, bleomycin, prednisone) followed by a consolidation therapy with high-dose methotrexate, ifosfamide, etoposide, asparaginase, and cytosine-arabinoside or m-BACOD (methotrexate, bleomycin, Adriamycin, cyclophosphamide, vincristine, dexamethasone), VIMMM (VM26, ifosfamide, mitoxantrone, methyl-gag, methotrexate)/ACVBP, and other chemotherapeutic strategies such as CHOP[61](cyclophosphamide, doxorubicin, vincristine, prednisone) showed important results is urgent to discover newer drugs, alone or in combination with cytotoxic agents, to overcome PTCLs clinical need.

US Food and Drug Administration (FDA) approved for relapsed/refractory PTCLs patients four single compounds: i) pralatrexate (antifolate agent), ii) romidepsin, iii) belinostat (HDAC inhibitor), iiii) brentuximab vedotin (SGN-35) that is a CD30 toxin-conjugated monoclonal antibody. Only brentuximab vedotin has a significant impact on patients' overall survival[5]. Interestingly, the ECHELON-2 clinical trial demonstrated that brentuximab vedotin used in combination with CHOP resulted in an increase in overall survival without added toxicity and supports the potential for brentuximab vedotin, cyclophosphamide, doxorubicin, and prednisone (A+CHP) to become a new standard of care for many patients with CD30-positive PTCL[62].

Targeted therapies and immunological approaches used also in combination with CHOP are the main strategies proposed for PTCLs treatment and clinical trials testing the combination efficacy are still ongoing[5].

PTCLs targeted therapies include the use of:

-Epigenetic modulators (such as azacytidine) in combination with CHOP, whose clinical trial is still ongoing (NCT03542266). In addition, multiple combinations of epigenetic modulators (azacytidine) with HDAC inhibitors (romidepsin), bortezomib, and durvalumab (PDL1 inhibitor) are in clinical trial (NCT03161223, NTC01998035, and NCT01129180) (*clinicaltrials.gov).*

-JAK/STAT inhibitors: JAK1 (AZD4205), JAK1, and JAK2 inhibitors (ruxolitinib) are in clinical trial (test of monotherapy regimen) in naïve or relapsed/refractory PTCLs and NK/T cell lymphomas (NCT04105010, NTC02974647) *(clinicaltrials.gov).*

-SYK inhibitors: novel dual inhibitor SYK-JAK (cerdulatinib) is showing significant efficacy in the clinical trials regarding refractory PTCLs and AITLs.

-PI3K inhibitors: duvelisib is an oral dual inhibitor of PI3K in clinical trial alone and in combination with HDAC inhibitors or bortezomib but have demonstrated a high rate of response in PTCL and CTCL.

Instead, immunotherapies for PTCL encompass the use of:

-Lenalidomide and CHOP: Lenalidomide is an immunomodulator that has antineoplastic activity and it was proposed in combination with CHOP for the treatment of AITLs.

-Brentuximab vedotin: is proposed as a treatment also for relapsed/refractory AITLs, PTCLs, and newly diagnosed PTCLs**.**

-Mogamulizumab: CCR4 monoclonal antibody with antitumor activity in PTCLs and ATLL preclinical models**.** It was approved in 2018 for the treatment of relapsed and refractory mycosis fungoides and Cezary syndrome.

-Camidanlumab tesirine: antiCD25 antibody-drug conjugated with a toxin (tesirine). Camidanlumab is internalized in the cells and the toxin is released causing cell death.

-Bifunctional antibodies such as AFM13 (CD30-CD16 antibody) are able to direct NK cells to CD30+ targets. Clinical trials are ongoing (NCT03192202, NCT04074746) *(clinicaltrials.gov)*.

-Checkpoint inhibitors: for PTCLs that express PD1-PDL1 (monoclonal antibody pembrolizumab, nivolumab).

-CAR-T cell-based therapies: CAR-T products are under investigation in several clinical trials[5].

In ALK^{+}ALCLs patients, *ALK* can be considered as the only onco-antigen required for neoplastic activation and maintenance. Crizotinib, an oral ALK-tyrosine kinase inhibitor, has also been employed to decrease NPM-ALK levels and induce tumor regression[63,64]. However, as for other target therapies, the use of ALK inhibitors may be limited by the occurrence of primary or secondary resistance[3]. In January 2021, FDA approved Crizotinib [65,66] for ALK^{+}ALCL in children and young adults. FDA approval is based on the results of this clinical trial NTC00939770*(ClinicalTrials.gov; FDA.gov).*

Chromatin remodeling

2. Description and functions

Chromatin dynamics such as regulation of proper gene expression, chromosome functions, and genome-wide nucleosome occupancy, require specialized ATP-dependent chromatin remodeling complexes to maintain DNA homeostasis. Indeed, chromatin remodelers can regulate nucleosome assembly and organization, chromatin accessibility, and nucleosome editing (in terms of removing or installing histone variants) by using the energy of ATP hydrolysis. Chromatin remodeling functions depend on cell lineage and stage, environmental stress, and also on cell cycle phase[67,68]**.** Chromatin remodelers are divided into four families: imitation switch (ISWI), chromodomain helicase DNA-binding (CHD), switch/sucrose non-fermentable (SWI/SNF), and INO80 (inositol-requiring 80) based on the similarities and differences in their catalytic domains. For all chromatin remodelers, the Tr domain is essential and sufficient to perform DNA translocation[67]**(Figure 10).**

The ISWI family ATPases consist of two RecA-like lobes separated from a small insertion, a carboxy-terminal HAND-SANT-SLIDE (HSS) domain that can interact and bind with the tail of Histone H3-H4 and the linker DNA flanking the nucleosome[69]. The activity of the ATPase domain is regulated by other two lobes: the autoinhibitory N terminal (AutoN) and the negative regulator of coupling (NegC). The main function of ISWI family complexes is to catalyze nucleosome assembly and spacing, limiting chromatin accessibility and leading to a state of repression.

The CHD family presents an ATPase domain similar to that of ISWI remodelers, two unique and characteristic tandemly arranged chromo-domains at the N-terminus. At the C-terminus, CHD remodelers have a NegC domain and a DNA binding domain (DBD) characterized only by SANT and SLIDE domain (SS)[67,70]. Functionally, their chromatin remodeling functions include all three general processes such as nucleosome assembly and spacing[71], regulation of chromatin accessibility, and nucleosome editing[72,73].

The SWI/SNF family is characterized by the presence of Helicase-SAINT associated domain (HSA) at N-terminus that bind actin and/or actin-related proteins (ARPs), an adjacent post-HSA domain, two RecA-like lobes. They present A-T hooks and C-terminal bromodomain that binds to the acetylated-lysines of histones tails. SWI/SNF chromatin remodelers mainly regulate chromatin accessibility (ejection/eviction of nucleosomes, gene expression/silencing)[67,70].

The INO80 family contains Helicase-SAINT associated domain (HSA) that can nucleate actin and bind ARPs, an adjacent post-HSA domain, two RecA-like lobes interspaced by a large and variable insertion. They are involved in the regulation of chromatin accessibility, transcriptional regulation, DNA replication, and DNA repair[74–78].

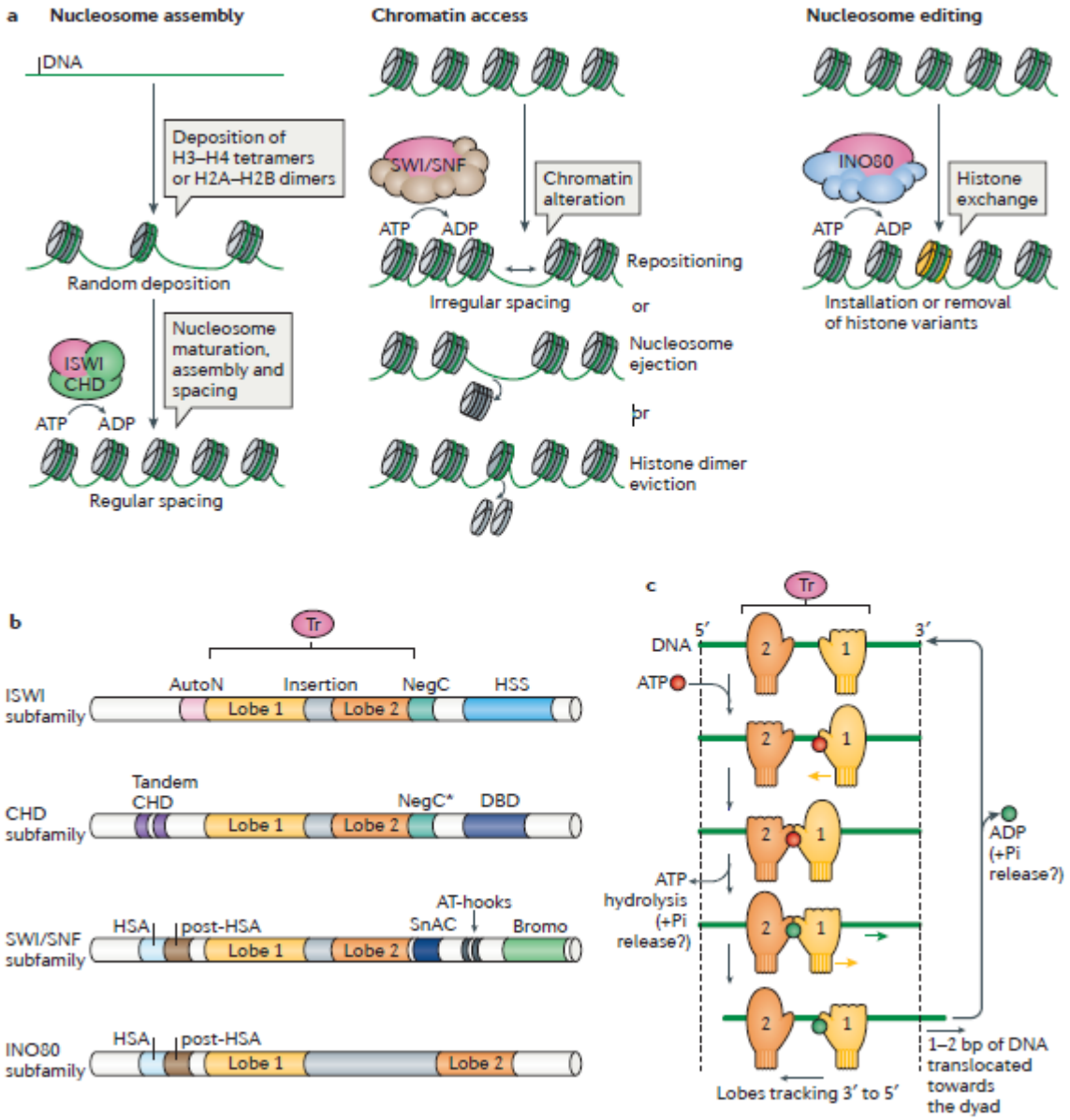

Figure 10. Functions and domain organization of chromatin remodelers. (a) | Functional classification of remodelers. The ATPase–translocase subunit of all remodelers is depicted in pink; additional subunits are depicted in green (imitation switch (ISWI) and chromodomain helicase DNA-binding (CHD)), brown (switch/sucrose non-fermentable (SWI/SNF)), and blue (INO80). Nucleosome assembly: particular ISWI and CHD subfamily remodelers participate in the random deposition of histones, the maturation of nucleosomes, and their spacing. Chromatin access: primarily, SWI/SNF subfamily remodelers alter chromatin by repositioning nucleosomes, ejecting octamers, or evicting histone dimers. Nucleosome editing: remodelers of the INO80 subfamily (INO80C or Swr1 complex (SWR1C)) change nucleosome composition by exchanging canonical and variant histones, for example, and installing H2A.Z variants (yellow). We note that this functional classification is a simplification, as INO80C, the ISWI remodeler nucleosome remodeling factor (NURF) and certain CHD remodelers can promote chromatin access. **(b)**| Domain organization of remodeler subfamilies. The ATPase–translocase domain (Tr) of all the remodelers is sufficient to carry out DNA translocation. It is comprised of two RecA-like lobes (lobe 1 and lobe 2, which are separated by a short or long (such as in the

INO80 subfamily) insertion (grey)). Remodelers can be classified into four subfamilies based on the length and function of the insertion and their domain organization. **(c)**| 'Inchworming' mechanism of DNA translocation. An ATP binding–hydrolysis-dependent conformational cycle of the RecA-like lobes ('mittens') drives DNA translocation. Mittens are depicted closed when lobes have high affinity for DNA and open when lobes have low affinity for DNA. Although the DNA can be double-stranded, only the tracking strand of DNA is depicted, along which the lobes move in the 3´–5´ direction (validated by single-stranded DNA studies from Saha, A. et al (Nat. Struct. Mol. Biol. 2005). Steps are depicted as sequential, but they may be concerted, and a similar model with mitten/lobe 1 being stationary is equally supported. The yellow arrows represent remodeler movement; the green arrow represents DNA translocation. The precise step in which inorganic phosphate (Pi) is released is not known. NegC* is a region with structural similarity to the ISWI negative regulator of coupling (NegC) domain. AutoN, autoinhibitory N-terminal; Bromo, bromodomain; DBD, DNA-binding domain; HSA, helicase/SANT-associated; HSS, HAND–SANT–SLIDE; SnAC, Snf2 ATP coupling. *(Cedric R Clapier, Mechanisms of action and regulation of ATP-dependent chromatin-remodeling complexes, Nature Reviews Molecular Cell Biology, DOI: 10.1038/nrm.2017.26,2017)(Reproduced with permission, license number: 5218200067478).*

Chromatin remodelers share several features: they have a greater affinity for nucleosome than DNA, one single catalytic subunit contains the ATPase domain and they have distinct domains for the interaction with specific transcriptional factors (TFs), chaperon, and other chromatin factors able to "read" and integrate signaling to control chromatin status and dynamics guaranteeing genomic stability. Indeed, these remodeling factors play an essential role in determining the expression of specific transcriptional gene programs. They act by organizing chromatin accessibility in terms of activation and repression, by dictating nucleosome editing and genome-wide nucleosome occupancy. In addition, chromatin factors are emerging as crucial players in maintaining RNA-DNA hybrid (R-loops) homeostasis, in which newly transcribed RNA anneals with the accessible and complementary single-stranded (ss) DNA, exposing DNA to increased risk of ruptures[79]. Recently, it has been demonstrated that SWI/SNF chromatin remodeling complex helps to resolve RNA-DNA hybrid structures caused by transcription-replication conflicts (TRCs) that occur when transcription and replication machinery collide, exposing DNA to increased replication forks damages that are the major source of genome instability[79,80]. Moreover, chromatin factors help cells to solve chromosomal lesions by acting as DNA helicases able to remodel replicative forks, recognize DNA damages and remove DNA damaged strands to protect and restore genome integrity[81] **(Figure 11)**. Indeed, DNA helicase's primary function is to resolve DNA helix and topological tensions, controlling many DNA-based processes and thus being the most important genome caretakers[82,83].

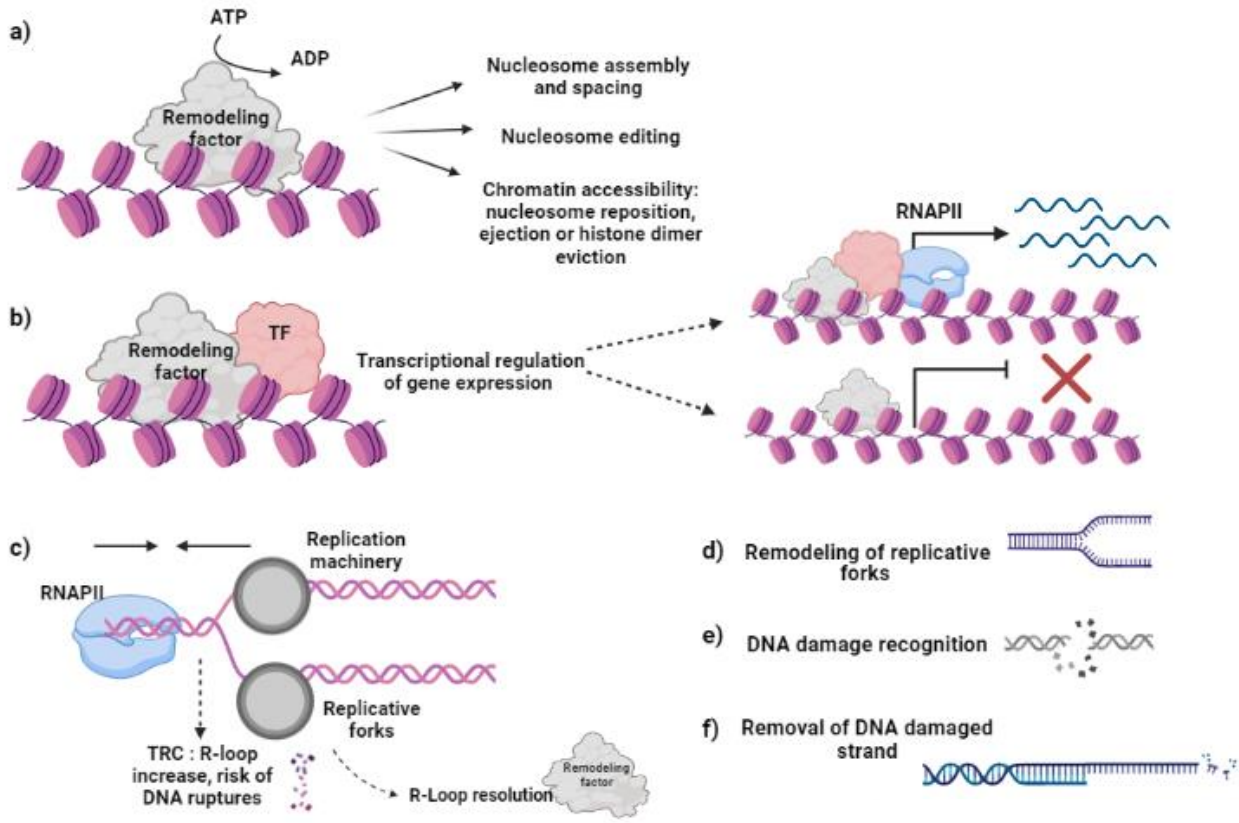

Figure 11. A wide spectrum of chromatin remodeling functions. **(a)** impact of chromatin remodeling function on nucleosome homeostasis and chromatin state; **(b)** transcriptional activity of chromatin remodeling factors, able to activate o inhibit transcription; **(c)** contribution of chromatin remodelers in resolving RNA-DNA hybrid caused by transcriptional-replication machinery collisions; **(d-f)** chromatin factors involvement in replicative forks remodeling, DNA damage sensing and recognition *(created with Biorender.com).*

2.1 The role of chromatin remodeling in T cell biology and PTCLs

It has been reported that chromatin remodeling functions are crucial in regulating T cell biology. Indeed, they are implicated in guaranteeing a proper gene expression program during T cell development in the thymus[84,85], in regulating thymic *T cell receptor (TCR)* gene rearrangement[86], in peripheral T helper differentiation modulating T cell plasticity. Moreover, together with lineage-specific transcription factors, they can change gene expression profiles after differentiation[87]. By orchestrating transcriptional changes and regulating chromatin accessibility in response to T cell perturbation, chromatin remodelers are also implicated in T cell activation, proliferation, and cytokine expression by directly acting on their regulatory regions[88,89]. Indeed, Jeong et al. demonstrated that SWI/SNF can increase AP-1 transcription factor expression and activity increasing cytokine production and proliferation of peripheral T cells.

Thus, it is not surprising that genetic or transcriptional alterations in many members of this remodeler family have been linked to different disease conditions including genetic disorders, aging, and predisposition to cancer[90,91]. Large-scale cancer genome sequencing studies (The Cancer Genome Atlas (TCGA), Pan-Cancer Atlas, Catalog of Somatic Mutation in Cancer (COSMIC)), reported that chromatin-related genes are mutated in >20% of human neoplasms[92]. In neoplastic T cells, chromatin modifiers overexpression is often related to increased cancer cell proliferation, DNA damage and altered forks homeostasis, aberrant regulation of gene expression, and resistance to therapy favoring tumor progression **(Figure 12)**. With the intent to correlate the PTCLs mutational landscape with patient's clinical outcome, Ye.Y et al. performed a retrospective study of 53 PTCLs patients using Next Generation Sequencing Technology (NGS) and showed that the most common mutations were those of epigenetic/chromatin modifications (n=40, 75%), indicating their relevance in supporting T neoplastic features. Indeed, epigenetic remodeler alterations are related to a worse prognosis and negative clinical outcome[93]. For this reason, understanding the mechanisms that underline the development and evolution of T lymphomas is crucial to define the molecular vulnerabilities of these neoplasms and to develop specific therapeutic strategies. Indeed, in virtue of their centrality in T cell biology, epigenetic modifiers are currently counted among the most appealing targets for cancer therapies and/or immunological approaches. Referring to ALCLs, we recently proved that the SWI/SNF2 DNA-helicase HELLS is required for proficient ALK$^-$ALCLs proliferation. We showed that *HELLS* is a downstream target of STAT3 transcription factor and that its expression is controlled by the ALK$^-$ALCLs specific lncRNA *BlackMamba*. Besides, we demonstrated that *BlackMamba* interacts with HELLS driving its positioning on target promoters, suggesting that the role of this chromatin modifier in this tumor setting may rely on its transcriptional activity[94].

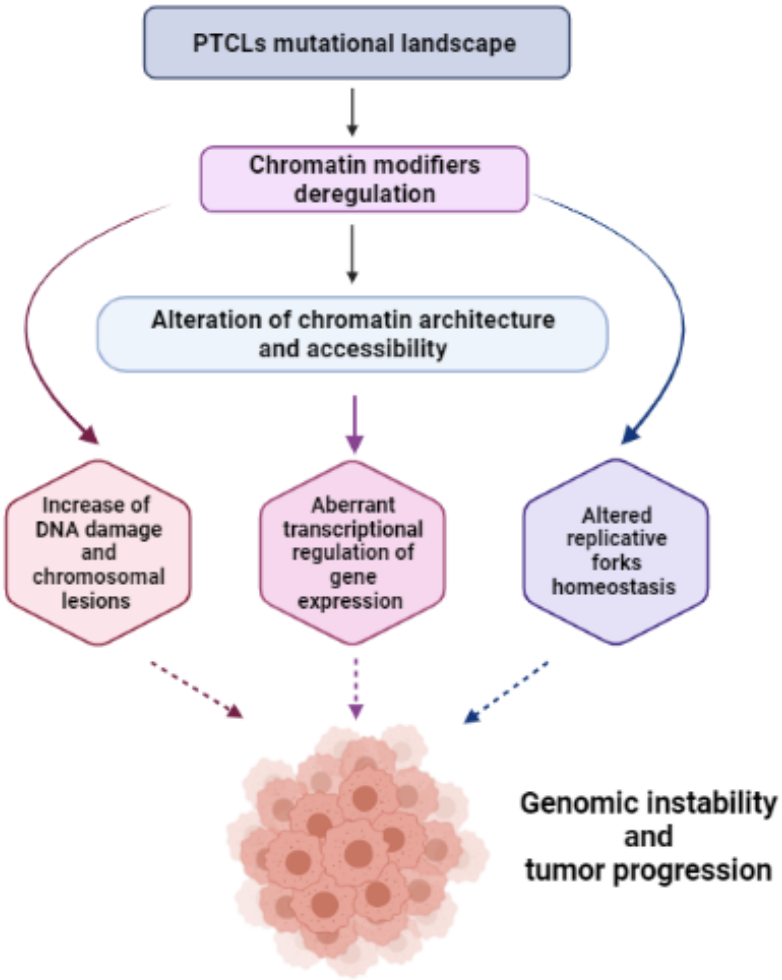

Figure 12. Deregulation of chromatin modifiers/chromatin modifications is essential in determining and increasing tumor instability, favoring tumor growth and progression. *(created with Biorender.com).*

3. The role of Rho-GTPases in T cell biology and PTCLs

Rho-GTPases are a family of 23 small G proteins that belong to the Ras superfamily[95]. Rho-GTPases are crucial signal-transducing proteins downstream several receptors playing key roles in the regulation of cytoskeleton dynamics(polarity, membrane transport, motility, and invasiveness), in the control of different biological processes such as cytokinesis, cell growth and proliferation, apoptosis, transcription, and nuclear signaling[96,97]. Mechanistically, Rho-GTPases cycles/switches from an inactive state(guanosine diphosphate-GDP-bound) to an active state (guanosine triphosphate-GTP-bound) changing their localization[98,99]. This balanced regulation is mediated by several guanine nucleotide exchange factors (GEFs), GTPase activating proteins (GAPs), and guanine nucleotide dissociation inhibitors (GDIs)[100] that guarantee the proper activation/inhibition in response to specific stimuli. RhoA, Rac1, and Cdc42 are the typical and most studied GTPases. It has been demonstrated that RhoA plays important role in T-cell development contributing to pre-and post-thymic selection of CD4+ and CD8+ lymphocytes, in T-lymphocytes polarization and migration in response to chemokines[101,102]and also TCR-dependent activation process and spreading after TCR-activation[103]. Once activated, RhoA can activate different downstream effectors such as Rho-associated coiled-coil-containing protein kinases (ROCKI and ROCKII), Citron Kinase, and diaphanous related formin 1 (mDia1) to change cytoskeleton flexibility promoting both depolymerization and polymerization of F-actin guaranteeing proper and complete cytokinesis through the regulation of actomyosin ring structure[104]. Furthermore, RhoA regulates the transcription of *serum response factor (SRF)* and *myocardin-related transcription factor (MRTFA)*[105,106]**,** two transcriptional factors that control the expression of cytoskeleton-related genes and that induce changes in cellular globular actin (G-actin) concentration, coupling cytoskeletal gene expression to cytoskeletal dynamics **(Figure 13).**

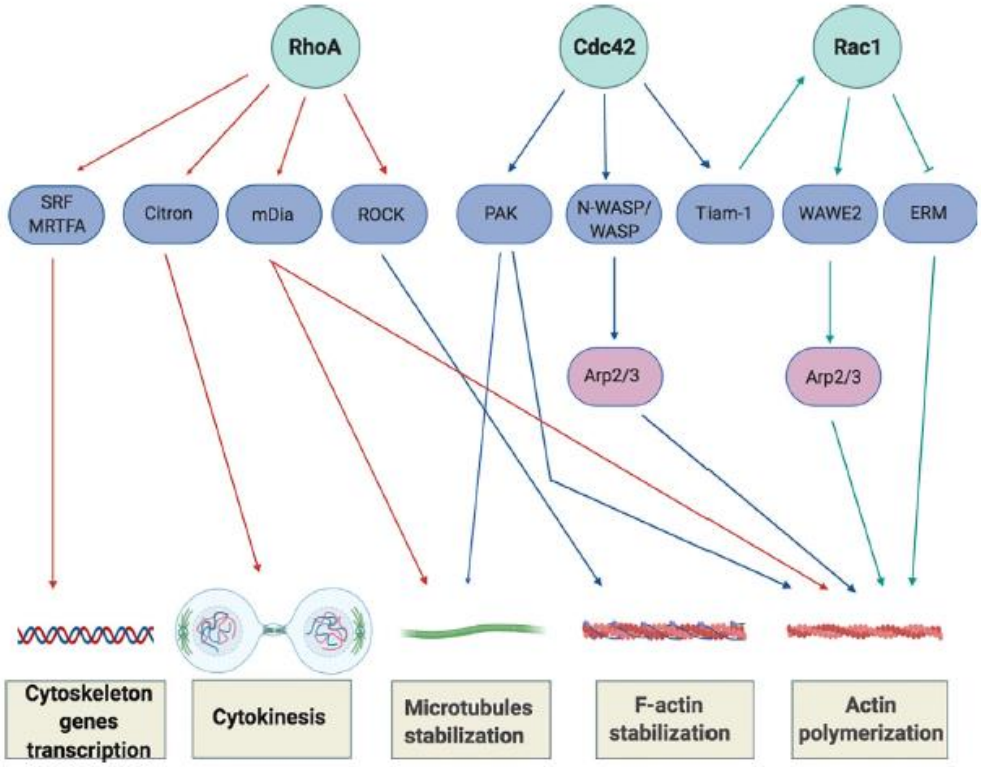

Figure 13. Overview of Rho-GTPase signaling in T-cells. Rho GTPases regulate several processes, including cytoskeletal rearrangement, proliferation, and cellular division. The best-characterized Rho GTPase proteins, RhoA, Cdc42, and Rac1 (light green), and some of their main effector proteins are shown (purple). The Activation or inactivation of cytoskeletal effectors leads to responses such as actomyosin contraction, filamentous (F)-actin disassembly, or F-actin polymerization, and microtubules stabilization. RhoA induces the activation of Rho-associated coiled-coil-containing protein kinases (ROCKI and ROCKII) leading to actomyosin assembly. Targeting Citron kinase at the cleavage furrow during the cytokinesis, RhoA also increases the actomyosin contractile ring tension and facilitates cell separation. Moreover, RhoA induces actin polymerization through the activation of the novo actin polymerizing agent formin mammalian diaphanous (mDIa1). The binding of Cdc42 to N-WASP or WASP (Neuronal-/Wiskott-Aldrich syndrome protein) and Rac1 to WAVE2 (Wiskott-Aldrich syndrome protein family member 2) initiates the assembly of protein machinery that is required for actin polymerization and involved the activation of actin-binding proteins (Arp2/3 complex) to stimulate actin polymerization by creating a new nucleation core. Cdc42 also phosphorylates and activates the effector proteins p21-activated kinases (PAKs) to mediate effects on microtubules and F-actin. Cdc42 and Rac1 are further interconnected by the exchange factor Tiam-1 that, acting mainly upstream of Rac1, is involved in the regulation of Rac1-mediated signaling pathways. *(Fragliasso V, Tameni A, Cytoskeleton Dynamics in Peripheral T Cell Lymphomas: An Intricate Network Sustaining Lymphomagenesis, Frontiers in Oncology,2021, doi.org/10.3389/fonc.2021.643620).*

As RhoA is crucial in signaling transduction and essential in regulating cytoskeleton and cytokinesis-related dynamics, its deregulation could have a role in lymphomagenesis. Indeed, it has been shown that *RHOA* is mutated in PTCLs, suggesting a driver role for its GTPase in the development of these lymphomas. The most frequent mutation is G17V, which has been detected in 50% to 70% of AITL[107,108], 18% of PTCL-NOS[109], 7% of SS, and 2% of ATLL[110]. In AITL, G17V *RHOA* mutation guarantees the onset of permissive genetic

background in which loss of function of Tet2 has occurred as first hit of lymphomagenesis suggesting a cooperative role of these alterations in the pathogenesis of AITL[111]. Apparently, this mutation confers suppressive functions to RhoA breaking many paradigms on the role of this protein in tumors. Mechanistically, glycine at residue 17 is critical for GTP binding and locks RhoA in its inactive conformation[109]. Its substitution with a valine residue confers the ability to act as dominant-negative preventing the activation of wild-type RhoA and its effectors proteins[111], and probably by altering the activity of the GEFs resulting in a reduction of *SRF* transcription and in the number of F-actin stress fibers[109]. However, G17V *RhoA* mutant can stimulate the Inducible T Cell Costimulator (ICOS) signaling leading to the differentiation of CD4+ T cells towards the follicular helper T lineage[111,112]. This indicates that G17V *RhoA* can induce transcriptional changes in neoplastic cells causing the establishment of the follicular helper T, exclusive aspects of AITL. In other PTCLs subtypes like Adult T-cell leukemia/lymphoma (ATLL) the effect of *RHOA* mutations in terms of loss or gain of function is diversified and context-specific. For example, in ATLL, HTLV-1 infection can prompt normal T cells to acquire either gain or loss of function mutations of *RHOA* that in turn guarantee different cells behavior in which T-reg and T-memory phenotypes co-exist[110]**.** Deeply characterizing RhoA protein should help to better understand its oncogenic role in PTCLs. As Rho-GTPases regulate dynamic changes and fast cytoskeleton re-organization through actin-microtubule dependent and independent activities, they can control transcription and drive cell cycle entry and progression[112]. After TCR-activation, Rac1 stimulates the creation of a new actin nucleation core by promoting the assembly of the molecular machinery required for actin polymerization. Through its effector p21-activated kinases (PAK), Rac1 regulates microtubules stabilization to balance the force of the mitotic spindle[113]. Furthermore, Rac1 is able to activate many transcriptional factors such as STATs, c-Jun, activator protein 1 (AP1), Nuclear factor kappa-light-chain-gene enhancer of activated B cells (NF-kB), and ETS-like transcriptional factor (ELK), that are required for T-cell proliferation and clonal expansion[114,115]. In PTCLs, Rac1 plays a key role in the ALK$^+$ALCL subtype where it is often hyperactivated and involved in the oncogenic program driven by NMP-ALK signaling[116,117]. Indeed, in the ALK$^+$ALCL subtype, NPM-ALK fusion protein affects Rac1 and Cdc42 activation and re-localization leading to the phosphorylation and activation of p21-activated kinase2 (Pak2) causing F-actin polarization[117,118]**.** In ALK$^+$ALCL, *CDC42*, and *RAC1* loss of function both in vitro and in vivo results in the impairment/loss of F-actin polarization and in the formation of round shape cells that are unable to disseminate suggesting that *RAC1* and *CDC42* cooperate in the regulation of cell morphology[38,117]. It is reported that NPM-ALK fusion protein affects also RhoA activity but

with an opposite mechanism of action. Indeed, one study demonstrated that NPM-ALK interacts and inhibits RhoA in a kinase-dependent manner[119], presumably to regulate cytoskeleton tension and cell morphology. These results highlight that the active regulation of NPM-ALK on cell shape and cytoskeleton dynamics/rearrangements is a fundamental part of the oncogenic program induced by these genetic defects in T-cells **(Figure 14).**
In mantle T cell lymphoma *RAC1* is overexpressed and correlates with poor prognosis and patient's overall survival, while in *p53*-deficient lymphoma cells its overexpression reduces cell proliferation[120]. The control of Rho-GTPases state and mechanism of action is a complex and tightly regulated process in which GEFs play an essential role and due to their activating functions, are considered as pro-oncogenic proteins[121]. In PTCLs, GEFs like *T Cell Lymphoma Invasion And Metastasis 1 (TIAM1)* and *VAV1* are emerging as drivers of T cell transformation[122]. Tiam-1 is a highly conserved protein[123] which activates and connects Rac1, Cdc42 and in a less extent RhoA promoting actin nucleation and branching[124], chemokine-induced polarization, and chemotaxis of T cells[125,126]. Recently, Tiam-1/Rac1 complex has been found to support Th17 differentiation program by the direct interaction and recruitment of transcriptional factor ROR$_{\gamma}$t on Il17 promoter[127]. Tiam-1 protein has been discovered as overexpressed in PTCLs, where it fosters T neoplastic cell infiltration into fibroblast monolayers[122]. Instead, in ATLL, the activation of Tiam-1/ Rac1 axis promotes the formation of lamellipodia sustaining the adhesion to stromal cells and tumor infiltration[128]. In chronic lymphoblastic leukemia, the overexpression of Tiam1-Rac1 axis guarantees cell cycle entry and neoplastic cell proliferation by activating c-Myc and cyclin D[129,130]. Similar to TIAM-1, Vav1 is a GEFs crucial for T cell proliferation[131], for cytokine production, and also for the accumulation of F-actin at immunological sinapses[132].

VAV1 is aberrantly expressed in many cancers[133]. *VAV1* deficient patients and *VAV1* loss of function murine models of lymphomas show alterations in F-actin accumulation, F-actin reorganization in response to TCR/CD28 co-engagement, and reveal defects of T cell selection in the thymus[134–136]. Gain of function mutations and fusions, such as *VAV1-THAP4, VAV1-MYO1F*, and *VAV1-S100A7* have been found in adult T cell leukemia[137] and PTCLs with dismal overall survival and results in a constitutively active conformation of Vav1 and a consequent transcriptional increase of chemokines[138]. As mentioned above, also Vav1-dependent RhoA activation is fundamental to modulate TCR signaling cascade[135,] and *VAV1* and *RHOA* mutations were found to be mutually exclusive in AITL. Both lead to enhanced TCR signaling, suggesting that this activation is critical for T-lymphomagenesis as already described for BCR in B-lymphomagenesis[139,140].

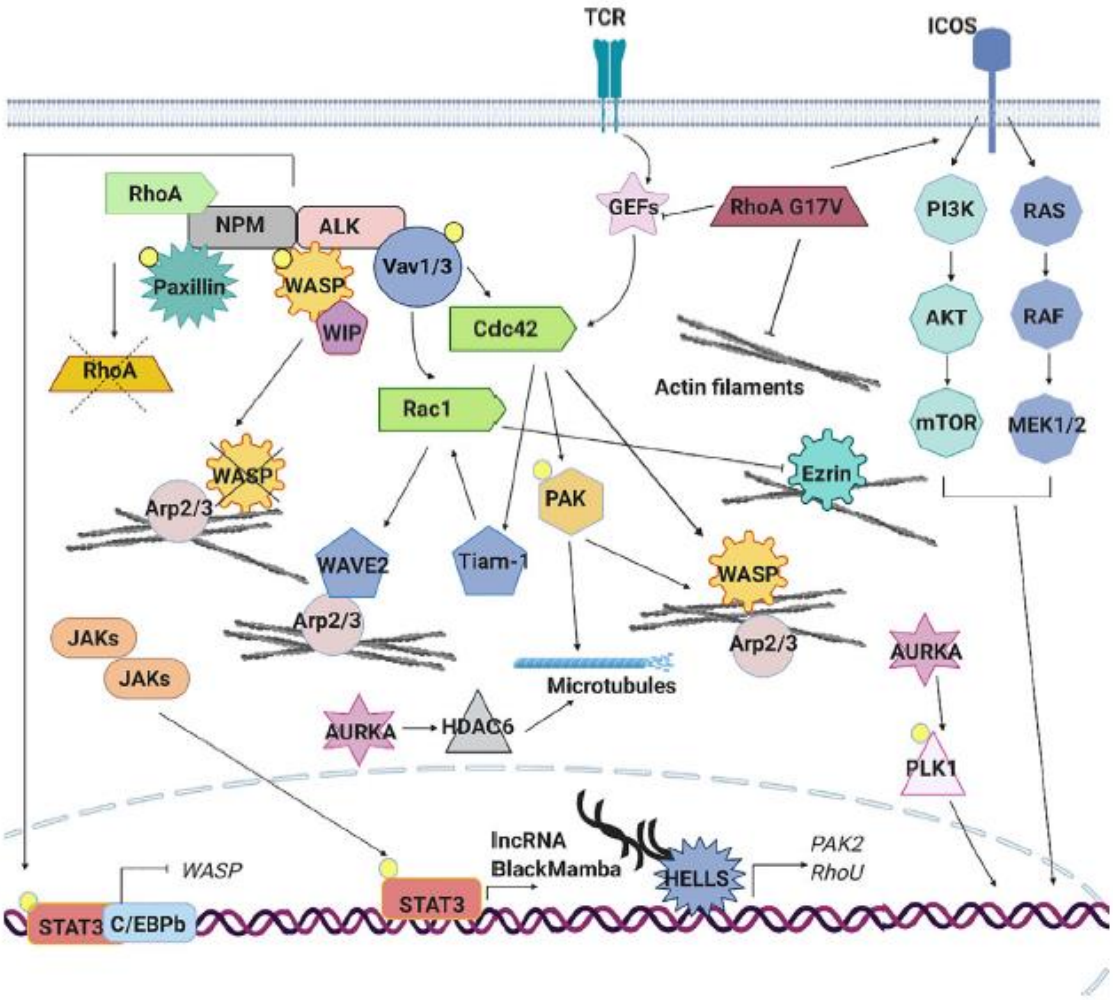

Figure 14. Signaling pathways aberrantly expressed in PTCLs. The aberrant cytoskeleton dynamics and regulation in PTCLs is sustained by several mechanisms. TCR signaling pathway is often constitutively active in PTCLs leading to an aberrant RhoGTPase signaling cascade and downstream effects. In anaplastic large cell lymphoma (ALCL), the nucleophosmin (NPM)–anaplastic lymphoma kinase (ALK) fusion hyperactivates Rac1 and Cdc42 leading to the constitutive activation of downstream effectors (PAK, Tiam1, WAVE, and N-WASP), to the increase of F-actin nucleation, polymerization and an altered microtubules dynamic. ALK fusion proteins can directly phosphorylate signal transducer and activator of transcription (STAT3) leading to its localization into the nucleus where, in association with C/EBPB, repress the expression of *WASP*. Moreover, NPM-ALK directly inhibits RhoA to regulate cytoskeleton tension and directly phosphorylates WASP to promote its proteasome-dependent degradation. In the ALK-ALCL subtype, activating mutations affecting cytokine receptors, Janus kinases (JAKs), and STAT3 lead to the constitutive activation of this pathway. The aberrant transcription of lncRNA *BlackMamba*, of *DNA helicase HELLS* and a set of genes regulating cytoskeleton architecture (*PAK2, RHOU*) leads to a reduction in the amount of F-actin. Mutations in the gene encoding *RHOA* (G17V) are detected in a subset of angioimmunoblastic T cell lymphoma (AITL), peripheral T cell lymphoma (PTCL)-NOS, and in adult T cell leukemia (ATLL). This mutation contributes to cellular transformation preventing the activation of wild-type *RHOA*, enhancing the expression of co-stimulatory molecules (ICOS), which in turn contributes to increased PI3K and MAPK signaling and by reducing the formation of stress fibers. Mutations in the gene encoding *VAV1* are found in ATLL, in PTCL-NOS, and AITL. These mutations lead to the hyperactivation of RhoGTPAses and their downstream targets increasing F-actin nucleation and polymerization. *AURKA* is overexpressed in ALK+ and ALK− ALCLs, PTCLs-NOS, and cutaneous T-cell lymphomas (CTCLs). Its overexpression leads to hyperactivation of PLK1 and its downstream targets as well as to hyperactivation of HDAC6 and enhanced microtubules stability. *(Fragliasso V, Tameni A, Cytoskeleton Dynamics in Peripheral T Cell Lymphomas: An Intricate Network Sustaining Lymphomagenesis, Frontiers in Oncology,2021, doi.org/10.3389/fonc.2021.643620).*

4. PRELIMINARY RESULTS

In collaboration with Weill Cornell Medicine (Dr. Inghirami, Head of Pathology unit and Dr. Elemento, Head of Cancer System Biology Lab), we investigated the role of the non-coding genome in ALCLs patients[141]. To do this, we performed high coverage and directional RNA sequencing of 21 ALK$^+$ALCL and 16 ALK$^-$ALCL primary samples, normal T-lymphocytes, corresponding to different stages of differentiation, and 10 ALCL cell lines (4 ALK$^+$ALCL and 6 ALK$^-$ALCL) **(Fig 15a).** Once confirmed the appropriateness of pathological samples, we performed de novo transcriptome analysis of the aligned primary tumor[142], which identified 106,014 new transcripts. Applying filtering cutoffs based on transcript length, exon count, and coding potential (based on cross-species comparisons), we discovered 1,208 previously unknown ALCL-specific lncRNAs **(Fig. 15b).** These lncRNAs showed transcript length >200 bp (a canonical lncRNAs feature), a stringent number of exons n = 2 for conserved spliced transcripts **(Fig. 15c, d),** and they displayed low coding potential compared to canonical coding RNAs **(Fig. 15e).** Next, we identified a set of lncRNAs significantly overexpressed in ALCL samples compared with normal T-lymphocytes (352/1,208) by unsupervised analysis **(Fig. 15f).** We also discovered that a part of them was differentially expressed by comparing ALK$^+$ALCL with ALK$^-$ALCL samples (24/1,208). As a result of the intersection of this data, we obtained 18 previously unknown lncRNAs associated with ALCL. Then, we restricted the analysis to lncRNAs expressed in at least 20% of ALCL samples (five or more samples) and this analysis led to the discovery of a pool of 14 lncRNAs (FDR < 0.05) **(Fig. 15g).** Since the deregulated STAT3 signaling is oncogenic in ALCL[18,143], we then searched for canonical STAT3 binding sites within putative promoter regions of these previously unknown lncRNAs **(Fig. 15g).** We identified the lncRNA *XLOC_043524*, which we named *BlackMamba*. *BlackMamba* is an intergenic lncRNA located on q26.3 of chromosome 10, predicted to be transcribed from the minus strand, with an estimated transcript length of 70,292 bp **(Fig. 15h)**. Inside of the discovery cohort, 9/ 16 ALK$^-$ALCL (56%) and 1/21 ALK$^+$ALCL (4.7%) expressed detectable levels of *BlackMamba*. The preferential expression of *BlackMamba* in ALK$^-$ALCL patient's samples was further confirmed in an independent cohort of 15 ALCLs and 9 PTCLs **(Fig. 15i).** Next, we evaluated *BlackMamba* expression in a panel of T-cell lines and we confirmed that its expression was consistently detectable in ALK$^-$ALCL and breast implanted associated (BIA)-ALCL cell lines. Low levels of expression were detected in ALK$^+$ALCL (L82 and Karpas299) in systemic and cutaneous ALK$^-$ALCL (FEPD, Mac1), and cutaneous T-cell lymphoma MJ, while in T-ALL lines (CUTLL1, KOPT-K1, and Jurkat), and mycosis fungoides, HUTL-78 cells were absent **(Fig. 15j).**

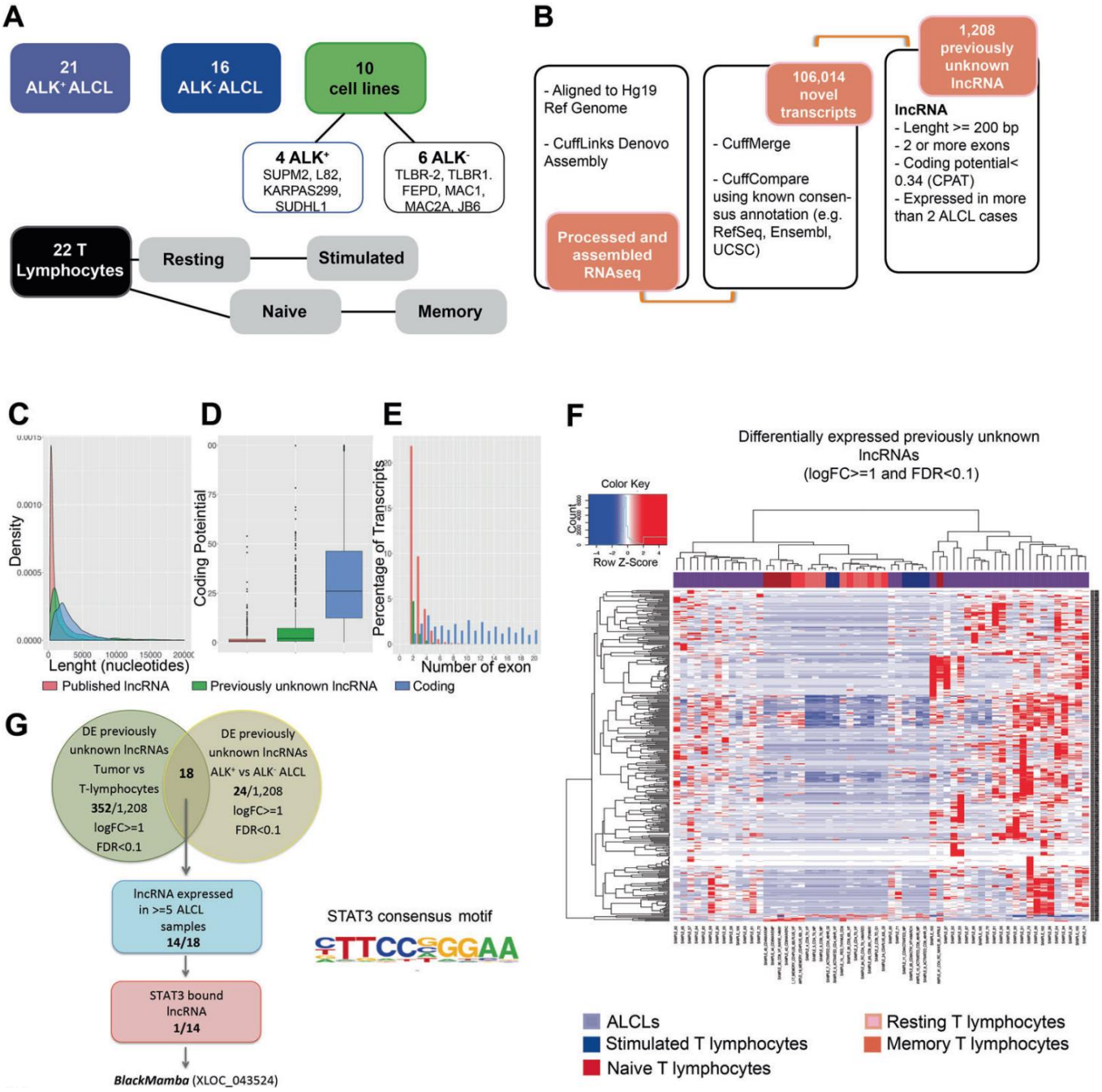
A
21 ALK+ ALCL
16 ALK- ALCL
10 cell lines
4 ALK+ SUPM2, L82, KARPAS299, SUDHL1
6 ALK- TLBR-2, TLBR1. FEPD, MAC1, MAC2A, JB6
22 T Lymphocytes
Resting
Stimulated
Naive
Memory
B
- Aligned to Hg19 Ref Genome
- CuffLinks Denovo Assembly
Processed and assembled RNAseq
106,014 novel transcripts
- CuffMerge
- CuffCompare using known consensus annotation (e.g. RefSeq, Ensembl, UCSC)
1,208 previously unknown lncRNA
lncRNA
- Lenght >= 200 bp
- 2 or more exons
- Coding potential< 0.34 (CPAT)
- Expressed in more than 2 ALCL cases
C
Density
Lenght (nucleotides)
D
Coding Poteintial
E
Percentage of Transcripts
Number of exon
Published lncRNA
Previously unknown lncRNA
Coding
F
Differentially expressed previously unknown lncRNAs
(logFC>=1 and FDR<0.1)
Color Key
Count
Row Z-Score
ALCLs
Stimulated T lymphocytes
Naive T lymphocytes
Resting T lymphocytes
Memory T lymphocytes
G
DE previously unknown lncRNAs Tumor vs T-lymphocytes 352/1,208 logFC>=1 FDR<0.1
18
DE previously unknown lncRNAs ALK+ vs ALK- ALCL 24/1,208 logFC>=1 FDR<0.1
lncRNA expressed in >=5 ALCL samples 14/18
STAT3 bound lncRNA 1/14
BlackMamba (XLOC_043524)
STAT3 consensus motif

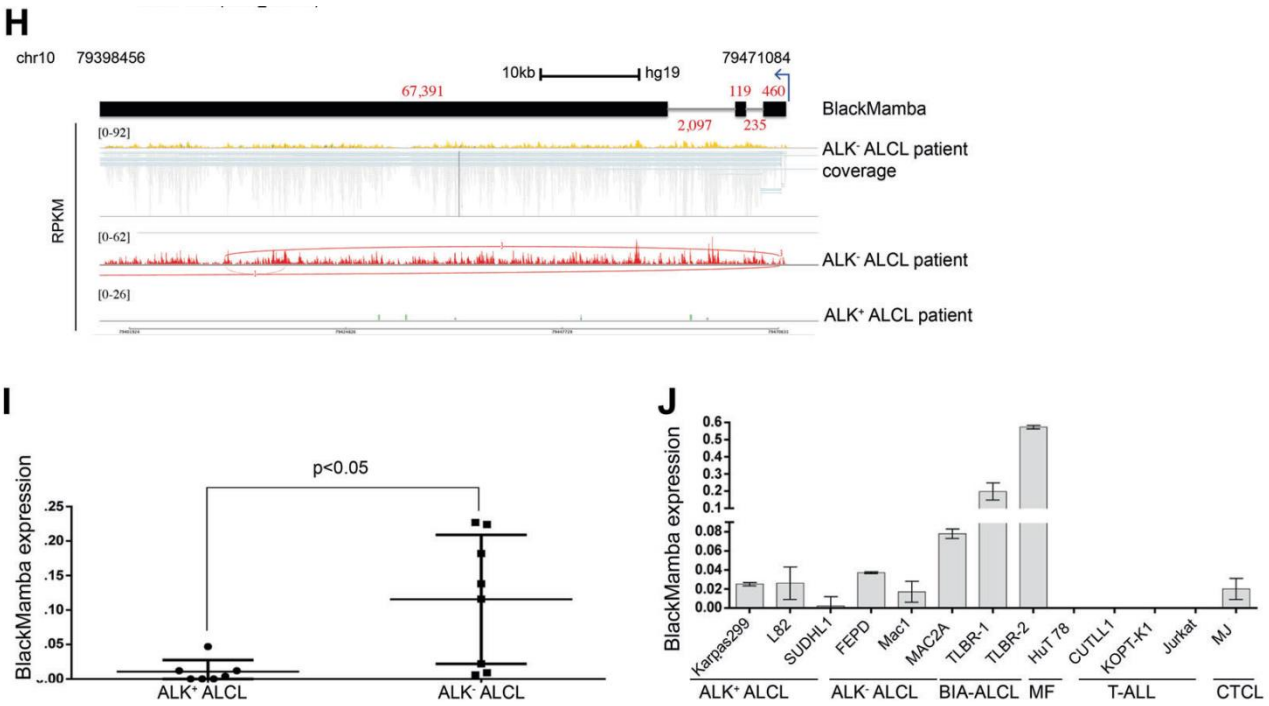

Figure 15. ALCL samples expressed a restricted set of aberrantly activated previously unknown lncRNAs. (a) Schematic representation of human samples used to perform directional RNA sequencing. (**b)** Bioinformatic pipeline for the discovery of previously unknown lncRNAs. **(c)** Density plot for transcript length shows shared pattern between previously unknown and known lncRNAs compared with protein-coding genes, which are much longer. **(d)** Coding Potential Score obtained from GENE ID shows that previously unknown lncRNAs and known lncRNAs have comparable and lower average coding potential than do protein-coding genes. **(e)** Comparing previously unknown lncRNAs against all transcripts with at least two or more exons shows a greater number of exons for the protein-coding genes. **(f)** Unsupervised analysis of previously unknown lncRNAs profile across normal T-cell lymphocytes and ALCL primary samples**. (g)** Flowchart for the discovery of *BlackMamba* in ALK− ALCL samples. **(h)** Schematic representation of locus, structure, and aligned reads of *BlackMamba.* Numbers represent the length (bp) of exons and introns (gray). Sashimi plots of representative ALK− and ALK+ ALCL samples were generated by Integrative Genomics Viewer software. The genomic coordinates are measured along the horizontal axis and the RPKM (Reads Per Kilobase per Million mapped reads) values up the vertical axis. qRT-PCR analysis of *BlackMamba* in a validation set of ALCLs samples **(i)** and a panel of cell lines **(j).**

Since STAT3 signaling is deregulated and hyper-activated also in the ALK+ALCL system, we wondered if, in L82 and Karpas299 that are ALK+ cell lines, STAT3 could regulate *BlackMamba* expression. To test this hypothesis and to explain why *BlackMamba* is not upregulated in ALK+ALCL cells, we used Crizotinib, a selective ALK inhibitor, and after 6 hours of treatment, we observed that *BlackMamba* expression was significantly downregulated in the examined cell lines **(Figure 16).** This data confirmed that STAT3 can regulate *BlackMamba* expression also in ALK+ALCL but it also suggests that additional transcriptional factors contribute to the transcriptional regulation of *BlackMamba*.

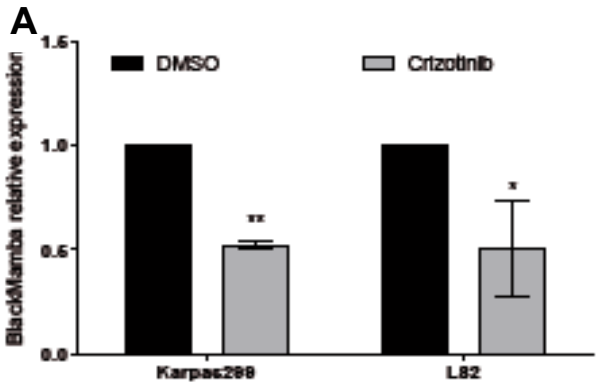

Figure 16. (a) qRT-PCR shows *BlackMamba* expression in ALK+ALCL cell lines after 6 hours of crizotinib treatment. The values represent mean ± SEM (n = 3) *p < 0.05; **p < 0.01.

BlackMamba is necessary for the proliferation and clonogenicity of ALK⁻ALCL cells

To characterize *BlackMamba* biological functions, we firstly silenced its expression by using two independent doxycycline (DOX) inducible shRNA and verified that its level of expression was significantly reduced after DOX induction. Both shRNA#2 and #6 could effectively knockdown (KD) the lncRNA in TLBR-2 and in MAC2A, although with different efficiency (−30%, shRNA#2 and −60%, shRNA#6 for TLBR-2, -50% for both shRNA #2 and #6 in MAC2A respectively) **(Fig. 17a).** Next, by performing cell fractioning and qRT-PCR analysis, we evaluated *BlackMamba* cellular localization showing that it is a chromatin-associated lncRNA **(Fig. 17b).** Then, we demonstrated that the loss of *BlackMamba* led to a reduction of cell proliferation **(Fig. 17c)** and delayed cell division **(Fig. 17d).** We also showed that *BlackMamba* functional KD led to a strong reduction of ALK⁻ALCL cells colony-forming ability **(Fig. 17e)**. Next, by using May–Grunwald Giemsa staining, we performed a cytological inspection of ALK⁻ALCL cells upon *BlackMamba* KD and showed an increased number of multi-nucleated cells **(Fig. 17f),** with a polyploid DNA content by partial FISH-based karyotyping **(Fig. 17g).**

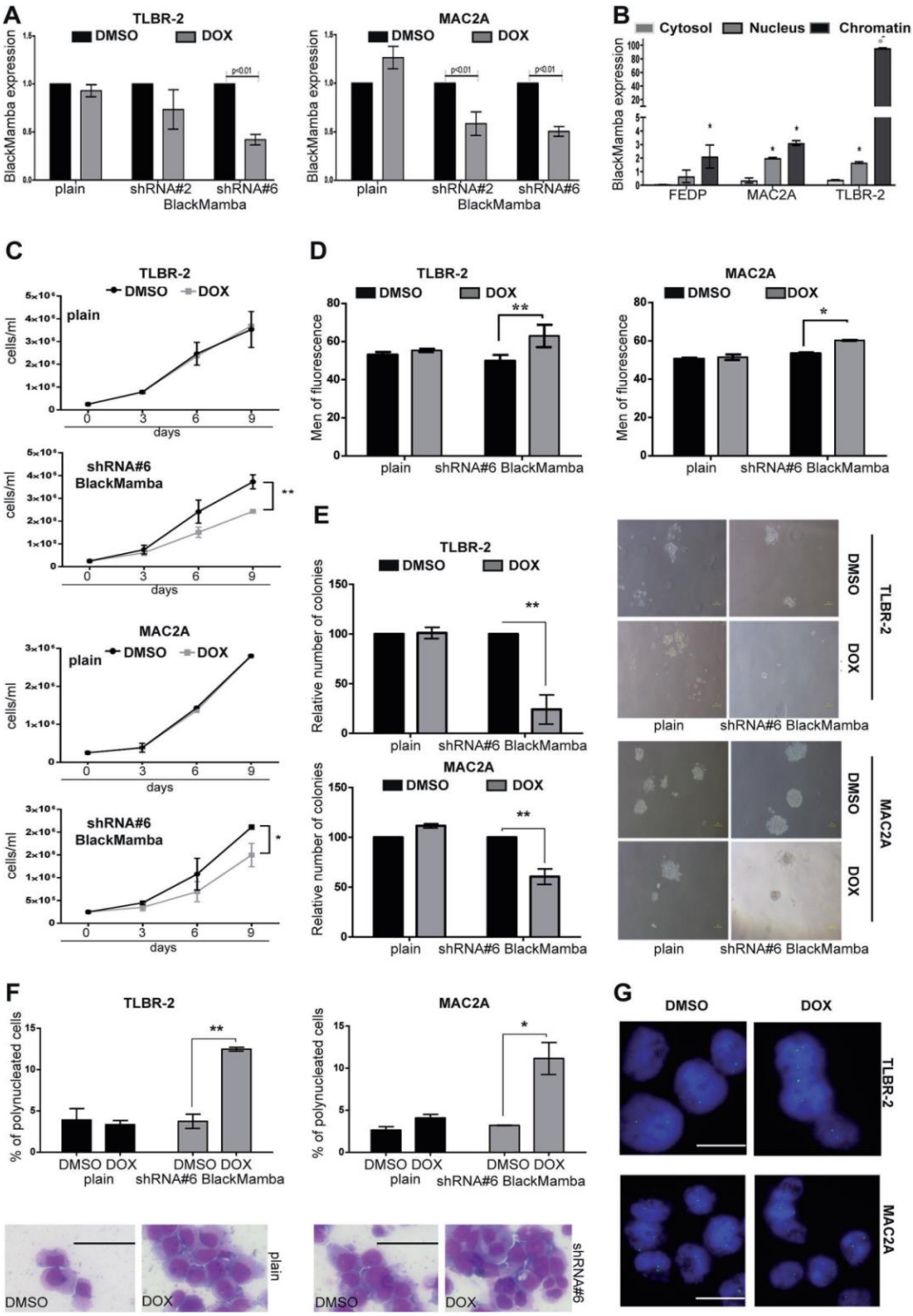

Figure 17. Loss of *BlackMamba* leads to impaired cell proliferation and clonogenicity of ALK⁻ALCL cells. **(a)** qRT-PCR analysis of BlackMamba expression after 6 days of doxycycline treatment in MAC2A and TLBR-2 cells. **(b)** Relative expression of *BlackMamba* in the cytoplasm, nucleus, and chromatin fraction of ALK− ALCL cell lines (average of three independent experiments ± S.D.) One-tailed t-test. *p ≤ 0.05. **(c)** Growth curve of MAC2A and TLBR-2 expressing pLKO-shRNA *BlackMamba* after induction with doxycycline. Each data point represents the mean ± S.D. (n = 3). One-tailed t-test. *p ≤ 0.05; **p ≤ 0.01. **(d)** The histograms show the fluorescent intensity of CFSE labeled TLBR-2 and MAC2A expressing pLKO-shRNA *BlackMamba* (9 days of treatment). Each data point represents the mean ± S.D. (n =3). One-tailed t-test. *p ≤ 0.05; **p ≤ 0.01. **(e)** Histogram shows methylcellulose colony formation of pLKO-shRNAs *BlackMamba* expressing cells pretreated with doxycycline for 6 days. Colonies were counted on day 10, after plating. Each data point represents the mean ± S.D. (n = 3). **(f)** The upper panel shows the percentage of polynucleated cells in at least 100 cells stained with May–Grunwald Giemsa (6 days after doxycycline induction). Each data point

represents the mean ± S.D. (n = 3). *p ≤ 0.05; **p ≤ 0.01. The lower panel shows the polynucleated cells in TLBR-2. The scale bar represents 100 µm. **(g)** FISH analysis of chromosome 17 centromere in pLKO-shRNAs *BlackMamba* expressing TLBR-2 and MAC2A cells (6 days of doxycycline induction). The scale bar represents 10 µm.

BlackMamba* regulates the transcription of the *DNA helicase HELLS

Having observed a multi-nucleated phenotype, we hypothesized that *BlackMamba* loss could be associated with cytoskeleton rearrangements and cytokinesis defects because an appropriate and complete cytokinesis requires an optimal cytoskeleton organization. By using immunofluorescence staining (phalloidin) we evaluated cytoskeleton architecture and F-actin organization in *BlackMamba* KD cell lines and showed that upon *BlackMamba* KD, cells lose actin polarization with actin filaments displacement from their membrane localization, supporting a role of BlackMamba in regulating cytoskeleton organization and cytokinesis **(Fig. 18a).** RNA sequencing analysis in TLBR-2 *BlackMamba* KD cell line highlighted that 59 genes were downregulated and 61 significantly upregulated genes (≥ 2-fold and FDR < 0.05) **(Fig. 18b)**. Concordantly with the observed phenotype, Gene ontology analysis of *BlackMamba*-target genes revealed the enrichment of several categories including actin cytoskeleton regulation, integrin-mediated cell adhesion, and focal adhesion genes (*i.e., RGS1, CCL22, CCL17, PAK2, RHOU*) **(Fig. 18c).** Next, we validated these genes in a separate set of experiments and confirmed that loss of *BlackMamba* leads to their dramatic downregulation **(Fig. 18d)**, suggesting that this lncRNA is involved in the maintenance of cytoskeleton organization and thus in guaranteeing an appropriate completion of cytokinesis.

As chromatin-enriched lncRNAs are spatially correlated with transcription factors[144], can act as cell type-specific activators of proximal gene transcription[145] and influence local chromatin organization, we decided to correlate *BlackMamba* expression with transcriptional factors and chromatin-remodeling genes in ALCL samples. The lymphoid-specific helicase (LSH) *HELLS*, the SET domain-containing protein *PRDM13*, and the polycomb repressive complex 2 histone-lysine N-methyltransferase *EZH2* were found to be positively correlated with *BlackMamba*. Conversely, the homeobox protein *HHEX* showed a negative correlation **(Fig. 18e).** To test whether this association was directly linked to *BlackMamba* expression, we quantified the mRNA levels of *HELLS* and *HHEX* in inducible shRNA *BlackMamba* ALCL cells. *HELLS* expression was consistently downregulated upon *BlackMamba* silencing, while *HHEX* was upregulated **(Fig. 18)**. In agreement with the opposite expression changes of *HELLS* and *HHEX* mRNA, H3K4me3 and H3K27me3 underwent chromatin

reorganization, with a significant reduction of H3K4me3 binding on *HELLS* promoter and a parallel loss of H3K27Me3 on *HHEX* promoter after *BlackMamba* silencing **(Fig. 18g).**

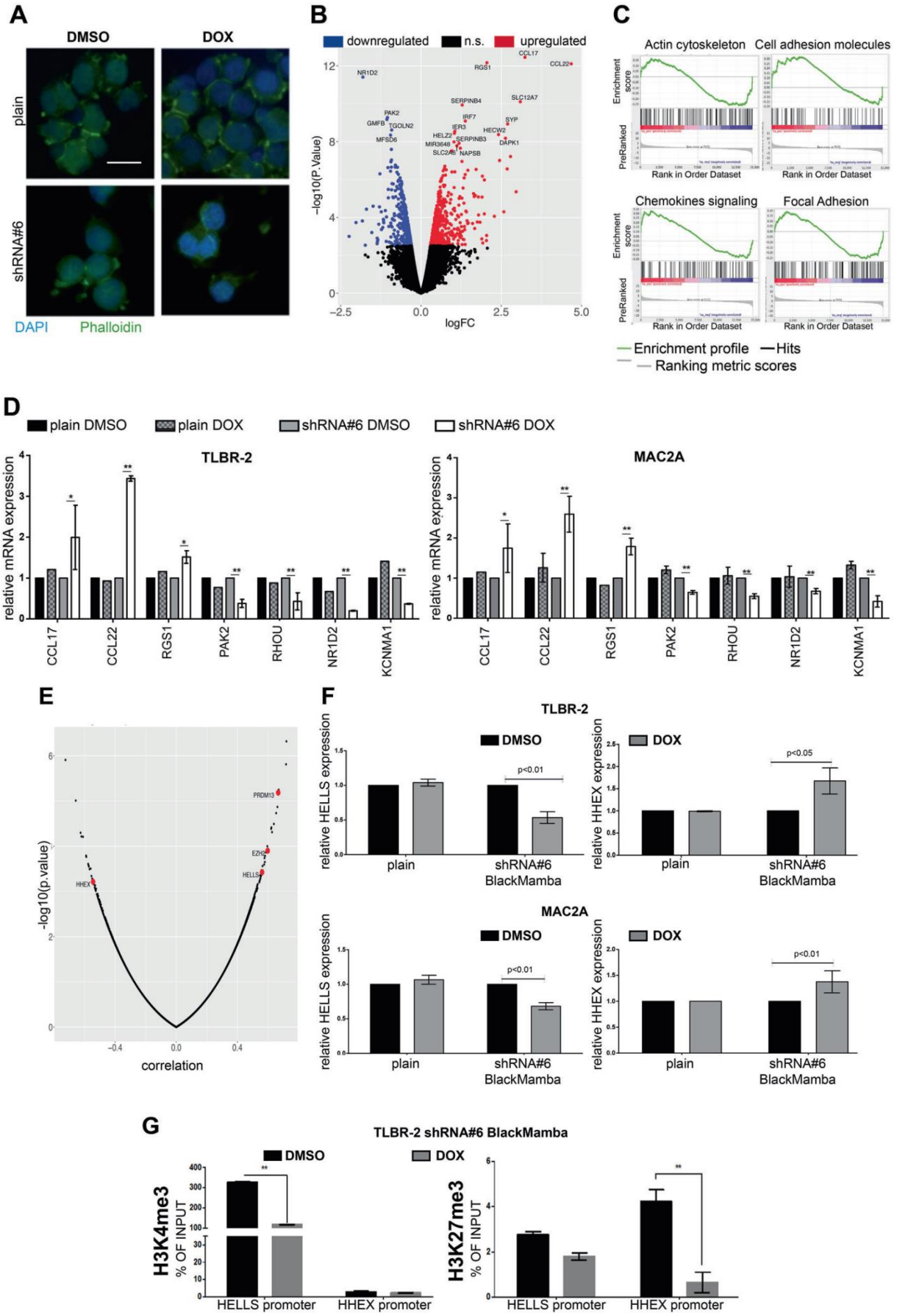

Figure 18. *BlackMamba* regulates the lymphoid-specific helicase *HELLS*. (a) Immunofluorescence images of TLBR-2 expressing pLKO-shRNA#6 *BlackMamba* stained with antiphalloidin antibody after doxycycline treatment (6 days). The scale bar represents 10 µm. **(b)** Volcano plot analysis of TLBR-2 expressing pLKO-shRNAs#6 *BlackMamba* after 6 days of doxycycline induction**. (c)** GSEA analyses of downregulated and upregulated pathways in TLBR-2 expressing pLKO-shRNA#6 *BlackMamba*. **(d)** qRT-PCR analysis of a panel of genes in MAC2a and TLBR-2 expressing pLKO-shRNA#6 *BlackMamba* after 6 days of doxycycline induction. **(e)** Graph shows the expression correlation between *BlackMamba* and protein-coding genes in ALK− ALCL samples. *PRDM13, HELLS, and EZH2* showed significant positive co-regulation while *HHEX* showed a negative coregulation. **(f)** qRT-PCR analysis of *HELLS* (6 days after doxycycline induction) and *HHEX* (9 days after doxycycline induction) expression in ALK− ALCL cell lines. Each data point represents the mean ± S.D. (n = 3). One-tailed t-test. *p ≤ 0.05; **p ≤ 0.01**. (g)** ChIP qRT-PCR detection of H3K4me3 and H3K27me3 antibodies on *HELLS* and *HHEX* promoters in TLBR-2 expressing pLKO-shRNA#6 *Black-Mamba* (6 days after doxycycline induction). The experiment was representative of a triplicate. The bars represent the mean ± SEM (n =3). **p ≤ 0.01.

5. AIM OF THE PROJECT

ALCLs are a group of heterogeneous and aggressive non Hodking T-lymphomas that arise from the transformation of mature T-cells. ALCL subtypes can be characterized by specific driving mutations for the ALK^{+}ALCL (*i.e* NPM-ALK) or different massive genomic rearrangements for the ALK^{-}ALCL subtype (*i.e DUSP22-IRF4, TP63, TP53, Blimp* loss/translocations*, JAK1* and/or *STAT3* activating mutations). Due to the lack of knowledge, the absence of biomarkers and therapeutic strategies for the ALK^{-}ALCL subtype, we dissected the molecular mechanism underlying this neoplasm by investigating the functional interplay between coding and noncoding genome. Indeed, the discovery of new key mediators of ALK^{-}ALCL oncogenic features is essential to provide a new druggable target for the design of new small molecules and targeted therapies. Recently, we discovered and characterized the novel lncRNA *BlackMamba* and demonstrated that its functional loss in ALK^{-}ALCL cell lines leads to a strong reduction of cell proliferation and clonogenicity, cytoskeleton rearrangements, and cytokinesis defects. Indeed, by performing RNA-sequencing analysis in *BlackMamba* silenced cell lines we showed a set of target genes primarily involved in cytoskeleton rearrangements, cytokinesis, and proliferation. Among these, the most interesting downstream targets that emerged was the DNA-helicase *HELLS*. HELLS is known to play an essential role in the development and survival of B and T-lymphocytes, also implicated in the maintenance of cancer genome stability by acting as an epigenetic modifier. The goal of my Ph.D. project was to characterize the molecular mechanism through which the *BlackMamba*-HELLS axis regulates ALK^{-}ALCL neoplastic features by pursuing two different aims:

I) to characterize the *BlackMamba*-HELLS-dependent gene expression program in ALK^{-} ALCL

II) To identify HELLS transcriptional partners that cooperate in the regulation of the ALK^{-} ALCL transcriptional gene program

6. MATERIALS AND METHODS

Cell culture and treatments

The human ALK⁻ALCL cell line MAC2A was a kind gift from Dr. Giorgio Inghirami. The human Breast Implanted Associated (BIA)-ALCL cell line TLBR-2 was a kind gift of Dr. Alain Epstein. Cell lines were authenticated. All cell lines were genotyped and routinely tested for Mycoplasma contamination. Cell lines were cultured in RPMI-1640 medium (Gibco) supplemented with 10% FBS at 37 °C in an atmosphere of 5% CO2. TLBR-2 cells are dependent from IL-2 and were supplemented with IL2 (20U/ml). For all the experiments cells were amplified and managed 3 times a week. Doxycycline was purchased from Sigma and dissolved in H2O.

Cell growth and cell division

For cell growth assays, cells were washed with phosphate-buffered saline, seeded at 2.5 × 105 cells/ml, and treated with 100 nM doxycycline. Viable cells were counted by trypan blue exclusion.

Transfection

HEK-293T cells were seeded at 1,5×10^6 cells/ml and transfected in a cell culture flask (T25) by using 3rd generation plasmids optimized concentrations:

Transfer plasmid (pLKO Tet-On-shRNA): 2.8 ug
pMD2g: 0.7ɥg
pRRE:1.75ɥg
pRSV-REV: 1.75ɥg
Optimem medium (Gibco): 600ɥl
Lipofectamine 2000:10ɥl

Plasmids and viral infections

pLKO Tet-On vectors expressing shRNAs against *HELLS* and lncRNA *BlackMamba* were generated by cloning synthetic double-stranded oligonucleotides (Broad Institute) into pLKO Tet-On vector (Addgene #21915). Vectors were packaged into lentiviral particles HEK 293T-cell line. Lentiviral particles were used for infection of low passages MAC2A or TLBR-2 at a multiplicity of infection (3 times, at 1400rpm, 7 min, 32°). Infected cells and control cells

(mock) were selected with 0.5 or1 µg/ml of puromycin (MAC2A and TLBR-2 respectively) for 3 days and *BlackMamba* or *HELLS* knockdown was assessed by quantitative qRT-PCR.

The list of shRNA is provided below:

shRNA#1 *HELLS*	GAATATGAAGTGCCGTCTAAT
shRNA#2 *HELLS*	GAACAAAGAAGTATCCATATT
ShRNA#6 *BlackMamba*	AGACAGATCTTGATAGAAATT
ShRNA#2 *BlackMamba*	GGACAAAACAGACGTAGAATT

pCDH-HELLS-HA-GFP was generated as follows: human *HELLS* was amplified by reverse transcription-PCR from TLBR-2 RNA with an upstream oligomer containing a 5′-flapping NheI site and a downstream oligomer containing a 3′-HA sequence and flapping NotI site. HELLS-HA PCR product was directionally cloned into the NheI-NotI-digested pCDH-GFP vector. The plasmid was DNA sequenced.

NheI_Hells_Fw	AATTGGCTAGCGCTAGCatgccagcggaacggcccg
NotI_Hells_HA_Rv	GCGGCCGCGCGGCCGCaaacaaaacattcaggactg

siRNA transfection

MAC2A and TLBR-2 cells were seeded at 1×10^6 cells/ml and were transfected with 30 nM siRNA concentration for single KD. SiRNA nucleofections/transfections were performed using the Cell Line Nucleofector Kit SF and Amaxa 4D Nucleofector (program DS-130 for TLBR-2, FI115 for MAC2A). Twenty-four hours after transfection, cells were harvested and plated 2.5 × 105 cells/ml. At forty hours were collected and analyzed for silencing efficiency. For siRNA scramble, we used 30nM a Silencer Select negative control no.1 (#4390843, Ambion, Life Technologies). For *PAK2* and *RHOA* we used a Silencer Select Validated siRNAs:

- siRNA *PAK2*: ID: s10022 (Ambion, Life Technologies).
- siRNA *RHOA*: ID: s759 (Ambion, Life Technologies).

For *RHOU* we used two different Silencer Selected Pre-designed (not validated) siRNAs:

- ID: 224502 (Ambion, Life Technologies).
- ID: s33826 (Ambion, Life Technologies).

For *YY1*, we used a Silencer Select Validated siRNAs: ID: s14958 (Ambion, Life Technologies).

RNA extraction and quantitative PCR (qRT-PCR)

Total RNA was extracted by TRIzol (Thermo Fisher Scientific) according to the manufacturer's instructions. Total RNA was also extracted by using Maxwell® RSC simply RNA Cells Kit. One microgram of total RNA was retrotranscribed using the iScript cDNA kit, (Biorad). The amplified transcript level of each specific gene was normalized on *CHMP2A*housekeeping. ΔΔCt quantification method was used for RT-qPCR analyses. The list of primers used is provided below:

qRTPCR	**FORWARD**	**REVERSE**
BlackMamba	TTGGAACTACTGCCGGTGTC	GTGCGAGGCTGTTTACCTCT
CHMP2A	ATGGACCTATTGTTCGGGCG	TCTCTAGTTTCTGTCGCTCGC
HELLS	AGCGGTTGTGAGGAGTTAGC	CATGCCTGGACACTCACCC
HHEX	CCCCCTGGGCAAACCTCTAC	TCGATGGTCTGGTCGTTGGA
PAK2	TGAGCAGAGCAAACGCAGTA	AGGGCCATAAGCTTTCCGTG
RHOU	GCCCCTCATCCTTCCAGAAC	GAGATCCGACTGCGTTCCAA
RGS1	TTGACTTCCGCACTCGAGAA	GCTTCATCAAAACACGTGGGG
CCL17	ACTTCAAGGGAGCCATTCCC	CCTGCCCTGCACAGTTACAA

CCL22	TTACGTCCGTTACCGTCTGC	GAAGGTTAGCAACACCACGC
CXCL10	TGCCATTCTGATTTGCTGCC	TGCAGGTACAGCGTACAGTT
KCNMA1	GGCACTCTCAAACCAGTGGA	CCTTCACGGAGGTCATCCAG
NR1D2	ATGCTGTTCGGTTTGGTCGT	AAGTGACCACTGAACTGGCT
RHOA	GGACTTAAGCGTCTGGCTC	AGTGCCACCCATGAGAACTG
ECT2	TTTTGAATCGGTTGTGGCGG	CTCTTCAAACGCCGACTCCT
PLK1	AGAAGACCCTGTGTGGGACT	ACCTCGAAACTGTGCCCTTT
ANLN	TCAGACCCAAAGGTTGAGCA	AGGACATCACTGAAGAGGTCA
AURKB	ATCAGCTGCGCAGAGAGATCGAAA	CTGCTCGTCAAATGTGCAGCTCTT
PRC1	AGCATCCTGAGTGGTGGGTA	AACTGTCAGAGAGGGACGGA
KIF23	TGGTGCAGAGTCTGAATGGAC	GCTTTTTGCGCTTGGGTTGT
KIF20A	AGTATCCCAGGAGGAGCAAGT	ATCGTCATCGGACAGCAAGC
KIF4A	AACCTTTGTTGGATGTGGGC	TGACTTAGCACCCTTCTGGAG
KLHL21	TTTGTCAGGGATGACTCCGC	CATGTACCTGATTCATGGACGG
PITPNM1	ACTACGCCAGAAGGCAATGT	ATAACCGGCCACGATGTTCA

CDC42SE2	GCGACGATAGGGCCAGATTT	TGCATACAGATGACCGCAGA
TFAP2A	ATATCCGTTCACGCCGATCC	CCTCGCAGTCCTCGTACTTG
E2F1	AGCTGGACCACCTGATGAAT	GAGGGGCTTTGATCACCATA
ETS1	TGGCCCCAGACTTTGTTGG	GCGGGATTCTGGATAGGCTG
ELK1	ATTACGACAAGCTCAGCCGG	TGTAGACGAACTTCTGGCCG
FOXP3	AACCTTCCAGGGCCGAGAT	ACCATGACTAGGGGCAGTGT
NFIC	ATGTATTCGTCCCCGCTCTG	TGAACCAGGTGTAGGCGAAG
SP1	GGTTCGCTTGCCTCGTCAG	TGATCTTGGTCGCTCATGGT
MYB	CTGGGAAGGGGACAGTCTGA	GCTGGTGCCATTAAAACGGA
C-MYC	TCAAGAGGCGAACACACAAC	GGCCTTTTCATTGTTTTC
KLF4	TCAACGATCTCCTGGACCTG	ATCGGATAGGTGAAGCTGCA
IL-6	CCAGAGCTGTCCAGATGAGT	GAGTTGTCATGTCCTGCAGC
YY1	CTGGAGGGCGAGTTCTCG	TCTGTTCTTCAACCACTGTCTCA

MLL1	ACCTGGAGGTAATGCTTTCAGT	ATTGCTCTGCCGCAGTTTTC
BMI-1	ATGCTGTTCGGTTTGGTCGT	AAGTGACCACTGAACTGGCT

RNA Immunoprecipitation

TLBR-2 cells were collected cells (15*10^6), centrifuged, washed in PBS 1X, and crosslinked in PBS 1X with fresh formaldehyde solution at 1% for 10 min.

Subsequently they were treated with 1.25 M glycine for 5 min and centrifuged at 1350g for 5 min at 4 °C. Cells were washed two times in PBS1X.

Cells were resuspended in PBS 1X (e.g., 10^7 cells in 2 mL PBS), 2ml of freshly prepared nuclear isolation buffer (1.28 M sucrose, 40 mM Tris-HCl pH 7.5, 20 mM MgCl2, 4% Triton X-100, 6 ml of water. Keep on ice for 20 min (with frequent mixing).

Nuclei were centrifuged at 2,500 g for 15 min. The nuclear pellet was resuspended in 1ml freshly prepared RIP buffer. Nuclei were resuspended into two fractions of 500 µL each (for mock and IP).

Nuclei were sonicated (2 cycles, 30 sec on/30 sec off); nuclear membrane and debris were centrifuged at 13,000 rpm for 10 min.

The precleared lysate was incubated with 6 µg of antibodies specific for HELLS (sc-46665, Santa Cruz Biotechnology, Inc.) or with IgG as a negative control for 2 hours at 4°C with gentle rotation.

A/G beads (40 µL) were added and the lysate with the antibody incubated for 1 h at 4ºC with gentle rotation.

Beads were centrifuged at 2,500 rpm for 30 s. The supernatant was removed and the beads were resuspended in 500 µL RIP buffer three times, followed by one wash in PBS1X.

Coprecipitated RNAs were isolated by resuspending in TRIzol RNA extraction reagent (500ɥl) according to the manufacturer's instructions.

RNA was eluted by using nuclease-free water (20 µL). Reverse transcribe DNAse treated RNA according to manufacturer instructions.

cDNA was analyzed by qRT-PCR.

All experiments were repeated at least three times.

The list of primers used is provided below:

RIP-primers	**FORWARD**	**REVERSE**
BlackMamba +438bp	AAGAGGCACCTAAGCTGATGAC	CACCCTCAGGTTCTCACCGT
BlackMamba +16885bp	TGACACACATTCAGAAAATTGCAC	AGTTACATGGATGTTGGCTTTTGA
BlackMamba +22482bp	TCTGCAGAGCTCCTCCATTTG	GTCTGGGGTTGGATGGCTAA
BlackMamba +33459 bp	TTGCCCTCTGCCTTTCTACG	ACACACCAGAATGCAGAGCA
BlackMamba +43126 bp	ACCAGGGATCTGCCAACCTA	GACTATACAGGAGCAGTGGCA
BlackMamba +54340 bp	TCCTCCCTTGATGTCTTTGCTC	TACAATGGCAGGTGGAGAAGG
BlackMamba +64710 bp	TTCTAGGCAGGGCATTGTGC	ACCTGCCTGCCAAGATACAA
BlackMamba +69715 bp	GATTCCCCTGGTGGTGTACG	GGCTCACCGTTCCCCATTTA

Chromatin Immunoprecipitation

MAC2A and TLBR-2 cells (30*10^6 of cells each IP) were collected, centrifuged, washed in PBS 1X, and crosslinked in PBS 1X with fresh formaldehyde solution at 1% for 10 min.

Subsequently they were treated with 1.25 M glycine for 5 min and centrifuged at 1350g for 5 min at 4 °C. Cells were washed two times in PBS1X.

Cells were lysed in LB1 (10mM Tris-HCl pH8; 85mN KCl; 0,5% NP40) supplemented with Protease Inhibitor Cocktail Tablets Complete, EDTA-free (Roche) for 10min at 4 °C.

Nuclei were pelleted at 1500g for 5 min at 4 °C and washed in LB2 (50 mM Tris-HCl pH 8.0, 10 mM EDTA, 10% SDS) supplemented protease inhibitors.

Nuclei were sonicated (15 cycles, 30 sec on/30 sec off) and cell debris were pelleted at 20000g for 10 min at 4 °C and a ChIP was set up in ChIP dilution buffer (0,01% SDS; 1% Triton; 1,2mM EDTA, 16.7 mM Tris-HCl pH8; 167nM NaCl) supplemented with protease inhibitors, Dynabeads® Protein G (Novex®), antibodies against HELLS (4ug, Rabbit Polyclonal, orb178580, Biorbyt), YY1 (D3D4Q, 1:100, Cell Signaling Technolgy), or IgG-isotype control (#66362, Cell Signaling Technology), left at 4 °C rocking overnight.

Then the beads were washed one time with Low salt wash buffer (20 mM Tris-HCl pH 8.0, 150 mM NaCl, 0.1% SDS, 2 mM EDTA, 1% Triton X-100) and one time with High salt wash buffer (20 mM Tris-HCl pH 8.0, 500 mM NaCl, 0.1% SDS, 2 mM EDTA, 1% Triton X-100). IPs were also washed one time with a LiCl solution (10 mM Tris-HCl pH 8.0, 250 mM LiCl, 1% NP-40, 1 mM EDTA) and two times with TE Buffer (50 mm Tris (pH 8.0). 10 mm EDTA).

Reverse crosslink was performed overnight at 65 °C with NaCl 5 M (Final concentration 0.2 M *NaCl*).

Samples were eluted by using 300ɥl of Elution Buffer (1%SDS/0.1M NaHCO3 pH8.0) and treated with 0.02 µg/µl RNase A (Sigma) for 2 h at 37 °C and with 0.04 µg/µl proteinase K (Sigma) for 1h at 45 °C. DNA was purified with QIAquick PCR Purification Kit (QIAGEN).

qRTPCR analysis was performed to evaluate. Values were normalized over the appropriate input control and reported in graphs as a relative fold on IgG.

The list of primers used is provided below:

ChIP promoters	**FORWARD**	**REVERSE**
***HELLS* promoter**	GTGAGGAGTTAGCTCGCGG	GCGCCCAAAAGGTTTTCCTC
***HHEX* promoter**	CTGGTCGCCAGTTAGGAAGG	CGGCTTATTTGTTAGGCCGC
***CCL22* promoter**	TCCTCTTCTCCACCCCACTC	TATAGCTGCCTGACCCCACT
***RGS1* promoter**	ACGTCACAGCACACCAAGAA	CGCTAGTCAACGTCTCTGCT
***KCNMA1* promoter**	TCAGCCCCCAGCTAACTACT	CCTTGAGGGCAGGAACTGAG
***PD5S4* promoter**	GAGACAGTGCCGCTCTCC	GTCCCGGACGGACACAAG
***KRAS* promoter**	GGAACGCATCGATAGCTCTG	GCCGCCTAGGAAAATCGAG
***MLL1* promoter**	TCGGGCTAACCCATCTTGTA	GGGAGAGCAGCTTCCAGTAT
***PAK2* promoter**	TGGCTGCTCCTCTCAATACAA	GCTGGGAGTAGTAGTTCGGTGA
***RHOU* promoter**	GTCACCCTCTTGGGAGCTG	GAGGACCTGGAACACACGTT
P4_BlackMamba	GGCGAGGTTGTAGCAGAGAA	CTGTCCCCAGAAAGCAGGAG
***RHOA* promoter**	ACAGCGACTTCGACTAAGCA	TGGGGTCTGTTTTGAGTGGA
***ANLN* promoter**	TCGGTGTTTCTGGGGCATATC	CACTCCTGAATGTGACAACGC

***ECT2* promoter**	CTTATCTCAGAGTGCGCCGT	GGCGGATGGCCTGGATTTAT
***PLK1* promoter**	GGAAAGAGTACCCAGCAAGGGAG	CAGAGCCAAGAAGCCCTTACCA
***AURKB* promoter**	CCCAACGGACCCTCTGATCT	GATTCAGTTGTTTGCGGGCG
***KIF20A* promoter**	CGAGGTGCCCTACTTTAGGC	CGGCATTTCTGAACGCGAAC
***KLHL21* promoter**	CACCCCGACAAAGGAGGTAG	AAACACTGCCGAGTCATGGT
***PITPNM1* promoter**	CAAGGCTGGGTTCATGGGAT	AGAGAGAAAGGGCACTGCTG
***CDC42SE2* promoter**	CCATCTTTCGGAGCGTCCTT	CGGGTTAGGAATTGGCCTCT
***KLF4* promoter**	ACTCACGTTATTCGGGGCAC	ATCTTTCTCCACGTTCGCGT
α-satellite	CATAGAGGCCTGTGGTGGAA	ACGATGACTCCCAAACTGCT

Co-Immunoprecipitation (Co-IP)

120*10^6 cells were collected, washed in PBS 1X, and crosslinked with 1% formaldehyde for 10 min, treated with 1.25M glycine for 5 min.

Cells were washed two times in PBS1X and resuspended in Buffer A (10mM HEPES pH 7.9, 1.5mM MgCl2, 10mM KCl, 0.5% NP-40) supplemented with protease inhibitor for 8 min in ice. After centrifugation at 3000 rpm for 2 min, the supernatant was collected as the cytoplasmic fraction and used as the quality control of the experiment.

The pellet was washed two times with BUFFER B (10mM HEPES pH7.9, 1.5mM MgCl2, 10mM KCl), centrifuged at 3000 rpm for 2 min, two times.

Nuclei were resuspended in lysis buffer (50mM Tris-HCl pH 7.4, 150mM NaCl, 1mM EDTA, 1% Triton X-100) supplemented with protease inhibitor and kept for 1 h in rotation at 4°C.

Nuclei extracts were sonicated 2 cycles (30 sec on/30 sec off) using a Bioruptor® Pico sonicator (Diagenode) and centrifuged at 16,000 g for 15 min.

Supernatant was kept and was quantified with Bradford. For each experiment, 4mg of nuclei extracts was used for immunoprecipitation and 150ɥg was kept as input control.

Protein A-Sepharose® CL-4B beads (GE Healthcare, Sigma Aldrich) were resuspended in demineralized water and washed 3 times at 500g/5min.

Precoating step was performed using Protein A-Sepharose® CL-4B beads (GE Healthcare, Sigma Aldrich), HELLS antibody (Rabbit Polyclonal, orb178580, Biorbyt).

Preclearing step was performed using total nuclear lysate and Protein A-Sepharose beads for aspecific removal for 1 h in rotation at 4°C.

After centrifugation at 500 g for 5 min, we combined the beads from precoating and supernatant from pre-clearing steps and kept in rotation overnight at 4°C.

After centrifugation of 500 g for 5 min, the supernatant was discarded and washed four times with TBS 1X (50mM Tris-HCl pH 7.4, 150mM NaCl). Laemmli Sample Buffer 4x (Biorad) was added to the immunoprecipitated samples and IPs were boiled for 20 min.

Co-IP was detected by western blot using the secondary antibody mouse anti-rabbit IgG HRP conjugate (L27A9) (#5127, 1:2000, Cell Signaling Technology).

Western Blot

3*10^6 cells were centrifuged for 5 min at 1,200 rpm, washed in PBS, lysed in 30 µl of Lysis Buffer (Promega), quantified by Bradford reagent (Biorad) and boiled at 100°C for 10 min. 25ug of proteins were loaded on 4-20% SDS-PAGE gel.

After blocking in 5% milk/TBST (TBST: 25 mM Tris-HCl, pH 7.4, 137 mM NaCl, 2.7 mM KCL, 0.1% Tween 20), membranes were stained with primary antibodies in 2.5% milk/TBST for 1h at room temperature and with horseradish peroxidase (HRP)–conjugated secondary antibodies at room temperature for 1 h.

The primary antibodies were diluted in 2% PBS/BSA and are: HELLS (Rabbit mAb#7998, 1:1000 Cell Signaling Technology), γ-PAK2 (E-9 Mouse mAb sc-373740, 1:1000 Santa Cruz Biotechnology, Inc), RHOA (26C4 Mouse mAb sc-418, 1:1000 Santa Cruz Biotechnology, Inc), RHOU (Rabbit, PA5-69128, 1:500 Invitrogen), YY1 (Rabbit, D3D4Q, 1:1000, Cell Signaling Technology), β-tubulin antibody (sc-23949, 1:100, Santa Cruz Biotechnology, Inc) and GAPDH (Rabbit mAb#2118, 1:2000, Cell Signaling Technology). All secondary antibodies (rabbit and mouse) were HRP-conjugated (GE Healthcare) and diluted 1:3000. Signals were detected by enhanced chemiluminescence and quantified by ImageJ software (National Institutes of Health).

Immunofluorescence

50.000 cells were spotted on glass slides using Cytospin (Thermo Scientific), fixed with 4% paraformaldehyde for 10 min, and permeabilized with 0.1% Triton X-100 for 3 min. Dots were blocked in 1% PBS-BSA solution for 1 hour at room temperature and incubated with phalloidin (Alexa Fluor® 488, Thermo Fisher) for actin staining for 50 min. Dots were washed in PBS three times and nuclei were stained with DAPI. For microtubules staining, we used the β-tubulin antibody (sc-23949, 1:100, Santa Cruz Biotechnology, Inc). As a secondary antibody we used Alexa Fluor® 555, Thermo Scientific). Immunofluorescences were detected with Nikon Eclipse (Ni) microscope using 60X.

Library preparation and RNA-sequencing

RNA seq libraries were obtained starting from 500 ng of total RNA following Illumina TruSeq Stranded TotalRNA preparation protocol. Sequencing was performed using Illumina NEXSeq high-output cartridge (double-stranded, reads length 75bp-2 ×75). A sequencing depth of at least 60 million reads for each sample was guaranteed. Sequencing quality was assessed using the FastQC v0.11.8 software (www.bioinformatics.babraham.ac.uk/

projects/fastqc/), showing on average a Phred score per base >34 in each sample. Raw sequences were then aligned to the human reference transcriptome (GRCh38, Gencode release 30) using STAR version 2.7[146] and gene abundances were estimated with RSEM algorithm (v1.3.1)[147]. Differential expression analysis was performed using DESeq2 R package[148], considering a False Discovery Rate (FDR) of 10% and excluding genes with low read counts. Heatmap representation and unsupervised hierarchical clustering with a complete linkage method were exploited to graphically depict differentially expressed genes (FRD < 0.1). Significant genes underwent enrichment analysis, performed on Gene Ontology biological processes, KEGG and Reactome pathways databases via enrichR package[149] using a significance threshold of 0.05 on p-value adjusted by Benjamini–Hochberg correction for multiple testing.

Transcriptional factors motif enrichment

For transcriptional factor motif search, JASPAR 2020 and PROMO (version 3.0.2) software tools were used. A motif similarity threshold of 80% and a dissimilarity level of 15% were respectively applied for JASPAR 2020 and PROMO prediction results. JASPAR and PROMO lists were merged to obtain the final results of this motif search prediction.

Statistical analysis

Statistical analyses were performed using the GraphPad Prism Software (GraphPad). Statistical significance was determined using Student's t-test. Each experiment was replicated multiple times (>3 up to 6).

7. RESULTS

BlackMamba physically interacts with HELLS to control the *BlackMamba*-dependent transcriptional program

To test whether HELLS can enforce *BlackMamba*-mediated transcription, we silenced its expression by specific shRNAs in our ALK$^-$ALCL cell lines (TLBR-2 and MAC2A). By qRT-PCR and WB analyses, we confirmed the effective silencing **(Fig. 19a, b and Fig.20a)** demonstrating the simultaneous downregulation of described target *BMI-1* and *MLL1* genes, used as a positive control **(Fig. 20b)**[152,153]. ALK-ALCL cell line MAC2A shows low levels of HELLS than BIA-ALCL cell line TLBR-2 in both RNA-seq and qRT-PCR validation experiments. This is in line with the observed *BlackMamba* basal expression level which is lower in MAC2A than in TLBR-2 **(reported in the preliminary results, Figure 15j).** This data is also in line with the less strong global phenotype observed in MAC2A after *HELLS* silencing. We demonstrated that loss of *HELLS* was associated with significant changes in the expression of *RGS1, CCL17, CCL22, PAK2*, and *KCNMA1*, mimicking the *BlackMamba* KD phenotype **(Fig. 19c)**. To functionally validate this interplay, we performed HELLS over-expression, by cloning *HELLS* in the constitutive pCDH vector. By using this method, we obtained an upregulation of 0.4-fold. Coherently with the modest upregulation obtained, the phenotype observed was not so striking. Despite this technical limitation, the overexpression of *HELLS* in *BlackMamba* KD TLBR-2 cells demonstrated that restored levels of this helicase rescued the *BlackMamba* phenotype, and recovered the baseline levels of these genes **(Fig. 19d, e)**. It is reported that lncRNAs can coordinate the binding of ribonucleoproteins, scaffolding molecules, and other effectors[154], and also that are key regulators of gene expression by recruiting chromatin remodeler complexes to regulatory regions, influencing and regulating chromatin accessibility[155]. Since the remodeling properties of HELLS can be mediated by the long noncoding *HOTAIR* [156], we argued that *BlackMamba* could interact with HELLS to mediate its recruitment to target genes and foster their expression. To test the physical interaction between *BlackMamba* and HELLS, we performed RNA immunoprecipitation experiments showing that HELLS binds *BlackMamba* at 3'-end of the lncRNA **(Fig. 19f)**. By using Chromatin Immunoprecipitation assays (ChIP), we proved that HELLS preferentially binds target genes promoters only in *BlackMamba* positive ALK$^-$ALCL cell lines independently from *HELLS* expression **(Fig. 19g, Fig. 20c).** Collectively, these results indicate that the *BlackMamba*-HELLS axis could be a part of a regulatory complex able to control the ALK$^-$ALCL oncogenic transcriptional program.

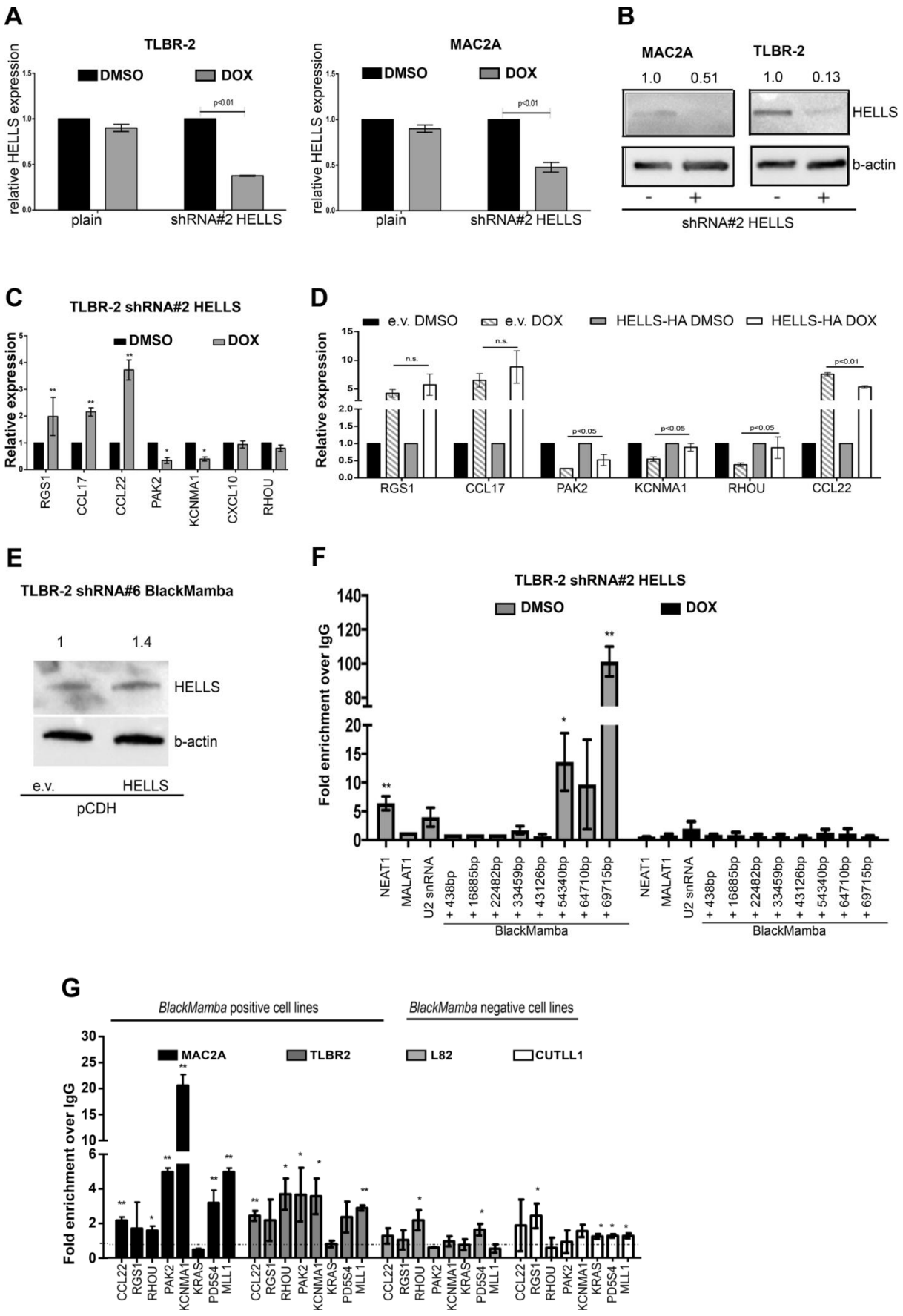
A
TLBR-2
DMSO
DOX
relative HELLS expression
p<0.01
plain
shRNA#2 HELLS
MAC2A
B
MAC2A
TLBR-2
1.0
0.51
1.0
0.13
HELLS
b-actin
shRNA#2 HELLS
C
TLBR-2 shRNA#2 HELLS
Relative expression
RGS1
CCL17
CCL22
PAK2
KCNMA1
CXCL10
RHOU
D
e.v. DMSO
e.v. DOX
HELLS-HA DMSO
HELLS-HA DOX
n.s.
p<0.05
p<0.01
E
TLBR-2 shRNA#6 BlackMamba
1
1.4
HELLS
b-actin
e.v.
pCDH
F
TLBR-2 shRNA#2 HELLS
Fold enrichment over IgG
NEAT1
MALAT1
U2 snRNA
+ 438bp
+ 16885bp
+ 22482bp
+ 33459bp
+ 43126bp
+ 54340bp
+ 64710bp
+ 69715bp
BlackMamba
G
BlackMamba positive cell lines
BlackMamba negative cell lines
MAC2A
TLBR2
L82
CUTLL1
CCL22
RGS1
RHOU
PAK2
KCNMA1
KRAS
PD5S4
MLL1

Figure 19. *BlackMamba* controls the recruitment of HELLS on target gene promoters. (a) qRT-PCR analysis of *HELLS* in ALK⁻ALCL cell lines expressing pLKO-shRNA#2 against *HELLS* (48 h after doxycycline induction). **(b)** Western blot shows the reduction of HELLS in cells expressing pLKO-shRNA#2 *HELLS* after 3 days of doxycycline induction. **(c)** qRT-PCR analysis of a panel of genes after 2 days of doxycycline induction in TLBR-2 expressing pLKO-shRNA# 2 *HELLS*. Each data point represents the mean ± SEM. (n = 3). *p ≤ 0.05; **p ≤ 0.01. **(d)** qRT-PCR analysis of TLBR-2 cells co-expressing shRNA#6 *BlackMamba* and pCDH-*HELLS*-HA vectors (6 days after doxycycline induction). **(e)** Western blot shows the overexpression of ectopic *HELLS*-HA in TLBR-2 overexpressing pLKO-shRNA# 6 *BlackMamba*. **(f)** RIP assay for HELLS in TLBR-2 expressing pLKO-shRNA#2 *HELLS* (2 days). Fold enrichment is relative to IgG (average of six independent experiments ±SEM; *p ≤ 0.05; **p ≤ 0.01). **(g)** ChIP qRT-PCR detection of HELLS antibody on several *BlackMamba* target gene promoters in a panel of T-cell lymphoma lines. *MLL1, PD5S4* were used as positive controls (average of six independent experiments ± SEM; *p ≤ 0.05; **p ≤ 0.01).

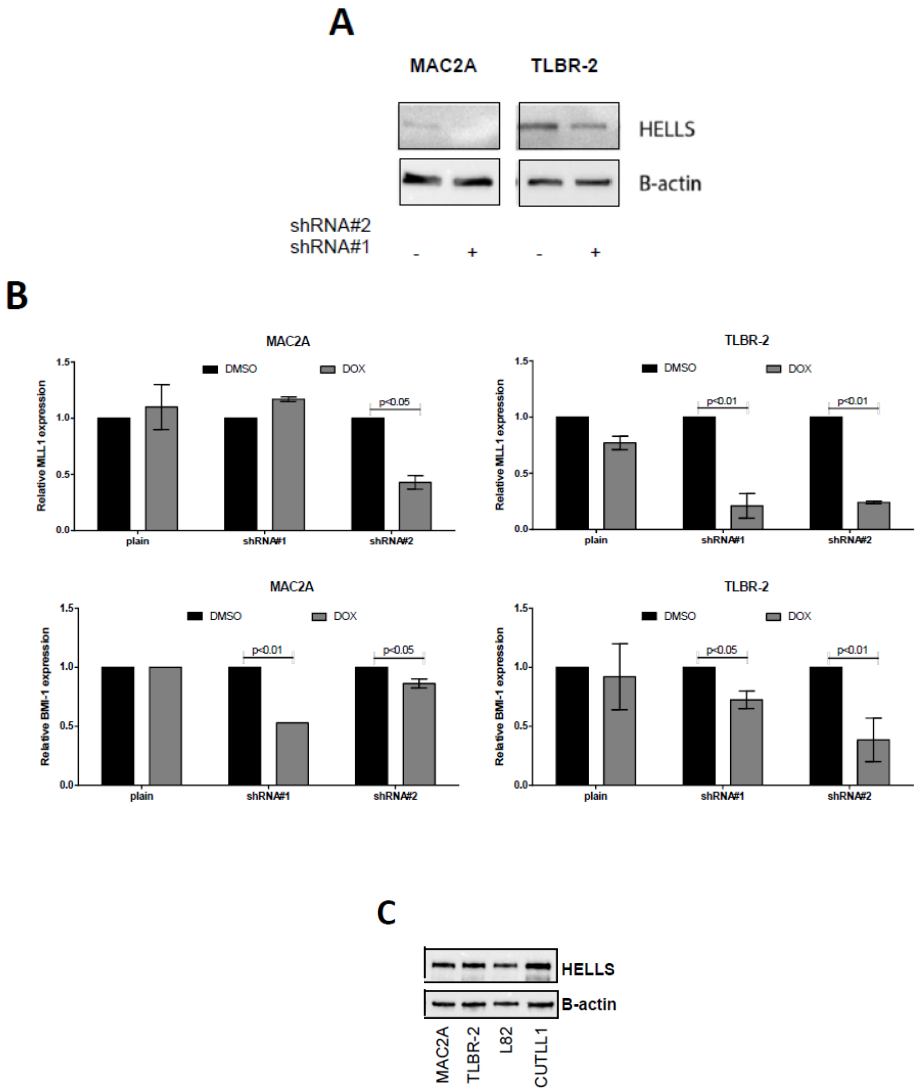

Figure 20. HELLS KD analysis. (a) Representative Western Blot of HELLS after 48hours of doxycycline induction. **(b)** qRT-PCR analysis of *BMI-1* and *MLL1* in ALK⁻ALCL cell lines expressing pLKO-shRNA#1 or 2-*HELLS* (48 hours after doxycycline induction). **(c)** Western Blot shows the basal level of HELLS in a panel of cell lines.

HELLS is necessary for the maintenance of ALK-ALCL neoplastic phenotype

To assess the contribution of *HELLS* and *BlackMamba* in maintaining ALK$^-$ALCL oncogenic features, we first analyzed cell proliferation and showed that loss of *HELLS* leads to decreased cell growth with reduced duplication rate with both shRNA#1 and shRNA#2 **(Fig. 21a, b and Fig. 22a)** and to a drastic decrease of colony-forming ability in both TLBR-2 and MAC2A HELLS KD cells **(Fig. 21c).** This phenotype was associated with an increased number of multinucleated cells, mimicking the *BlackMamba* KD cells phenotype **(Fig. 21d).** Next, we showed that *HELLS* overexpression could counterbalance the *BlackMamba* KD-related phenotype, as cell growth impairment and the number of multinucleated cells of TLBR-2 expressing inducible shRNA against *BlackMamba* were effectively rescued **(Fig. 21e, f)**. Collectively, these data indicate that HELLS is a crucial downstream mediator of *BlackMamba* and that the *BlackMamba*-HELLS axis represents a new vulnerability of ALK$^-$ ALCL cells at the base of cancer cell proliferation.

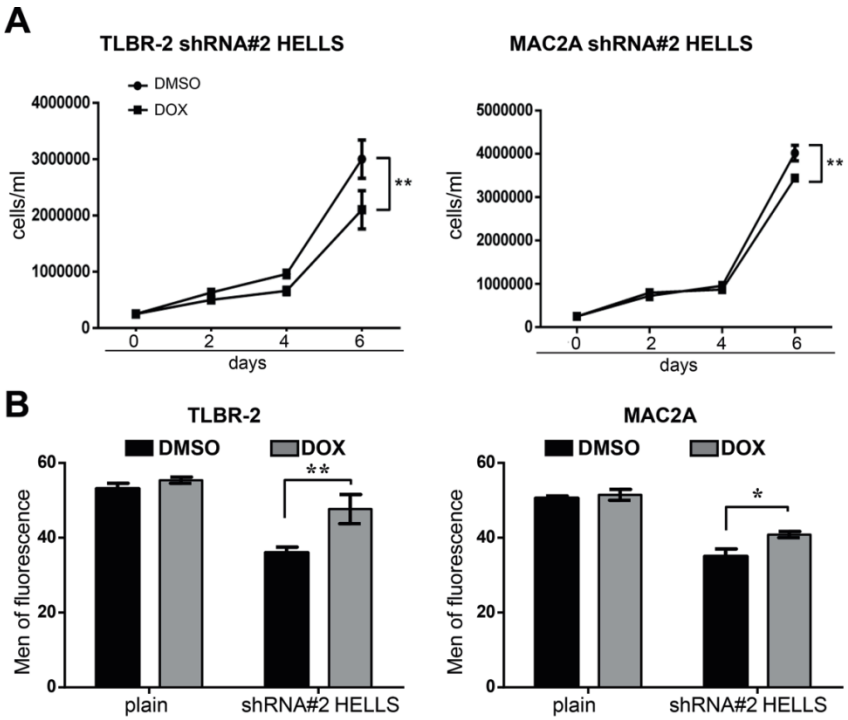

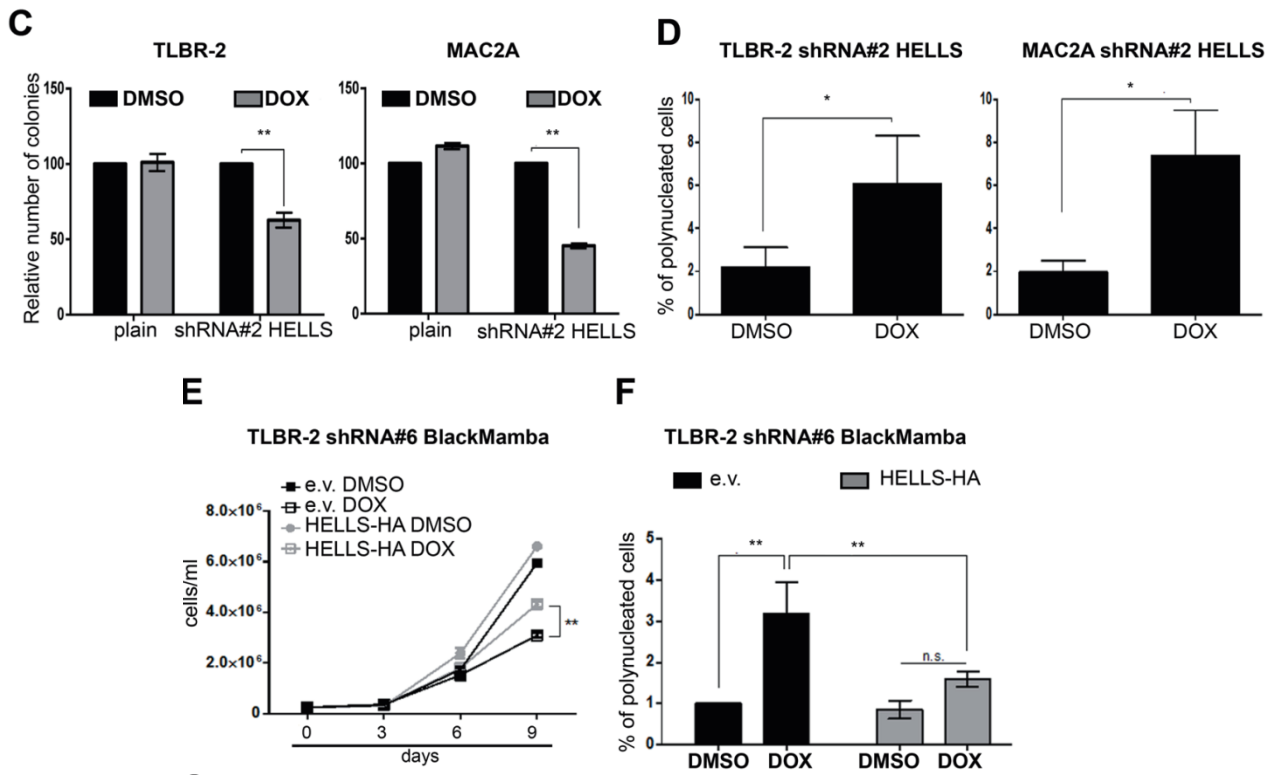

Figure 21. Silencing of *HELLS* mimics *BlackMamba* KD phenotype. **(a)** Growth curve of cells expressing pLKO-shRNA#2 *HELLS*. Each data point represents the mean ± S.D. (n = 3). ** p ≤ 0.01. **(b)** The histograms show the fluorescent intensity of CFSE-labeled ALK⁻ALCL cells (6 days after doxycycline treatment). **(c)** Histograms show methylcellulose colony formation of 3 days doxycycline pretreated cells expressing pLKO-shRNA#2 *HELLS*. Colonies were counted on day 10, after plating. Each data point represents the mean ± S.D. (n =3). **p ≤ 0.01. **(d)** Histograms show the percentage of polynucleated cells in at least 100 cells stained with May–Grunwald Giemsa (2 days of doxycycline induction). Each data point represents the mean ± S.D. (n = 3). *p ≤ 0.05. **(e)** Growth curve of TLBR-2 cells co-expressing pLKO-shRNA#6 *BlackMamba* and pCDH-*HELLS*-HA. Each data point represents the mean ± S.D. (n = 3). **p ≤ 0.01. **(f)** The panel shows the percentage of polynucleated cells in at least 100 cells stained with May–Grunwald Giemsa (2 days of treatment). Each data point represents the mean ± S.D. (n = 3). **p < 0.01.

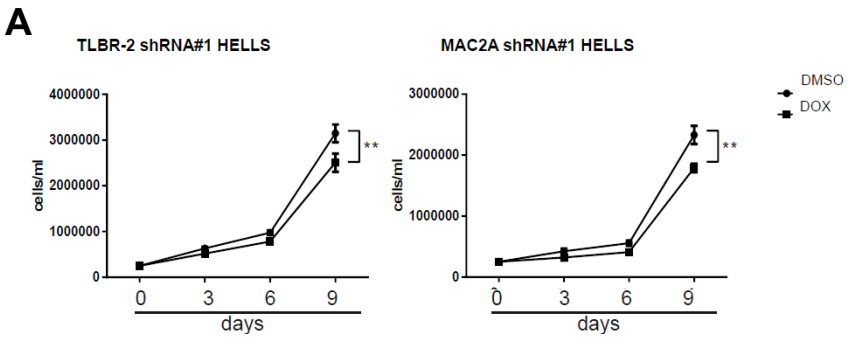

Figure 22. Cell proliferation analysis upon *HELLS* KD. (a) Growth curve of cells expressing pLKO-shRNA#1 *HELLS*. Each data point represents the mean ± S.D. (n =3). **p<0.01.

HELLS controls ALK⁻ALCL proliferation by transcriptionally coordinating a panel of cytoskeleton related genes involved in cytokinesis

To get insight into the transcriptional regulation of HELLS, we performed RNA-sequencing profiling in TLBR-2 cells which represent the ALK⁻ALCL subtype known as Breast Implanted Associated (BIA)-ALCL. We used the previously described inducible *HELLS* knockdown (KD) lines (TLBR-2 HELLS KD). *HELLS* silencing was analyzed by western blot and qRT-PCR **(Fig. 23a, b)** and functionally confirmed by the reduction of the expression mRNA levels of already defined HELLS-downstream targets both for TLBR-2 HELLS KD and MAC2A HELLS KD[152] previously demonstrated and showed in **Fig. 20b**. After DOX induction, the gene expression profile of TLBR-2 HELLS KD cells was analyzed and compared to the one obtained from untreated cells used as control. Transcriptional changes observed after *HELLS* KD revealed 728 differentially expressed genes. 413 were downregulated and 315 were upregulated upon *HELLS* KD with an FDR < 0.1 **(Fig. 23c)**. Gene ontology analysis of HELLS-target genes revealed the enrichment of several categories including cell cycle, DNA damage, histone modification, and chromatin organization. Noticeably, top-scoring in this list, there were multiple Rho GTPases and cytoskeleton related categories, including cytoskeleton regulation by Rho GTPases and Rho GTPases signaling **(Fig. 23d, e).** This was particularly interesting since we previously reported that the reduction of cell proliferation of ALK⁻ALCL cells upon *HELLS* silencing is associated with cytokinesis defects and with a marked increase in multinucleated cells in which Rho-GTPases are major players[157]. To give a phenotypic readout to these results, we evaluated the organization of cytoskeleton in T-cells[158] performing immunostaining for β-tubulin (as a principal constituent of microtubules) and for F-actin upon *HELLS* KD in TLBR-2 and in an additional cell line representing the systemic ALK⁻ALCL subtype (MAC2A) **(Fig. 23f)**. We detected a less organized localization of β-tubulin in the midzone of central spindle in HELLS KD cells as compared to control cells **(Fig. 23f)**. By contrast, we observed a profound reorganization of the F-actin with a reduced alignment and compaction in the cleavage furrow structure. This phenomenon resulted in an incomplete actomyosin ring formation in HELLS KD cells as compared to control cells **(Fig. 23f),** in agreement with the multinucleated phenotype previously reported[157]. Taken together, these data indicate that, in ALK⁻ALCL, HELLS supports and contributes to appropriate cytokinesis through the transcriptional control of genes involved in contractile ring structure and regulation.

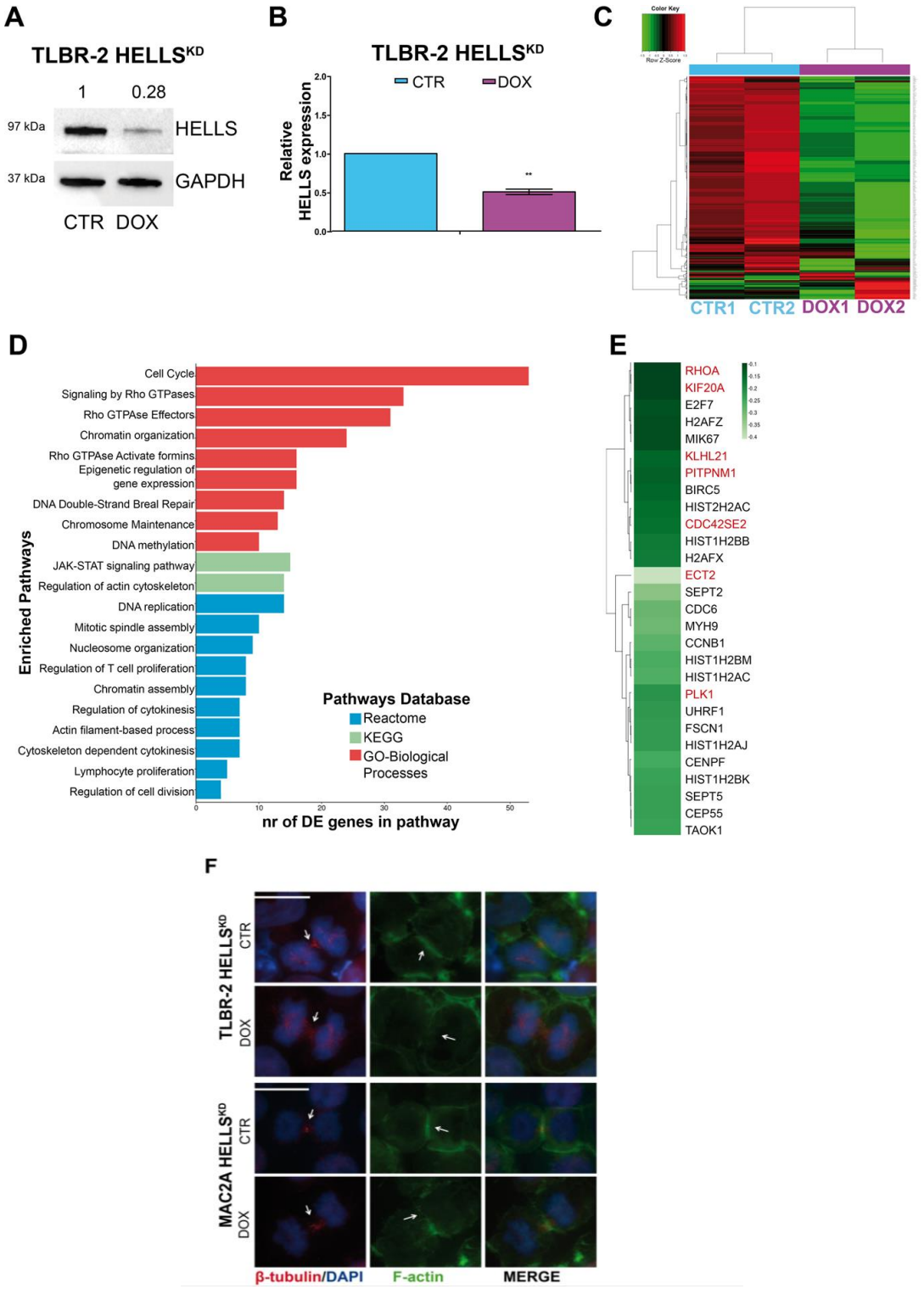

Figure 23. HELLS transcriptionally controls cytokinesis. (a) Western blot shows HELLS expression in TLBR-2 HELLS KD cells after 48 h of doxycycline (DOX) induction. GAPDH was used as a housekeeping gene. **(b)** qRT-PCR analysis of *HELLS* expression in TLBR-2 HELLS KD cells after 48 h of doxycycline induction. The values represent mean ± SEM (n = 3) *p < 0.05; **p < 0.01. **(c)** The heatmap depicts hierarchical clustering based on the 728 differentially expressed genes, whose read counts are Z-score normalized. Unsupervised hierarchical clustering was performed between DOX and CTRL samples (as indicated by the colored bar on columns) with a complete linkage method. Color intensity for each gene shows Z-score values ranging from red for upregulation and green for downregulation. **(d)** Most significant enriched pathways (adjusted p-value<0.05) are represented showing the number of DE genes mapped in each considered pathway. **(e)** The heatmap depicts validated significantly downregulated genes. Green color bar shows the

fold difference on the Log2 scale calculated between DOX and CTRL samples. Darker green represents the most downregulated genes. Genes in red were selected for further validations. **(f)** Immunofluorescence images of TLBR-2 HELLS KD cells and MAC2A HELLS KD cells after 48 h of doxycycline (DOX) induction. Cells were stained with DAPI, F-actin, and β-tubulin antibodies. The white scale bar represents 10 µm.

HELLS controls cytokinesis by directly binding to target gene promoters

Using qRT-PCR, we validated a representative set of genes involved in cytoskeleton and cytokinesis confirming the RNA-sequencing results and the effect of *HELLS* KD on these processes **(Fig. 24a).** Since we showed that HELLS cooperates with the lncRNA *BlackMamba* for transcriptional activity in ALK⁻ALCL and concurs to the lncRNA *BlackMamba* pro-oncogenic role in these cells[157], we investigated whether lncRNA *BlackMamba* was involved in the HELLS-dependent regulation of these genes. Taking advance of the previously generated TLBR-2 and MAC2A *BlackMamba* KD inducible cell lines[157], we showed that silencing of this lncRNA resulted in an important reduction of all tested HELLS-target genes **(Fig. 24b)** confirming the functional synergy between *BlackMamba* and HELLS and further indicating the cytoskeleton related genes as a central node of the transcriptional program supported by this axis in ALK⁻ALCL. To further investigate the direct role of HELLS in the regulation of these genes, we performed ChIP experiments to assess the binding of HELLS on their promoters. We observed a significant and specific enrichment of HELLS binding on 10 out of 11 promoter regions tested in both MAC2A and TLBR-2 cells **(Fig. 24c).** These data confirm that HELLS acts as a transcriptional activator of these genes.

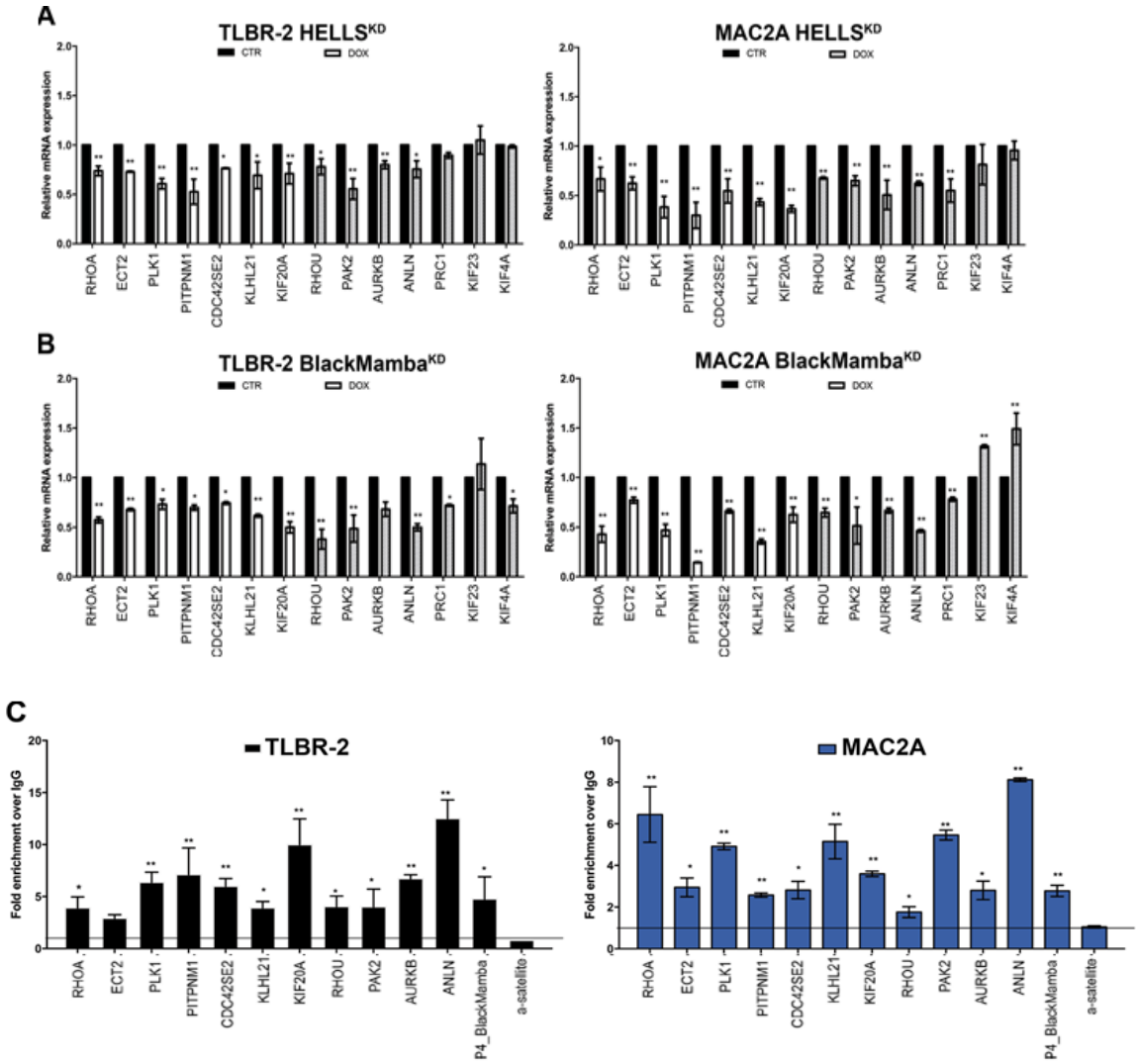

Figure 24. HELLS binds target gene promoters. (a) qRT-PCR validation of significantly downregulated genes obtained from RNA-sequencing. White bars represent the most significantly downregulated genes (FDR < 0.1) and gray bars represent less significant downregulated genes (FDR > 0.1) in TLBR-2 HELLS KD cells and MAC2A HELLS KD cells after 48 h of doxycycline (DOX) induction. Each data represent mean ± SEM (n = 3). Two-tailed t-test. *p < 0.05; **p < 0.01**. (b)** qRT-PCR validation of significantly downregulated genes obtained from RNA-sequencing. White bars represent the most significantly downregulated genes (FDR < 0.1) and gray bars represent less significant downregulated genes (FDR > 0.1) in TLBR-2 *BlackMamba* KD cells and MAC2A *BlackMamba* KD cells after 6 days of doxycycline (DOX) induction. Each data represent mean ± SEM (n =3). Two-tailed t-test. *p < 0.05; **p < 0.01. **(c)** ChIP qRT-PCR detection of HELLS antibody in a panel of target gene promoters in TLBR-2 and MAC2A.P4_*BlackMamba* and α-satellite were used as positive and negative controls, respectively. The values represent the relative fold enrichment over IgG and are indicated as mean ± SEM (n = 3). Two-tailed t-test. *p < 0.05; **p < 0.01.

YY1 is a transcriptional partner of HELLS in ALK⁻ALCL

Little is still known about the transcriptional function of helicases. Thus, to explore how HELLS controls the expression of its target genes we searched for putative transcriptional factors (TFs) that cooperate with HELLS in ALK⁻ALCL. A region spanning 500 bp around the transcriptional starting site (TSS) of each HELLS target gene was selected **(Fig. 25a).** A prediction search for TF binding sites enriched in these regions was performed using JASPAR[159] and PROMO[160]. 607 TFs and 26 TFs were significantly identified by JASPAR and PROMO, respectively. Merge of these lists resulted in a final list of 9 top scoring TFs and HELLS potential co-factors (predicted to bind up to 90% of the promoter regions used in this search): Yin Yang 1(YY1), Transcription Factor AP-2 Alpha (TFAP2A), Sp1 transcriptional factor (SP1), Nuclear Factor 1C (NFIC), MYB Proto-Oncogene Transcription Factor (MYB), Forkhead Box P3 (FOXP3), ETS Proto-Oncogene 1 (ETS1), ETS Transcription Factor ELK1 (ELK1) and E2F Transcription Factor 1(E2F1) **(Fig. 25b, c).** To validate this analysis, we first tested the basal expression of each of these TFs in ALK⁻ALCL cell lines. 7 out of 9 (78%) TFs were expressed in all tested cell lines even if with variable levels. By contrast, no expression was observed for *FOXP3* and *SP1* **(Fig. 25d).** Next, we investigated the potential interaction of these factors with HELLS by co-immunoprecipitation experiments in nuclear extracts. Among all the TFs investigated, only YY1 was found to interact with HELLS in both TLBR-2 and MAC2A cells **(Fig. 25e),** although the levels of YY1 in MAC2A cells are significantly lower than in TLBR2.To enforce the idea of cooperation between HELLS and YY1, we performed ChIP assay to investigate the binding of YY1 on the promoter regions of HELLS target genes both in MAC2A and TLBR-2 cell lines. We showed that 80% of the tested promoter (9/11) were simultaneously bound by both factors supporting the hypothesis of functional cooperation between these two factors **(Fig. 25f).** To establish a hierarchy within their relationship, we analyzed how HELLS KD affects YY1 binding on target promoters. Noticeably, YY1 was displaced by these regions in the absence of HELLS **(Fig. 25f)** indicating that HELLS is crucial in positioning YY1 on specific target genes in the context of ALK⁻ALCL.

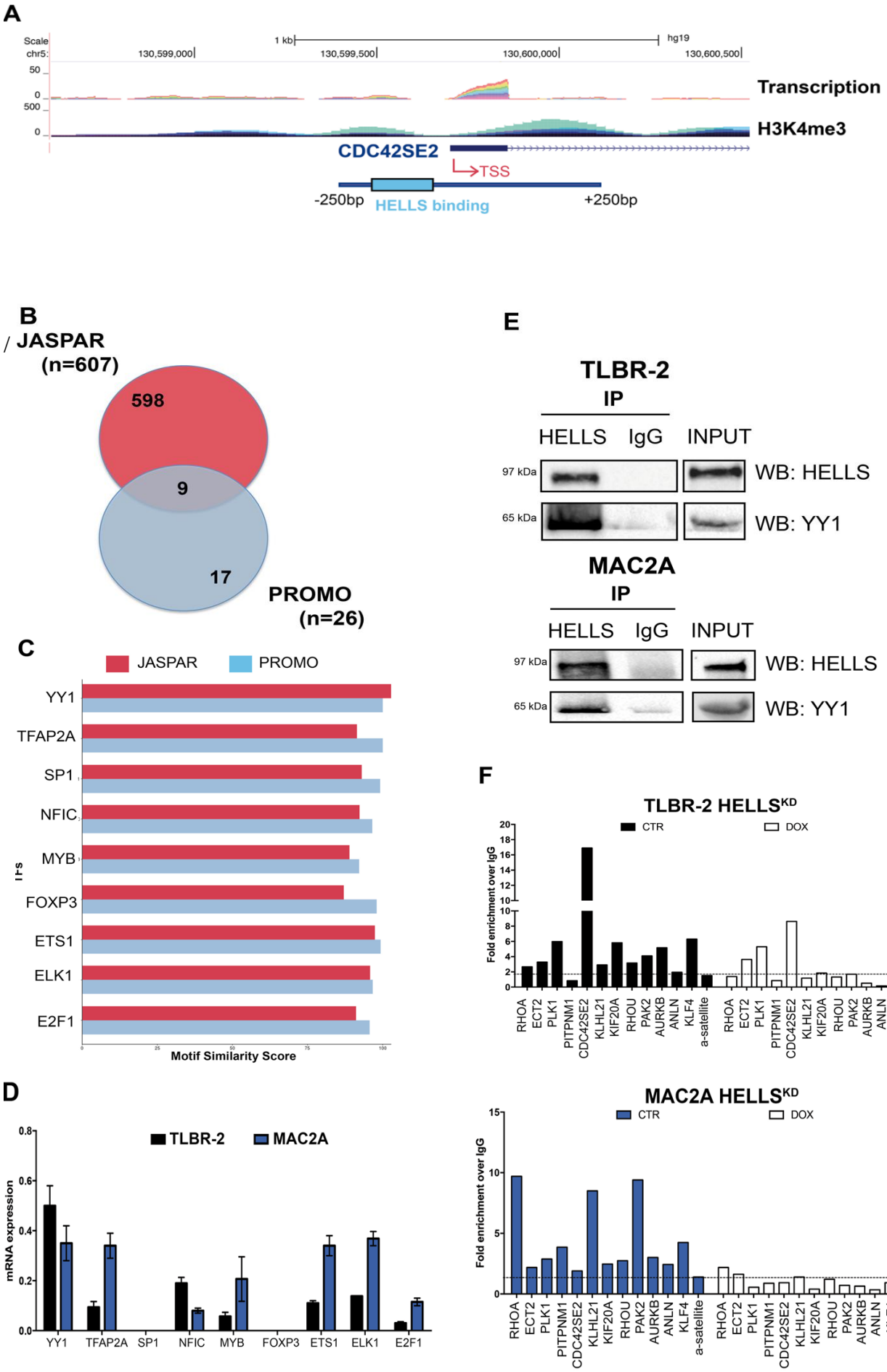
A
Scale
chr5:
1 kb
hg19
130,599,000
130,599,500
130,600,000
130,600,500
Transcription
H3K4me3
CDC42SE2
TSS
-250bp
HELLS binding
+250bp
B
JASPAR
(n=607)
598
9
17
PROMO
(n=26)
C
JASPAR
PROMO
YY1
TFAP2A
SP1
NFIC
MYB
FOXP3
ETS1
ELK1
E2F1
Motif Similarity Score
D
TLBR-2
MAC2A
mRNA expression
E
TLBR-2
IP
HELLS
IgG
INPUT
97 kDa
65 kDa
WB: HELLS
WB: YY1
MAC2A
IP
HELLS
IgG
INPUT
97 kDa
65 kDa
WB: HELLS
WB: YY1
F
TLBR-2 HELLSKD
CTR
DOX
Fold enrichment over IgG
RHOA
ECT2
PLK1
PITPNM1
CDC42SE2
KLHL21
KIF20A
RHOU
PAK2
AURKB
ANLN
KLF4
a-satellite
MAC2A HELLSKD
CTR
DOX
Fold enrichment over IgG

Figure 25. HELLS interacts with the transcriptional factor YY1. **(a)** Schematic representation of *CDC42SE2* genomic locus showing the position, the level of transcription, and the enrichment of H3K4me3 on its putative promoter**. (b)** The Venn diagram represents the intersection between transcriptional factors (TFs) identified by JASPAR (n = 607) and PROMO (n = 26) TFs binding prediction tools. The intersection shows the number of HELLS-predicted and common TFs (n = 9). **(c)** JASPAR and PROMO similarity scores are represented for top-ranked enriched transcription factors (TFs). (**d)** qRT-PCR analysis of top-scoring TFs in TLBR-2 and MAC2A cell lines. Each data represent mean ± SEM (n = 3). **(e)** Nuclear extract from TLBR-2 and MAC2A cells were tested for the presence of a multi-protein complex. Co-immunoprecipitation experiments were performed to evaluate the binding of HELLS to YY1. Western blots are representative of two independent experiments. **(f)** ChIP qRT-PCR detection of YY1 in TLBR-2 HELLS KD and MAC2A HELLS KD after 48 h of doxycycline (DOX) induction. *KLF4 and α-satellite* were used as positive and negative controls, respectively. The values represent the fold enrichment over IgG (representative of three independent experiments).

YY1 cooperates with HELLS to foster transcription of cytokinesis-related genes

YY1 is a ubiquitous transcriptional factor known to have a fundamental role in normal and cancer-related processes [161]. Thus, to consolidate its role as HELLS partner in the transcriptional program of ALK−ALCL, we silenced *YY1* with specific siRNA. WB analyses and qRT-PCR confirmed the efficiency of the silencing **(Fig. 26a, b).** Parallel analysis demonstrated that previously reported YY1 target genes[162,163] were coherently altered upon its KD and that no perturbation of *YY1* expression levels was detected upon *HELLS* KD **(Fig. 27a, b, c).** Proliferation analysis of TLBR2 and MAC2A transfected with either siRNA against *YY1* or scramble oligos as control did not evidence a significant effect on cell proliferation **(Fig. 26c).** However, we observed a significant increase in the number of multinucleated cells in YY1 KD cells **(Fig. 26d, e).**

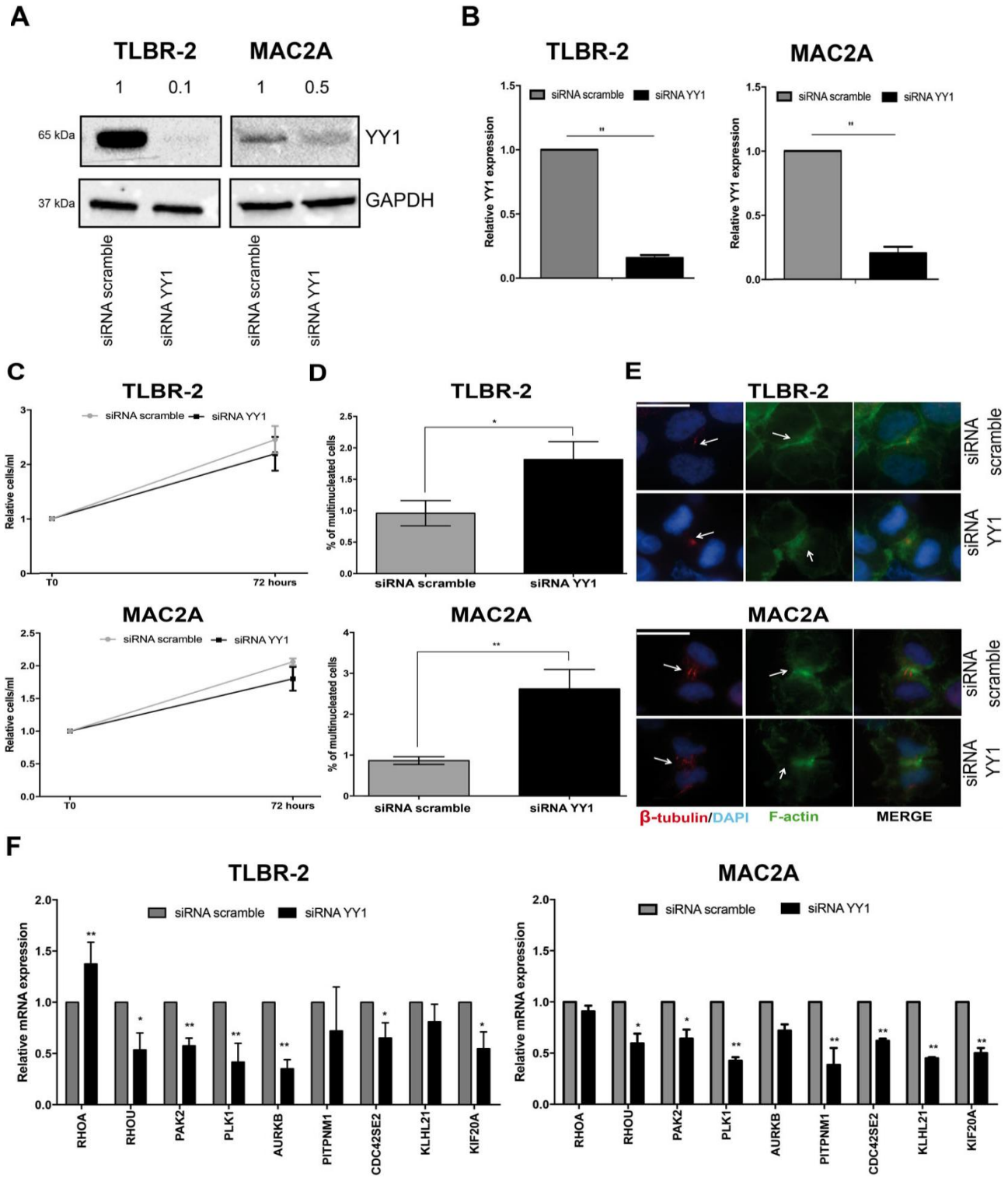

Figure 26. YY1 cooperates with HELLS to regulate the multi-nucleated phenotype. **(a)** Western Blot shows the knockdown of YY1 36 h post-nucleofection with a specific siRNA in TLBR-2 and MAC2A. GAPDH was used as a housekeeping gene. **(b)** qRT-PCR analysis of *YY1* expression after siRNA in TLBR-2 and MAC2A cell lines (36 h post-nucleofection). Each data represent mean ± SEM (n = 3). Two-tailed t-test. **p < 0.01. **(c)** The graph represents the relative growth curve of TLBR-2 and MAC2A 72 h post-nucleofection with *YY1* specific siRNA. Data were normalized on siRNA scramble values. Each data point represents the mean ± SEM (n = 3). Two-tailed t-test. **(d)** The panels show the percentage of multinucleated cells in at least 500 cells stained with β-tubulin and F-actin antibodies (48 h post-nucleofection). Each data point represents the mean ± SEM (n = 3). Two-tailed t-test. *p < 0.05; **p < 0.01. **(e)** Panels show representative immunofluorescences of TLBR-2 and MAC2A stained with DAPI, F-actin, and β-tubulin antibodies 48 h post nucleofection. The scale bar represents 10 μm. **(f)** qRT-PCR analysis of a panel of selected HELLS-target

genes in TLBR-2 and MAC2A 36 h post-nucleofection with specific *YY1* siRNA. The values represent mean ± SEM (n = 3). Two-tailed t-test. *p < 0.05; **p < 0.01.

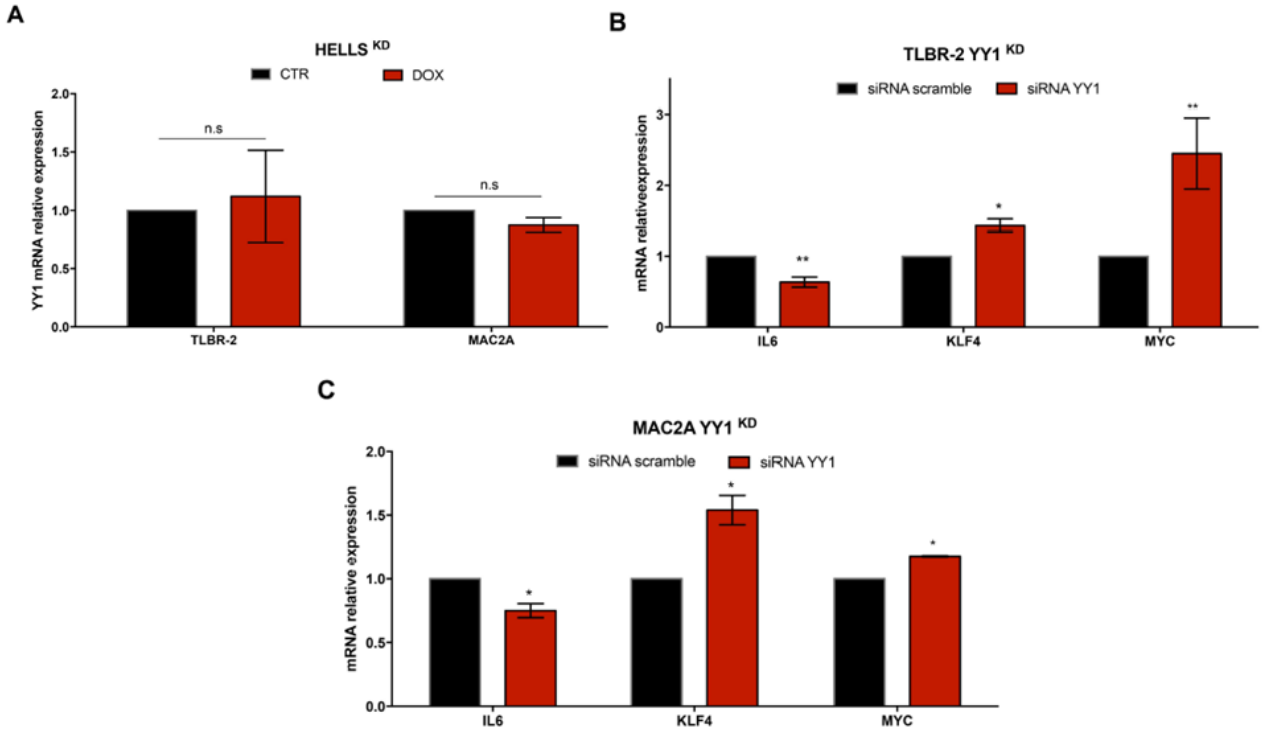

Figure 27. *YY1* KD analysis. (a) qRT-PCR analysis of *YY1* expression in TLBR-2 HELLS KD and MAC2A HELLS KD after 48 hours of doxycycline induction (DOX). The values represent mean ± SEM (n = 3). Two-tailed t-test. n.s.= not significant. **(b, c)** qRT-PCR analysis of YY1 targets *IL-6, KLF4*, and *MYC* in TLBR-2 and MAC2A nucleofected with specific *YY1* siRNA (36 hours post nucleofection).

Downstream effects of HELLS are mediated by multiple Rho-GTPases and effector

Rho-GTPases are a family of small GTPase proteins involved in many aspects of intracellular actin dynamics including cell division. During the cytokinesis, Rho-GTPases trigger the initiation of the cleavage furrow from which cytosol division begins[164,165]. Rho-GTPases are also known for their role in the regulation of cell growth and proliferation and cytoskeleton rearrangements in T lymphomas[166]. Thus, to consolidate the relevance of the transcriptional program associated with HELLS, we investigated the relevance of these genes in ALK⁻ALCL. To this end, we knocked down the expression of RhoA, RhoU, and Pak2 with specific siRNAs. Since Rho-GTPases are known to work in a highly cooperative manner[167,168] we also combined siRNAs to simultaneously knockdown two or more of these proteins. **Figures 28a** and **28b** show the efficiency of the silencing at the mRNA and protein level in both MAC2A and TLBR-2 cells. We noticed that while RhoA KD or Pak2 KD did not alter the expression of the others, RhoU KD exerted a significant effect on RhoA expression,

suggesting a tight interplay between these two proteins. Morphologically, *RHOA* KD and *RHOU* KD led to the increase in the percentage of multinucleated cells relative to siRNA scramble. By contrast, no such effect was observed for *PAK2* silencing. This phenomenon slightly increased when *RHOA* KD and *RHOU* KD were combined. On the contrary, combined *RHOU* KD/*PAK2* KD and *RHOA* KD/ *PAK2* KD did not increase the percentage of multinucleated cells relative to *RHOU* KD and *RHOA* KD, respectively. Consistently, triple KD resulted in an induction of multi nuclei comparable to combined *RHOA* KD/*RHOU* KD or *RHOA* KD **(Fig. 28c).** To assess if the multi-nucleated phenotype resulted from cytokinesis failure[169], we quantified cytokinetic cells by immunofluorescence using F-actin and β-tubulin staining. A significant decrease in the percentage of total cytokinetic cells and a relative increase in abnormal cytokinetic cells were observed in single and combined *RHOA* KD/*RHOU* KD compared to siRNA scramble **(Fig. 28d).** Immunofluorescences showed that both *RHOA* KD and *RHOU* KD affected β-tubulin organization at central spindles or midbody structures. The proper F-actin organization at the contractile ring was also dramatically affected resulting in an abnormal formation of cleavage furrow **(Fig. 28e).** As expected, combined *RHOA* KD and *RHOU* KD resulted in a more pronounced phenotype close to the one observed in HELLS KD cells **(Fig. 28e).** The analysis of cell proliferation was coherent with these observations. Single silencing of *RHOU* and *PAK2* did not affect significantly cell growth while a significant decrease in cell proliferation was observed in *RHOA* KD in both cell models. Combined *RHOU* KD/*RHOA* KD resulted in a cell proliferation reduction similarly to single *RHOA* KD whereas combined *RHOU* KD/ *PAK2* KD enhanced the effects of single *RHOU* KD and *PAK2* KD but only in TLBR-2. Notably, triple KD resulted in a significant decrease in cell proliferation, but this reduction was similar to *RHOA* KD or *RHOU* KD/*PAK2* KD **(Fig. 28f).** Collectively, these data demonstrated that RhoA and RhoU mediate HELLS effects on cell proliferation and cell division of ALK⁻ALCLs and that RhoA has a prominent role in this process.

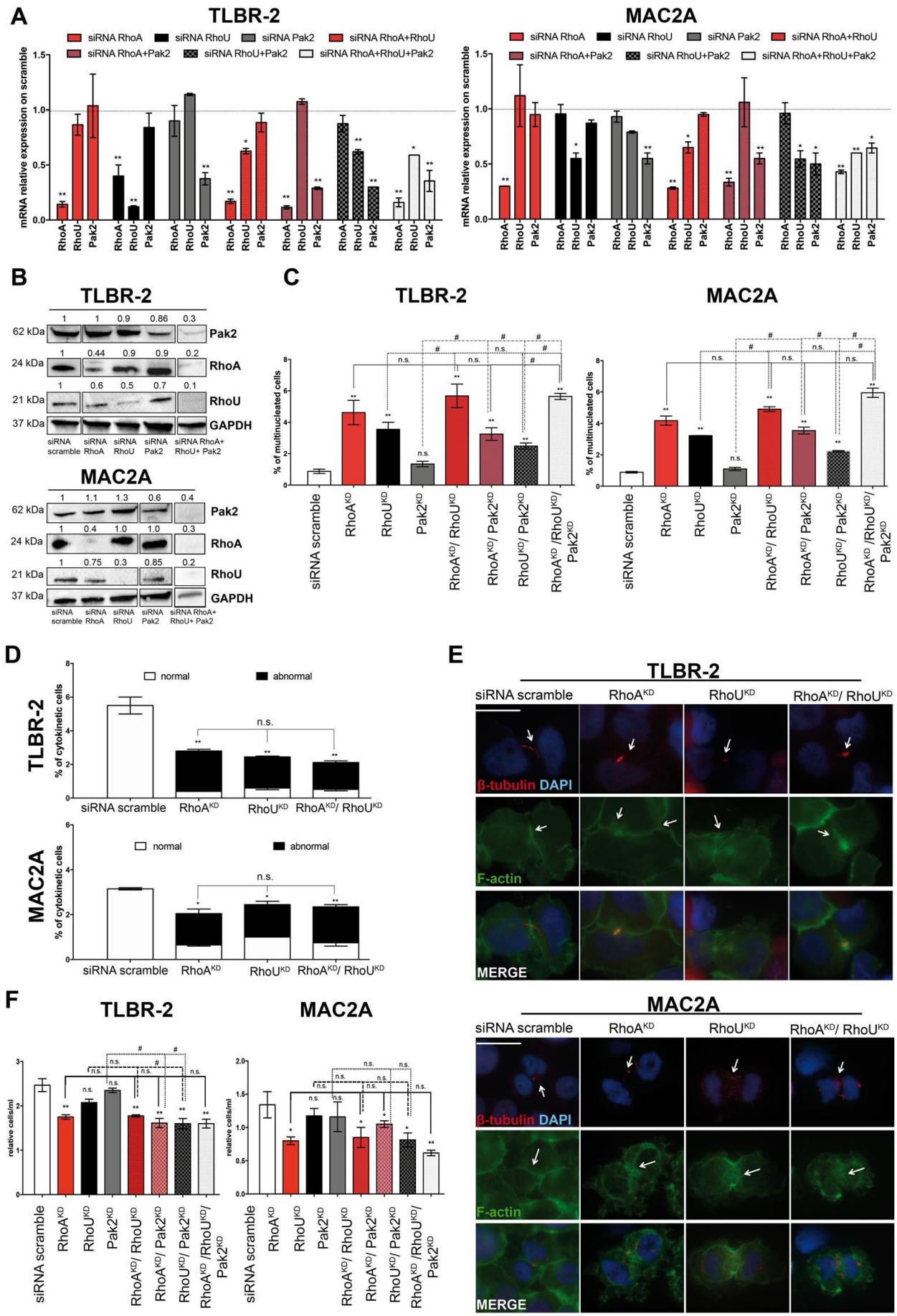

Figure 28. Rho-GTPases mediate HELLS-downstream effects. **(a)** qRT-PCR analysis of *RHOA, RHOU* and *PAK2* expression after single or combined siRNAs in TLBR-2 and MAC2A cell lines (36 h post-

nucleofection). Each data represent mean ± SEM (n = 3). Two-tailed t-test. *p < 0.05, **p < 0.01. **(b)** Western blots show knockdown of RhoA, RhoU, or Pak2 36 h post-nucleofection with specific siRNAs in TLBR-2 and MAC2A. GAPDH was used as a housekeeping gene. **(c)** The histograms show the percentage of multi-nucleated cells in at least 500 cells TLBR-2 and MAC2A stained with DAPI, F-actin, and β-tubulin antibodies (48 h post-nucleofection). Cells were nucleofected with single and combined specific siRNAs against *RHOA, RHOU, and PAK2.* Each data point represents the mean ± SEM (n = 3). Two-tailed t-test. *p < 0.05 and **p < 0.01 relative to siRNA scramble. # p < 0.05 relative to *RHOA* KD, *RHOU* KD, or *PAK2* KD. **(d)** The histograms show the percentage of cytokinetic cells in at least 500 cells TLBR-2 and MAC2A stained with DAPI, F-actin, and β-tubulin antibodies (48 h post-nucleofection). The term “abnormal” refers to cytokinetic cells with defects in cleavage furrow and/or microtubules structures. Cells were nucleofected with single and combined specific siRNAs against *RHOA* and *RHOU*. Each data point represents the mean ± SEM (n =3). Two-tailed t-test. *p < 0.05 and **p < 0.01 relative to siRNA scramble. **(e)** Immunofluorescence of TLBR-2 and MAC2A nucleofected with siRNA scramble and single and combined *RHOA* and *RHOU* siRNAs (48 h post-nucleofection). Cells were stained with DAPI, F-actin, and β-tubulin antibodies. The scale bar represents 10 µm**. (f)** Relative growth curve of TLBR-2 and MAC2A nucleofected with siRNA scramble and single or combined *RHOA* and *RHOU* and *Pak2* siRNAs (72 h post-nucleofection). Each data was normalized to siRNA scramble and represented the mean ± SEM (n = 3). Two-tailed t-test. *p < 0.05 and **p < 0.01 relative to siRNA scramble. # p < 0.05 relative to *RHOA* KD, *RHOU* KD, or *PAK2* KD.

8. MOLECULAR MODEL

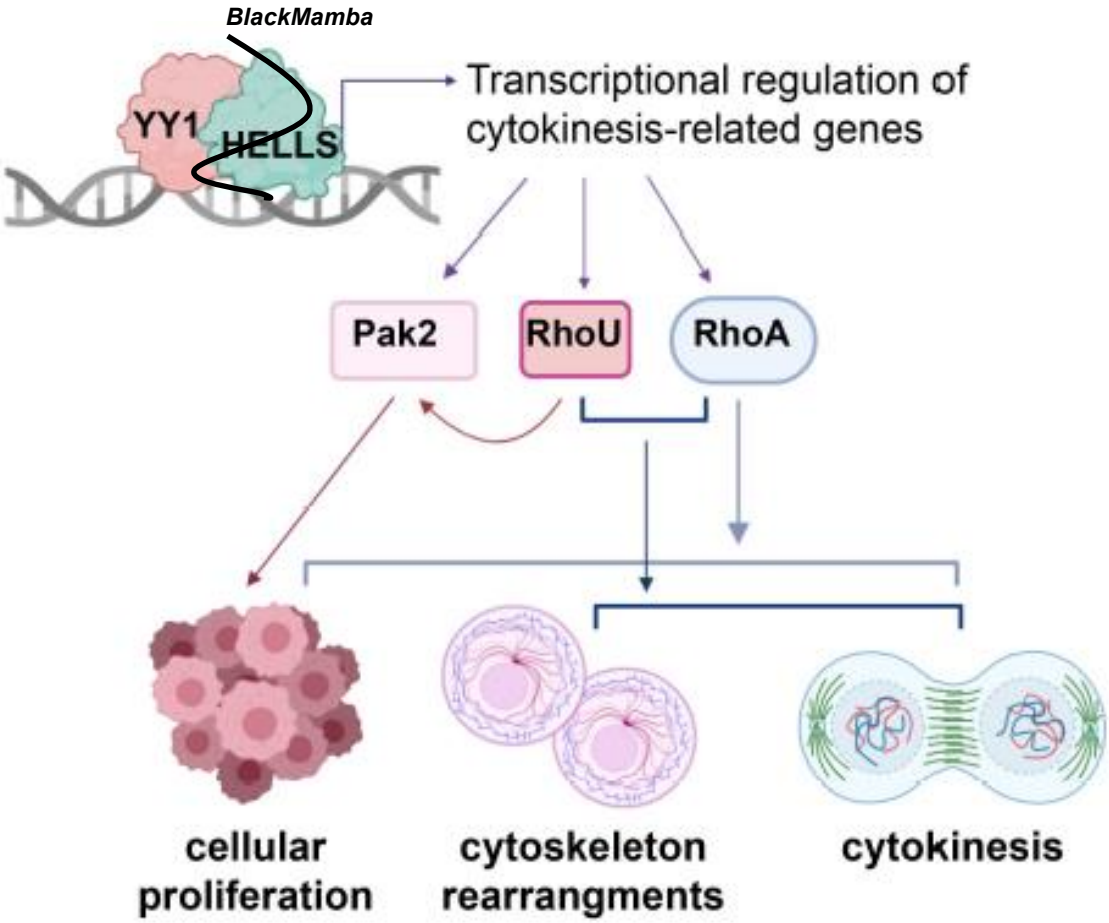

Figure 29. Schematic representation of *BlackMamba*-HELLS axis in the regulation of ALK⁻ALCLs cytoskeleton and cytokinesis-related program *(created with BioRender.com).*

9. DISCUSSION

Peripheral T cell lymphomas (PTCLs) are a complex and heterogeneous group of orphan neoplasms. Despite the introduction of chemotherapy protocols with or without hematopoietic transplantation and the discovery of new agents, the progression-free survival of patients needs to be improved.

The rarity of these lymphomas, the limited knowledge regarding the driving defects, the lack of experimental and preclinical models have impaired clinical success making the discovery of new target therapies an urgent clinical need.

Several mechanisms have been shown to contribute to PTCLs pathogenesis and transformation including: 1) acquired intrinsic defects deregulating many signaling pathways that are at the base of T cell development, maturation, and differentiation; 2) a plethora of structural and somatic mutations that affect TCR signaling and deregulated activation of signaling that control cell proliferation, survival, and apoptosis such as JAK-STAT pathway; 3) expression of membrane antigens that allow tumor evasion; 4) mechanisms regarding the remodeling of the tumor microenvironment; 5) genomic and epigenomic changes that modify T cell transcriptional profile/landscape; 6) metabolic dysregulation and reprogramming able to sustain cancer cell growth in stress conditions; 7) virus-mediated oncogenesis[5].

Taking advantage of massive genomic sequencing approaches, important steps forward have been made in the discovery of PTCLs molecular defects that foster T cell transformation[5,170,171]. The understanding of genomic alterations and the integration of these with functional data have led to: 1) genomic-based patient stratification, 2) establishment of new clinical/diagnostic criteria, 3) more detailed risk assessment, and 4) well-designed therapeutic approaches.

These therapeutic options will include conventional compounds, new targeted agents with immune regulators, and chimeric antigen receptor-expressing natural killer and T cells with the intent to improve PTCLs patients' overall survival.

The human genome transcribes many thousands of lncRNAs that display cell/state-specific expression patterns and play key regulatory functions in cells as epigenetic modulation, regulation of chromatin states and gene expression, post-transcriptional regulation, and cell homeostasis. For this reason, aberrant loss or gain of function of lncRNAs is observed in different human cancers and diseases.

XIST, HOTAIR, MALAT1, NEAT1, KCNQ1OT1 are the main examples of lncRNAs aberrantly expressed in cancer where they modulate the expression of several oncogenes and tumor suppressors. They are considered initiators and drivers of malignancies able to sustain neoplastic phenotype. Furthermore, they are recognized as biomarkers/predicting factors, and their expression levels are related to good or poor prognosis.

While for human B-cell hematological neoplasms and solid tumors there is evidence about the pathogenic role of lincRNAs, little is known about their function in T cell neoplasms[172–175]. Particularly, the potential involvement of lncRNAs in the maintenance of neoplastic phenotype in ALCLs has never been studied before and represents a crucial point for the investigation of the molecular mechanisms able to sustain T cell proliferation, survival, and drive ALCLs progression.

In our study, we demonstrate, for the first time, that ALK$^-$ALCL patients display a restricted and specific set of previously unknown lincRNAs expression.

We performed a comprehensive genome-wide analysis of coding and non-coding transcripts in ALCLs samples compared to normal T-lymphocytes discovering 1208 unknown lncRNAs preferentially expressed in ALCLs. A third of these lncRNAs were co-shared by both ALCL subtypes further supporting the idea that they share some similarities[176].
To deeply characterize the interplay between coding and non-coding genome, we selected the unique lincRNA expressed in ALK$^-$ALCL setting, identified as STAT3 regulated that we named *BlackMamba*. STAT3 activation is deregulated in many cancers[177] including ALCLs where the constitutive JAK/STAT signaling pathway is mainly caused by gene fusions, somatic mutations, and loss of negative regulators[18,178–181]. These lead to a different transcriptional program associated with defined pathological entities[176,182]. It is known that lincRNAs are linked to STAT signaling by modulating metabolic pathways[183] and, by contrast, STAT3 can regulate cell differentiation by regulating lncRNA expression[184].
Given the importance of chromatin-associated long noncoding RNA in regulating gene expression by controlling epigenetic chromatin states and in coordinating RNA-RNA, RNA-DNA, and RNA-protein interactions, it is not surprising that their deregulation, in terms of overexpression or loss, is related to human disease and cancer[185–187].
Coherently, we demonstrated that *BlackMamba*, a chromatin-associated lncRNA, plays a crucial role in regulating ALK$^-$ALCL neoplastic phenotype and this is achieved mainly through the action of the DNA helicase HELLS and the transcriptional regulation of genes controlling G-protein and cytoskeletal organization, cell migration, tissue recruitment, and inflammation. The top-scoring deregulated target genes encode chemokines and

chemokine receptors (*CCL17, CCL22, CXCL10*), *G protein regulators (RGS1)*, multiple effectors involved in cell growth, and motility (*PAK2, ERBB2, RHOU, KIF12B*).

Among *BlackMamba* target genes, we found the DNA-helicase *HELLS* (16,550,000 bp from *BlackMamba* locus) and demonstrated that its functional loss mimics *BlackMamba* silencing phenotype leading to a strong reduction of cell proliferation and colony-forming ability, F-actin cytoskeleton rearrangements, and an increase of multi-nucleated cells without changes in polyploidy.

It is reported that lncRNAs can recruit chromatin-modifying proteins to target sites by the association with DNA-binding proteins and influence the chromatin states thereby modulating gene expression.

In accordance with these observations, we showed that *BlackMamba* physically interacts with HELLS and it can control its recruitment on target genes regulatory regions and its expression in ALK$^-$ALCL lymphoma. The DNA helicase HELLS is a multifunctional protein proved to play, among the others, critical roles in DNA methylation[188], chromatin packaging, and development of lymphoid tissue[151,188]. Indeed, known also as Lymphoid-specific helicase (Lsh), HELLS is required for normal development and survival of lymphoid and other tissues via chromatin organization[189,190], promotion of DNA double-strand break repair, replicative fork protection, and chromatin accessibility modification[191,192] favoring genome stability[193–195].

In cancer, HELLS is deregulated in several settings i.e. gliomas[196], retinoblastoma[197,198], prostate[152], breast carcinomas[199,200], medulloblastoma[201], leukemia[202] where it promotes cellular proliferation and stemness.

It is known that a significant part of HELLS activity in these processes is mediated by its transcriptional function even if the way through which HELLS controls gene expression is still partially undefined. Its interaction with the epigenetic silencer factor G9a [203], DNA methyltransferases (DNMTs)[204] as well as with E2F transcriptional factor 3(E2F3)[152,198] and c-Myc[196] has been described.

In line with this evidence, we demonstrated that HELLS is able to act as a transcriptional regulator of a set of cytokinesis-related genes.

We contributed to unveiling a new mechanism showing that, in the specific context of ALK$^-$ALCL, HELLS interacts and functionally cooperates with the transcription factor YY1. We demonstrated that DNA binding motif for YY1 is enriched within the HELLS binding sites and that these two factors physically interact and co-occupy the same regions at the level of target promoters to ensure transcription of a large set of cytokinesis-related genes.

YY1 is a ubiquitously expressed transcriptional factor with a fundamental role in embryogenesis, adult hematopoiesis, differentiation, replication, and cellular proliferation[161,205,206]. YY1 ensures the proper completion of mitosis and its knockdown leads to defects in cytokinesis and accumulation of multi-nucleated cells[207].

YY1 is often deregulated in hematopoietic malignancies where it controls the survival and growth of neoplastic cells[208,209]. Coherently, here we reported that in ALK⁻ALCL, the loss of *YY1* is associated with the accumulation of multinucleated cells likely attributable to incomplete cytokinesis. The functional relationship between HELLS and YY1 has never been described before. Interestingly, we showed that the loss of HELLS protein leads to YY1 displacement from DNA. This seems to indicate that HELLS, by altering chromatin accessibility, works by priming the binding of specific transcription factors to target promoters, therefore, regulating a specific set of context-specific genes. By RNA-sequencing profiling, we showed that a significant part of the HELLS transcriptional program in ALK⁻ALCL converges on the regulation of cytoskeleton and cytokinesis.

To the best of our knowledge, this is the first time that the transcriptional activity of HELLS is linked to these biological processes.

Cytoskeleton is the structure responsible for cell shape maintenance and organization.

It also confers mechanical support to every cellular process from proliferation and division to cell migration, adhesion, and interaction with the surrounding microenvironment.

Of note, recent genetic and molecular profiling studies have unveiled several alterations targeting the cytoskeleton, highlighting its critical role during the transformation and progression of T-cells[111,210].

Indeed, defects in cytoskeleton structure and functions support tumorigenesis leading to aberrant proliferation and promoting inappropriate migratory and invasive features.

Aberrant signaling pathways, like JAK/STAT3, NPM-ALK, Rho-GTPase, and Aurora Kinase, can contribute to lymphomagenesis by modifying cytoskeleton structure and signaling properties.

Although we still lack a definitive overall view of how cytoskeleton changes during lymphomagenesis, the emerging picture suggests that the cytoskeleton transcends the maintenance of cell morphology and polarity providing a more complex support to T-cells in the response to intrinsic and environmental clues. Among HELLS-downstream effectors, we identified several Rho-GTPases and their related proteins including RhoA, RhoU, and Pak2. Single and combined KDs of these proteins highlight that RhoA and RhoU are key effectors of the HELLS program controlling both cell proliferation and cell division. RhoA is a key player in T-cell processes[211] and its deregulation has emerged as a central issue of T-

lymphoma biology[107,110,111,211,212]. Coherently, our results demonstrate that RhoA is a fundamental effector of the HELLS-dependent oncogenic program. At the transcriptional level, *RHOA* is regulated by HELLS but not by YY1 suggesting a more complex regulation of this Rho-GTPase in this setting. Limited information is available on the regulation of *RHOA*[213], and given its centrality, additional studies are needed to better clarify this point. As RhoU can mediate the effects of WNT and STAT3 signaling pathways in regulating cell morphology, cytoskeletal organization, and proliferation[214,215], our data provide a new layer of complexity demonstrating a new role of RhoU in cytokinesis via the STAT3-*BlackMamba*-HELLS axis. The cooperative role of Rho-GTPases in the execution of the neoplastic program driven by HELLS is in agreement with their fundamental role in the regulation of cell proliferation, cell division, and actin polymerization in cancer[216].

Interestingly, deregulation of chromatin modifiers fostering the transcriptional program of neoplastic T-cell is emerging as a common feature and potential vulnerability of ALK$^-$ALCL[5,54]. Since HELLS is expressed in many tumors and plays a relevant role in the transcription and genomic stability of cancers, its pharmacological inhibition may represent a promising therapeutic strategy in lymphomas and in other human neoplasms.

Collectively, our data provide novel insights into the mechanism sustaining the progression of ALK$^-$ALCL showing that the *BlackMamba*-HELLS axis supports ALK$^-$ALCL neoplastic phenotype by controlling a specific gene expression program that is crucial for proper and complete cytokinesis, and thus for proficient cell division and proliferation **(Figure 27)**.

10. RECENT OBSERVATIONS AND FUTURE PERSPECTIVES

It is known that T cell lymphomas are a rare and heterogeneous group of neoplasm characterized by poor prognosis, lack of effective therapies, and whose molecular mechanisms are quite elusive. They are associated with genome instability and high transcriptional activity that is required to sustain cancer cell proliferation, increasing the risk of DNA damages and ruptures. In this context, the DNA helicases, by controlling many DNA-based processes, are considered as the master keeper of genome stability.

In our recent work, we demonstrated that HELLS orchestrate a transcriptional program specific to neoplastic T cell sustaining disease progression. My work aims to study how HELLS manages and coordinates transcription by modulating chromatin landscape and to investigate its ability to promote gene expression by solving DNA topological conflicts and by preventing DNA damages. To understand how HELLS manages transcription and to define a HELLS-associated gene signature, we performed RNA-Sequencing analysis in the BIA-ALCL cell line silenced for *HELLS*. Gene expression profiling and gene ontology analysis showed a plethora of genes primarily involved in cell cycle and DNA replication, chromatin remodeling and maintenance, and DSB repair highlighting the key role of HELLS in these processes as we reported in **Figure 23** of the thesis.

Next, we validated the RNA-Sequencing results in TCLs cell lines (MAC2A, TLBR-2, and CUTLL-1 that are representative of Human T-Cell Lymphoblastic Lymphoma) showing that HELLS not only decisively affects the expression of genes involved in cytoskeleton/cytokinesis- mediated processes but also genes that are essential in regulating DNA dynamics. Next, to evaluate changes in chromatin landscape associated with *HELLS* silencing, we performed Chip-sequencing analysis on active and repressive H3 histone markers such as K4me3 and K9me3 respectively. We observed a modest but significant change in K4me3 level at promoters and distal intergenic regions while no changes were observed for the K9me3 repressive marker.

Notably, gene ontology analysis on the identified 59 genes resulting from the intersection of RNA-sequencing and ChIP-sequencing data analysis revealed the enrichment in T cell activation, T helper differentiation, and lineage commitment processes accordingly with the role of HELLS in lymphocyte development.

To deeply study the transcriptional function of HELLS, we investigate its ability to promote transcription by solving DNA topological tension.

We performed immunostaining of RNA-DNA hybrid structures, called R-loops, on a panel of TCLs cell line and showed that the loss of *HELLS* leads to an accumulation of R-loops that co-localize with the active form of RNA-PolymeraseII (RNAPII), suggesting that HELLS can facilitate RNAPII progression along the gene body by avoiding R-loops collision.

Co-Immunoprecipitation experiments showed that HELLS physically interacts with RNAPII and chromatin-IP assays in BIA-ALCL cells demonstrated that *HELLS* silencing leads to an accumulation of the active form of RNAPII at the transcriptional starting site of selected target genes. To enforce this hypothesis, we performed ethynyl uridine staining (EU, marker of nascent RNA) and we detected that the RNAPII decreased activity was strictly associated with a significant decrease in the nascent RNA confirming the attenuation of the transcription process across all transcriptome.

Since R-loops accumulation and persistence are associated with DNA damages, we studied the level of γ-H2AX (DNA damage marker) and showed that *HELLS* functional loss causes an increase in γ-H2AX signal and foci in TCLs cells. In addition, γ-H2AX foci were observed in correspondence of R-loops structures and in colocalization with the active form of RNAPII**.**

Collectively, our data indicate that HELLS orchestrates a transcriptional program essential to the survival and proliferation of TCLs and its genetic ablation profoundly impairs mitosis and cell proliferation. HELLS supports TCLs progression promoting gene expression by solving DNA topological conflicts, easing RNAPII progression, and protecting DNA from damaging events. These key functions qualify HELLS as a new dependency of TCLs and as a potential vulnerability of these aggressive lymphomas, making HELLS an attractive target for the design of new small molecules.

BIBLIOGRAPHY

1. Vose, J., Armitage, J., Weisenburger, D., & International T-Cell Lymphoma Project. International peripheral T-cell and natural killer/T-cell lymphoma study: pathology findings and clinical outcomes. *J. Clin. Oncol. Off. J. Am. Soc. Clin. Oncol.* **26**, 4124–4130 (2008).

2. Weltgesundheits organisation. *WHO classification of tumours of haematopoietic and lymphoid tissues*. (International Agency for Research on Cancer, 2017).

3. Tabbó, F. ALK signaling and target therapy in anaplastic large cell lymphoma. *Front. Oncol.* **2**, (2012).

4. Delabie, J. *et al.* Enteropathy-associated T-cell lymphoma: clinical and histological findings from the international peripheral T-cell lymphoma project. *Blood* **118**, 148–155 (2011).

5. Fiore, D. *et al.* Peripheral T cell lymphomas: from the bench to the clinic. *Nat. Rev. Cancer* **20**, 323–342 (2020).

6. Strachan, T. & Read, A. P. *Human molecular genetics*. (Wiley, 1999).

7. Swerdlow, S. H. *et al.* The 2016 revision of the World Health Organization classification of lymphoid neoplasms. *Blood* **127**, 2375–2390 (2016).

8. Scarfò, I. *et al.* Identification of a new subclass of ALK-negative ALCL expressing aberrant levels of ERBB4 transcripts. *Blood* **127**, 221–232 (2016).

9. Montes-Mojarro, I. A., Steinhilber, J., Bonzheim, I., Quintanilla-Martinez, L. & Fend, F. The Pathological Spectrum of Systemic Anaplastic Large Cell Lymphoma (ALCL). *Cancers* **10**, E107 (2018).

10. Hossfeld, D. K. World Health Organization Classification of Tumours: Pathology and Genetics of Tumours of Haematopoietic and Lymphoid Tissues. *Ann. Oncol.* **13**, 490 (2002).

11. Morris, S. *et al.* Fusion of a kinase gene, ALK, to a nucleolar protein gene, NPM, in non-Hodgkin's lymphoma. *Science* **263**, 1281–1284 (1994).

12. Parrilla Castellar, E. R. *et al.* ALK-negative anaplastic large cell lymphoma is a genetically heterogeneous disease with widely disparate clinical outcomes. *Blood* **124**, 1473–1480 (2014).

13. Savage, K. J. *et al.* ALK− anaplastic large-cell lymphoma is clinically and immunophenotypically different from both ALK+ ALCL and peripheral T-cell lymphoma, not otherwise specified: report from the International Peripheral T-Cell Lymphoma Project. *Blood* **111**, 5496–5504 (2008).

14. Ferreri, A. J. M., Govi, S., Pileri, S. A. & Savage, K. J. Anaplastic large cell lymphoma, ALK-negative. *Crit. Rev. Oncol. Hematol.* **85**, 206–215 (2013).

15. and The Spanish Cooperative Group for the study of T-cell lymphomas *et al.* Differential expression of NF-κB pathway genes among peripheral T-cell lymphomas. *Leukemia* **19**, 2254–2263 (2005).

16. Stein, H. *et al.* CD30(+) anaplastic large cell lymphoma: a review of its histopathologic, genetic, and clinical features. *Blood* **96**, 3681–3695 (2000).

17. Hapgood, G. & Savage, K. J. The biology and management of systemic anaplastic large cell lymphoma. *Blood* **126**, 17–25 (2015).

18. Crescenzo, R. *et al.* Convergent Mutations and Kinase Fusions Lead to Oncogenic STAT3 Activation in Anaplastic Large Cell Lymphoma. *Cancer Cell* **27**, 516–532 (2015).

19. Luchtel, R. A. *et al.* Recurrent MSCE116K mutations in ALK-negative anaplastic large cell lymphoma. *Blood* **133**, 2776–2789 (2019).

20. Ben-Neriah, Y. & Bauskin, A. R. Leukocytes express a novel gene encoding a putative transmembrane protein-kinase devoid of an extracellular domain. *Nature* **333**, 672–676 (1988).

21. Krolewski, J. J. & Dalla-Favera, R. The ltk gene encodes a novel receptor-type protein tyrosine kinase. *EMBO J.* **10**, 2911–2919 (1991).

22. Bai, R. Y., Dieter, P., Peschel, C., Morris, S. W. & Duyster, J. Nucleophosmin-anaplastic lymphoma kinase of large-cell anaplastic lymphoma is a constitutively active tyrosine kinase that utilizes phospholipase C-gamma to mediate its mitogenicity. *Mol. Cell. Biol.* **18**, 6951–6961 (1998).

23. Chiarle, R., Voena, C., Ambrogio, C., Piva, R. & Inghirami, G. The anaplastic lymphoma kinase in the pathogenesis of cancer. *Nat. Rev. Cancer* **8**, 11–23 (2008).

24. Hernández, L. *et al.* TRK-fused gene (TFG) is a new partner of ALK in anaplastic large cell lymphoma producing two structurally different TFG-ALK translocations. *Blood* **94**, 3265–3268 (1999).

25. Lamant, L., Dastugue, N., Pulford, K., Delsol, G. & Mariamé, B. A new fusion gene TPM3-ALK in anaplastic large cell lymphoma created by a (1;2)(q25;p23) translocation. *Blood* **93**, 3088–3095 (1999).

26. Colleoni, G. W. B. *et al.* ATIC-ALK: A Novel Variant ALK Gene Fusion in Anaplastic Large Cell Lymphoma Resulting from the Recurrent Cryptic Chromosomal Inversion, inv(2)(p23q35). *Am. J. Pathol.* **156**, 781–789 (2000).

27. Touriol, C. *et al.* Further demonstration of the diversity of chromosomal changes involving 2p23 in ALK-positive lymphoma: 2 cases expressing ALK kinase fused to CLTCL (clathrin chain polypeptide-like). *Blood* **95**, 3204–3207 (2000).

28. Tort, F. *et al.* Molecular Characterization of a New ALK Translocation Involving Moesin (MSN-ALK) in Anaplastic Large Cell Lymphoma. *Lab. Invest.* **81**, 419–426 (2001).

29. Debelenko, L. V. *et al.* Identification of CARS-ALK Fusion in Primary and Metastatic Lesions of an Inflammatory Myofibroblastic Tumor. *Lab. Invest.* **83**, 1255–1265 (2003).

30. Lamant, L. *et al.* Non-muscle myosin heavy chain (MYH9): A new partner fused to ALK in anaplastic large cell lymphoma. *Genes. Chromosomes Cancer* **37**, 427–432 (2003).

31. Wong, D. W.-S. *et al.* A novel *KIF5B-ALK* variant in nonsmall cell lung cancer: *KIF5B-ALK* in NSCLC. *Cancer* **117**, 2709–2718 (2011).

32. Takeuchi, K. *et al.* KIF5B-ALK, a Novel Fusion Oncokinase Identified by an Immunohistochemistry-based Diagnostic System for ALK-positive Lung Cancer. *Clin. Cancer Res.* **15**, 3143–3149 (2009).

33. Bonzheim, I. *et al.* Anaplastic large cell lymphomas lack the expression of T-cell receptor molecules or molecules of proximal T-cell receptor signaling. *Blood* **104**, 3358–3360 (2004).

34. Watanabe, M. *et al.* JunB Induced by Constitutive CD30–Extracellular Signal-Regulated Kinase 1/2 Mitogen-Activated Protein Kinase Signaling Activates the CD30 Promoter in Anaplastic Large Cell Lymphoma and Reed-Sternberg Cells of Hodgkin Lymphoma. *Cancer Res.* **65**, 7628–7634 (2005).

35. Hsu, F. Y.-Y., Johnston, P. B., Burke, K. A. & Zhao, Y. The Expression of CD30 in Anaplastic Large Cell Lymphoma Is Regulated by Nucleophosmin-Anaplastic Lymphoma Kinase–Mediated JunB Level in a Cell Type–Specific Manner. *Cancer Res.* **66**, 9002–9008 (2006).

36. Staber, P. B. *et al.* The oncoprotein NPM-ALK of anaplastic large-cell lymphoma induces JUNB transcription via ERK1/2 and JunB translation via mTOR signaling. *Blood* **110**, 3374–3383 (2007).

37. Cussac, D. Nucleophosmin-anaplastic lymphoma kinase of anaplastic large-cell lymphoma recruits, activates, and uses pp60c-src to mediate its mitogenicity. *Blood* **103**, 1464–1471 (2003).

38. Ambrogio, C. *et al.* The Anaplastic Lymphoma Kinase Controls Cell Shape and Growth of Anaplastic Large Cell Lymphoma through Cdc42 Activation. *Cancer Res.* **68**, 8899–8907 (2008).

39. Fujimoto, J. *et al.* Characterization of the transforming activity of p80, a hyperphosphorylated protein in a Ki-1 lymphoma cell line with chromosomal translocation t(2;5). *Proc. Natl. Acad. Sci.* **93**, 4181–4186 (1996).

40. Pulford, K., Morris, S. W. & Mason, D. Y. Anaplastic lymphoma kinase proteins and malignancy: *Curr. Opin. Hematol.* **8**, 231–236 (2001).

41. Bai, R. Y. *et al.* Nucleophosmin-anaplastic lymphoma kinase associated with anaplastic large-cell lymphoma activates the phosphatidylinositol 3-kinase/Akt antiapoptotic signaling pathway. *Blood* **96**, 4319–4327 (2000).

42. Levy, D. E. & Inghirami, G. STAT3: A multifaceted oncogene. *Proc. Natl. Acad. Sci.* **103**, 10151–10152 (2006).

43. Bournazou, E. & Bromberg, J. Targeting the tumor microenvironment: JAK-STAT3 signaling. *JAK-STAT* **2**, e23828 (2013).

44. Andreesen, R., Osterholz, J., Lohr, G. & Bross, K. A Hodgkin cell-specific antigen is expressed on a subset of auto- and alloactivated T (helper) lymphoblasts. *Blood* **63**, 1299–1302 (1984).

45. Chiarle, R. *et al.* CD30 in normal and neoplastic cells. *Clin. Immunol. Orlando Fla* **90**, 157–164 (1999).

46. Dürkop, H. *et al.* Expression of the CD30 antigen in non-lymphoid tissues and cells. *J. Pathol.* **190**, 613–618 (2000).

47. Hsi, E. D. *et al.* Diagnostic Accuracy of a Defined Immunophenotypic and Molecular Genetic Approach for Peripheral T/NK-cell Lymphomas: A North American PTCL Study Group Project. *Am. J. Surg. Pathol.* **38**, 768–775 (2014).

48. Lee, J.-H. Breast implant-associated anaplastic large-cell lymphoma (BIA-ALCL). *Yeungnam Univ. J. Med.* **38**, 175–182 (2021).

49. K Groth, A. & Graf, R. Breast Implant-Associated Anaplastic Large Cell Lymphoma (BIA-ALCL) and the Textured Breast Implant Crisis. *Aesthetic Plast. Surg.* **44**, 1–12 (2020).

50. Laurent, C. *et al.* Breast implant-associated anaplastic large cell lymphoma: two distinct clinicopathological variants with different outcomes. *Ann. Oncol. Off. J. Eur. Soc. Med. Oncol.* **27**, 306–314 (2016).

51. Talagas, M. *et al.* Breast Implant-Associated Anaplastic Large-Cell Lymphoma Can Be a Diagnostic Challenge for Pathologists. *Acta Cytol.* **58**, 103–107 (2014).

52. Aladily, T. N., Medeiros, L. J., Alayed, K. & Miranda, R. N. Breast implant-associated anaplastic large cell lymphoma: a newly recognized entity that needs further refinement of its definition. *Leuk. Lymphoma* **53**, 749–750 (2012).

53. Letourneau, A. *et al.* Dual JAK1 and STAT3 mutations in a breast implant-associated anaplastic large cell lymphoma. *Virchows Arch.* **473**, 505–511 (2018).

54. Laurent, C. *et al.* Gene alterations in epigenetic modifiers and JAK-STAT signaling are frequent in breast implant-associated ALCL. *Blood* **135**, 360–370 (2020).

55. Oishi, N. *et al.* Genetic subtyping of breast implant–associated anaplastic large cell lymphoma. *Blood* **132**, 544–547 (2018).

56. Naoki Oishi *et al.* Molecular profiling reveals a hypoxia signature in breast implant-associated anaplastic large cell lymphoma. *Haematologica* **106**, 1714–1724 (2020).

57. Popplewell, L., Thomas, S. H., Huang, Q., Chang, K. L. & Forman, S. J. Primary anaplastic large-cell lymphoma associated with breast implants. *Leuk. Lymphoma* **52**, 1481–1487 (2011).

58. Story, S. K., Schowalter, M. K. & Geskin, L. J. Breast implant-associated ALCL: a unique entity in the spectrum of CD30+ lymphoproliferative disorders. *The Oncologist* **18**, 301–307 (2013).

59. Zain, J. M. Aggressive T-cell lymphomas: 2019 updates on diagnosis, risk stratification, and management. *Am. J. Hematol.* **94**, 929–946 (2019).

60. Zhang, Y., Lee, D., Brimer, T., Hussaini, M. & Sokol, L. Genomics of Peripheral T-Cell Lymphoma and Its Implications for Personalized Medicine. *Front. Oncol.* **10**, 898 (2020).

61. Suzuki, R. *et al.* Prognostic significance of CD56 expression for ALK-positive and ALK-negative anaplastic large-cell lymphoma of T/null cell phenotype. *Blood* **96**, 2993–3000 (2000).

62. Horwitz, S. *et al.* Brentuximab vedotin with chemotherapy for CD30-positive peripheral T-cell lymphoma (ECHELON-2): a global, double-blind, randomised, phase 3 trial. *The Lancet* **393**, 229–240 (2019).

63. Foyil, K. V. & Bartlett, N. L. Brentuximab Vedotin and Crizotinib in Anaplastic Large-Cell Lymphoma. *Cancer J.* **18**, 450–456 (2012).

64. Harrer, D. C. *et al.* Unusual Late Relapse of ALK-Positive Anaplastic Large Cell Lymphoma Successfully Cleared Using the ALK-Inhibitor Crizotinib: Case Report. *Front. Oncol.* **10**, 585830 (2020).

65. Mossé, Y. P. *et al.* Safety and activity of crizotinib for paediatric patients with refractory solid tumors or anaplastic large-cell lymphoma: a Children's Oncology Group phase 1 consortium study. *Lancet Oncol.* **14**, 472–480 (2013).

66. Gambacorti-Passerini, C. *et al.* Long-term effects of crizotinib in ALK-positive tumors (excluding NSCLC): A phase 1b open-label study. *Am. J. Hematol.* **93**, 607–614 (2018).

67. Clapier, C. R., Iwasa, J., Cairns, B. R. & Peterson, C. L. Mechanisms of action and regulation of ATP-dependent chromatin-remodeling complexes. *Nat. Rev. Mol. Cell Biol.* **18**, 407–422 (2017).

68. Li, M. *et al.* Dynamic regulation of transcription factors by nucleosome remodeling. *eLife* **4**, e06249 (2015).

69. Boyer, L. A., Latek, R. R. & Peterson, C. L. The SANT domain: a unique histone-tail-binding module? *Nat. Rev. Mol. Cell Biol.* **5**, 158–163 (2004).

70. Längst, G. & Manelyte, L. Chromatin Remodelers: From Function to Dysfunction. *Genes* **6**, 299–324 (2015).

71. Lusser, A., Urwin, D. L. & Kadonaga, J. T. Distinct activities of CHD1 and ACF in ATP-dependent chromatin assembly. *Nat. Struct. Mol. Biol.* **12**, 160–166 (2005).

72. Murawska, M. & Brehm, A. CHD chromatin remodelers and the transcription cycle. *Transcription* **2**, 244–253 (2011).

73. Konev, A. Y. *et al.* CHD1 Motor Protein Is Required for Deposition of Histone Variant H3.3 into Chromatin in Vivo. *Science* **317**, 1087–1090 (2007).

74. Jin, J. *et al.* A Mammalian Chromatin Remodeling Complex with Similarities to the yeast INO80 Complex. *J. Biol. Chem.* **280**, 41207–41212 (2005).

75. Bakshi, R. *et al.* Characterization of a human SWI2/SNF2 like protein hINO80: Demonstration of catalytic and DNA binding activity. *Biochem. Biophys. Res. Commun.* **339**, 313–320 (2006).

76. Cai, Y. *et al.* YY1 functions with INO80 to activate transcription. *Nat. Struct. Mol. Biol.* **14**, 872–874 (2007).

77. Hur, S.-K. *et al.* Roles of human INO80 chromatin remodeling enzyme in DNA replication and chromosome segregation suppress genome instability. *Cell. Mol. Life Sci. CMLS* **67**, 2283–2296 (2010).

78. Jiang, Y. *et al.* INO80 chromatin remodeling complex promotes the removal of UV lesions by the nucleotide excision repair pathway. *Proc. Natl. Acad. Sci.* **107**, 17274–17279 (2010).

79. Bayona-Feliu, A., Barroso, S., Muñoz, S. & Aguilera, A. The SWI/SNF chromatin remodeling complex helps resolve R-loop-mediated transcription–replication conflicts. *Nat. Genet.* **53**, 1050–1063 (2021).

80. Abakir, A. & Ruzov, A. SWI/SNF complexes as determinants of R-loop metabolism. *Nat. Genet.* **53**, 940–941 (2021).

81. Brosh, R. M. DNA helicases involved in DNA repair and their roles in cancer. *Nat. Rev. Cancer* **13**, 542–558 (2013).

82. C., J., D., M. & Melendy, T. Replicative Helicases as the Central Organizing Motor Proteins in the Molecular Machines of the Elongating Eukaryotic Replication Fork. in *The Mechanisms of DNA Replication* (ed. Stuart, D.) (InTech, 2013). doi:10.5772/52335.

83. Chu, W. K. & Hickson, I. D. RecQ helicases: multifunctional genome caretakers. *Nat. Rev. Cancer* **9**, 644–654 (2009).

84. Chi, T. H. *et al.* Reciprocal regulation of CD4/CD8 expression by SWI/SNF-like BAF complexes. *Nature* **418**, 195–199 (2002).

85. Bultman, S. J. A Brg1 mutation that uncouples ATPase activity from chromatin remodeling reveals an essential role for SWI/SNF-related complexes in -globin expression and erythroid development. *Genes Dev.* **19**, 2849–2861 (2005).

86. Osipovich, O. *et al.* Essential function for SWI-SNF chromatin-remodeling complexes in the promoter-directed assembly of Tcrb genes. *Nat. Immunol.* **8**, 809–816 (2007).

87. O'Shea, J. J. & Paul, W. E. Mechanisms Underlying Lineage Commitment and Plasticity of Helper $CD4^+$ T Cells. *Science* **327**, 1098–1102 (2010).

88. Bediaga, N. G. *et al.* Multi-level remodeling of chromatin underlying activation of human T cells. *Sci. Rep.* **11**, 528 (2021).

89. Jeong, S. M., Lee, C., Lee, S. K., Kim, J. & Seong, R. H. The SWI/SNF Chromatin-remodeling Complex Modulates Peripheral T Cell Activation and Proliferation by Controlling AP-1 Expression. *J. Biol. Chem.* **285**, 2340–2350 (2010).

90. Chan, E. M. *et al.* WRN helicase is a synthetic lethal target in microsatellite unstable cancers. *Nature* **568**, 551–556 (2019).

91. Thijssen, P. E. *et al.* Mutations in CDCA7 and HELLS cause immunodeficiency–centromeric instability–facial anomalies syndrome. *Nat. Commun.* **6**, 7870 (2015).

92. Centore, R. C., Sandoval, G. J., Soares, L. M. M., Kadoch, C. & Chan, H. M. Mammalian SWI/SNF Chromatin Remodeling Complexes: Emerging Mechanisms and Therapeutic Strategies. *Trends Genet.* **36**, 936–950 (2020).

93. Ye, Y. *et al.* Correlation of mutational landscape and survival outcome of peripheral T-cell lymphomas. *Exp. Hematol. Oncol.* **10**, 9 (2021).

94. Tameni, A. *et al.* The DNA-helicase HELLS drives ALK− ALCL proliferation by the transcriptional control of a cytokinesis-related program. *Cell Death Dis.* **12**, 130 (2021).

95. Madaule, P. & Axel, R. A novel ras-related gene family. *Cell* **41**, 31–40 (1985).

96. Saoudi, A., Kassem, S., Dejean, A. S. & Gaud, G. Rho-GTPases as key regulators of T lymphocyte biology. *Small GTPases* **5**, e983862 (2014).

97. Etienne-Manneville, S. & Hall, A. Rho GTPases in cell biology. *Nature* **420**, 629–635 (2002).

98. Van Aelst, L. & D'Souza-Schorey, C. Rho GTPases and signaling networks. *Genes Dev.* **11**, 2295–2322 (1997).

99. Johnson, J. L., Erickson, J. W. & Cerione, R. A. New Insights into How the Rho Guanine Nucleotide Dissociation Inhibitor Regulates the Interaction of Cdc42 with Membranes. *J. Biol. Chem.* **284**, 23860–23871 (2009).

100. Durand-Onaylı, V., Haslauer, T., Härzschel, A. & Hartmann, T. Rac GTPases in Hematological Malignancies. *Int. J. Mol. Sci.* **19**, 4041 (2018).

101. Heasman, S. J., Carlin, L. M., Cox, S., Ng, T. & Ridley, A. J. Coordinated RhoA signaling at the leading edge and uropod is required for T cell transendothelial migration. *J. Cell Biol.* **190**, 553–563 (2010).

102. Infante, E. & Ridley, A. J. Roles of Rho GTPases in leucocyte and leukemia cell transendothelial migration. *Philos. Trans. R. Soc. B Biol. Sci.* **368**, 20130013 (2013).

103. Borroto, A. *et al.* Rho regulates T cell receptor ITAM-induced lymphocyte spreading in an integrin-independent manner. *Eur. J. Immunol.* **30**, 3403–3410 (2000).

104. Parsons, J. T., Horwitz, A. R. & Schwartz, M. A. Cell adhesion: integrating cytoskeletal dynamics and cellular tension. *Nat. Rev. Mol. Cell Biol.* **11**, 633–643 (2010).

105. Hill, C. S., Wynne, J. & Treisman, R. The Rho family GTPases RhoA, Racl, and CDC42Hsregulate transcriptional activation by SRF. *Cell* **81**, 1159–1170 (1995).

106. Miralles, F., Posern, G., Zaromytidou, A.-I. & Treisman, R. Actin Dynamics Control SRF Activity by Regulation of Its Coactivator MAL. *Cell* **113**, 329–342 (2003).

107. Palomero, T. *et al.* Recurrent mutations in epigenetic regulators, RHOA and FYN kinase in peripheral T cell lymphomas. *Nat. Genet.* **46**, 166–170 (2014).

108. Yoo, H. Y. *et al.* A recurrent inactivating mutation in RHOA GTPase in angioimmunoblastic T cell lymphoma. *Nat. Genet.* **46**, 371–375 (2014).

109. Sakata-Yanagimoto, M. *et al.* Somatic RHOA mutation in angioimmunoblastic T cell lymphoma. *Nat. Genet.* **46**, 171–175 (2014).

110. Nagata, Y. *et al.* Variegated RHOA mutations in adult T-cell leukemia/lymphoma. *Blood* **127**, 596–604 (2016).

111. Cortes, J. R. *et al.* RHOA G17V Induces T Follicular Helper Cell Specification and Promotes Lymphomagenesis. *Cancer Cell* **33**, 259-273.e7 (2018).

112. Ng, S. Y. *et al.* RhoA G17V is sufficient to induce autoimmunity and promotes T-cell lymphomagenesis in mice. *Blood* **132**, 935–947 (2018).

113. Whalley, H. J. *et al.* Cdk1 phosphorylates the Rac activator Tiam1 to activate centrosomal Pak and promote mitotic spindle formation. *Nat. Commun.* **6**, 7437 (2015).

114. Boyer, L. *et al.* Rac GTPase Instructs Nuclear Factor-κB Activation by Conveying the SCF Complex and IkBα to the Ruffling Membranes. *Mol. Biol. Cell* **15**, 1124–1133 (2004).

115. Malek, T. R. The Biology of Interleukin-2. *Annu. Rev. Immunol.* **26**, 453–479 (2008).

116. Colomba, A. *et al.* Inhibition of Rac controls NPM–ALK-dependent lymphoma development and dissemination. *Blood Cancer J.* **1**, e21–e21 (2011).

117. Choudhari, R. *et al.* Redundant and nonredundant roles for Cdc42 and Rac1 in lymphomas developed in NPM-ALK transgenic mice. *Blood* **127**, 1297–1306 (2016).

118. Colomba, A. *et al.* Activation of Rac1 and the exchange factor Vav3 are involved in NPM-ALK signaling in anaplastic large cell lymphomas. *Oncogene* **27**, 2728–2736 (2008).

119. Lim, M. S. *et al.* The proteomic signature of NPM/ALK reveals deregulation of multiple cellular pathways. *Blood* **114**, 1585–1595 (2009).

120. Bosco, E. E. *et al.* Rac1 targeting suppresses p53 deficiency–mediated lymphomagenesis. *Blood* **115**, 3320–3328 (2010).

121. Rossman, K. L., Der, C. J. & Sondek, J. GEF means go: turning on RHO GTPases with guanine nucleotide exchange factors. *Nat. Rev. Mol. Cell Biol.* **6**, 167–180 (2005).

122. Habets, G. G. M. *et al.* Identification of an invasion-inducing gene, Tiam-1, that encodes a protein with homology to GDP-GTP exchangers for Rho-like proteins. *Cell* **77**, 537–549 (1994).

123. Habets, G. G., van der Kammen, R. A., Stam, J. C., Michiels, F. & Collard, J. G. Sequence of the human invasion-inducing TIAM1 gene, its conservation in evolution and its expression in tumor cell lines of different tissue origin. *Oncogene* **10**, 1371–1376 (1995).

124. ten Klooster, J. P. *et al.* Interaction between Tiam1 and the Arp2/3 complex links activation of Rac to actin polymerization. *Biochem. J.* **397**, 39–45 (2006).

125. Gérard, A., van der Kammen, R. A., Janssen, H., Ellenbroek, S. I. & Collard, J. G. The Rac activator Tiam1 controls efficient T-cell trafficking and route of transendothelial migration. *Blood* **113**, 6138–6147 (2009).

126. Gérard, A., Mertens, A. E. E., van der Kammen, R. A. & Collard, J. G. The Par polarity complex regulates Rap1- and chemokine-induced T cell polarization. *J. Cell Biol.* **176**, 863–875 (2007).

127. Kurdi, A. T. *et al.* Tiam1/Rac1 complex controls Il17a transcription and autoimmunity. *Nat. Commun.* **7**, 13048 (2016).

128. Masuda, M. *et al.* CADM1 Interacts with Tiam1 and Promotes Invasive Phenotype of Human T-cell Leukemia Virus Type I-transformed Cells and Adult T-cell Leukemia Cells. *J. Biol. Chem.* **285**, 15511–15522 (2010).

129. Buongiorno, P., Pethe, V. V., Charames, G. S., Esufali, S. & Bapat, B. Rac1 GTPase and the Rac1 exchange factor Tiam1 associate with Wnt-responsive promoters to enhance beta-catenin/TCF-dependent transcription in colorectal cancer cells. *Mol. Cancer* **7**, 73 (2008).

130. Hofbauer, S. W. *et al.* Tiam1/Rac1 signals contribute to the proliferation and chemoresistance, but not motility, of chronic lymphocytic leukemia cells. *Blood* **123**, 2181–2188 (2014).

131. Guy, C. S. *et al.* Distinct TCR signaling pathways drive proliferation and cytokine production in T cells. *Nat. Immunol.* **14**, 262–270 (2013).

132. Helou, Y. A., Petrashen, A. P. & Salomon, A. R. Vav1 Regulates T-Cell Activation through a Feedback Mechanism and Crosstalk between the T-Cell Receptor and CD28. *J. Proteome Res.* **14**, 2963–2975 (2015).

133. Katzav, S. Flesh, and blood: The story of Vav1, a gene that signals in hematopoietic cells but can be transforming in human malignancies. *Cancer Lett.* **255**, 241–254 (2007).

134. Paccani, S. R. *et al.* Defective Vav expression and impaired F-actin reorganization in a subset of patients with common variable immunodeficiency characterized by T-cell defects. *Blood* **106**, 626–634 (2005).

135. Fischer, K.-D. *et al.* Vav is a regulator of cytoskeletal reorganization mediated by the T-cell receptor. *Curr. Biol.* **8**, 554-S3 (1998).

136. Turner, M. *et al.* A Requirement for the Rho-Family GTP Exchange Factor Vav in Positive and Negative Selection of Thymocytes. *Immunity* **7**, 451–460 (1997).

137. Robles-Valero, J. *et al.* A Paradoxical Tumor-Suppressor Role for the Rac1 Exchange Factor Vav1 in T Cell Acute Lymphoblastic Leukemia. *Cancer Cell* **32**, 608-623.e9 (2017).

138. Oshima, K. *et al.* Mutational landscape, clonal evolution patterns, and role of RAS mutations in relapsed acute lymphoblastic leukemia. *Proc. Natl. Acad. Sci.* **113**, 11306–11311 (2016).

139. Young, R. M., Shaffer, A. L., Phelan, J. D. & Staudt, L. M. B-cell receptor signaling in diffuse large B-cell lymphoma. *Semin. Hematol.* **52**, 77–85 (2015).

140. Fujisawa, M. *et al.* Activation of RHOA-VAV1 signaling in angioimmunoblastic T-cell lymphoma. *Leukemia* **32**, 694–702 (2018).

141. Fragliasso, V. *et al.* The novel lncRNA BlackMamba controls the neoplastic phenotype of ALK-anaplastic large cell lymphoma by regulating the DNA helicase HELLS. *Leukemia* **34**, 2964–2980 (2020).

142. Verma, A. *et al.* Transcriptome sequencing reveals thousands of novel long noncoding RNAs in B cell lymphoma. *Genome Med.* **7**, 110 (2015).

143. Chiarle, R. *et al.* Stat3 is required for ALK-mediated lymphomagenesis and provides a possible therapeutic target. *Nat. Med.* **11**, 623–629 (2005).

144. Herriges, M. J. *et al.* Long noncoding RNAs are spatially correlated with transcription factors and regulate lung development. *Genes Dev.* **28**, 1363–1379 (2014).

145. Werner, M. S. *et al.* Chromatin-enriched lncRNAs can act as cell-type-specific activators of proximal gene transcription. *Nat. Struct. Mol. Biol.* **24**, 596–603 (2017).

146. Dobin, A. *et al.* STAR: ultrafast universal RNA-seq aligner. *Bioinformatics* **29**, 15–21 (2013).

147. Li, B. & Dewey, C. N. RSEM: accurate transcript quantification from RNA-Seq data with or without a reference genome. *BMC Bioinformatics* **12**, 323 (2011).

148. Love, M. I., Huber, W. & Anders, S. Moderated estimation of fold change and dispersion for RNA-seq data with DESeq2. *Genome Biol.* **15**, 550 (2014).

149. Kuleshov, M. V. *et al.* Enrichr: a comprehensive gene set enrichment analysis web server 2016 update. *Nucleic Acids Res.* **44**, W90–W97 (2016).

150. He, Y. *et al.* Lsh/HELLS is required for B lymphocyte development and immunoglobulin class switch recombination. *Proc. Natl. Acad. Sci.* **117**, 20100–20108 (2020).

151. Geiman, T. M. & Muegge, K. Lsh, an SNF2/helicase family member, is required for the proliferation of mature T lymphocytes. *Proc. Natl. Acad. Sci.* **97**, 4772–4777 (2000).

152. von Eyss, B. *et al.* The SNF2-like helicase HELLS mediates E2F3-dependent transcription and cellular transformation. *EMBO J.* **31**, 972–985 (2012).

153. Xi, S. *et al.* Lsh controls Hox gene silencing during development. *Proc. Natl. Acad. Sci. U. S. A.* **104**, 14366–14371 (2007).

154. Hogan, D. J., Riordan, D. P., Gerber, A. P., Herschlag, D. & Brown, P. O. Diverse RNA-Binding Proteins Interact with Functionally Related Sets of RNAs, Suggesting an Extensive Regulatory System. *PLoS Biol.* **6**, e255 (2008).

155. Ørom, U. A. & Shiekhattar, R. Long noncoding RNAs usher in a new era in the biology of enhancers. *Cell* **154**, 1190–1193 (2013).

156. Wang, R. *et al.* The ratio of FoxA1 to FoxA2 in lung adenocarcinoma is regulated by LncRNA HOTAIR and chromatin remodeling factor LSH. *Sci. Rep.* **5**, 17826 (2015).

157. Fragliasso, V. *et al.* The novel lncRNA BlackMamba controls the neoplastic phenotype of ALK-anaplastic large cell lymphoma by regulating the DNA helicase HELLS. *Leukemia* **34**, 2964–2980 (2020).

158. Billadeau, D. D., Nolz, J. C. & Gomez, T. S. Regulation of T-cell activation by the cytoskeleton. *Nat. Rev. Immunol.* **7**, 131–143 (2007).

159. Fornes, O. *et al.* JASPAR 2020: update of the open-access database of transcription factor binding profiles. *Nucleic Acids Res.* **48**, D87–D92 (2020).

160. Messeguer, X. *et al.* PROMO: detection of known transcription regulatory elements using species-tailored searches. *Bioinformatics* **18**, 333–334 (2002).

161. Lu, Z. *et al.* Polycomb Group Protein YY1 Is an Essential Regulator of Hematopoietic Stem Cell Quiescence. *Cell Rep.* **22**, 1545–1559 (2018).

162. Morales-Martinez, M. *et al.* Regulation of Krüppel-Like Factor 4 (KLF4) expression through the transcription factor Yin-Yang 1 (YY1) in non-Hodgkin B-cell lymphoma. *Oncotarget* **10**, 2173–2188 (2019).

163. Lin, J. *et al.* A critical role of transcription factor YY1 in rheumatoid arthritis by regulation of interleukin-6. *J. Autoimmun.* **77**, 67–75 (2017).

164. Liu, Z. & Weiner, O. D. Positioning the cleavage furrow: All you need is Rho. *J. Cell Biol.* **213**, 605–607 (2016).

165. Piekny, A., Werner, M. & Glotzer, M. Cytokinesis: welcome to the Rho zone. *Trends Cell Biol.* **15**, 651–658 (2005).

166. Voena, C. & Chiarle, R. RHO Family GTPases in the Biology of Lymphoma. *Cells* **8**, E646 (2019).

167. Guo, F., Cancelas, J. A., Hildeman, D., Williams, D. A. & Zheng, Y. Rac GTPase isoforms Rac1 and Rac2 play a redundant and crucial role in T-cell development. *Blood* **112**, 1767–1775 (2008).

168. Dumont, C. *et al.* Rac GTPases play critical roles in early T-cell development. *Blood* **113**, 3990–3998 (2009).

169. Lens, S. M. A. & Medema, R. H. Cytokinesis defects and cancer. *Nat. Rev. Cancer* **19**, 32–45 (2019).

170. Pizzi, M., Margolskee, E. & Inghirami, G. Pathogenesis of Peripheral T Cell Lymphoma. *Annu. Rev. Pathol. Mech. Dis.* **13**, 293–320 (2018).

171. Zeng, Y. & Feldman, A. L. Genetics of anaplastic large cell lymphoma. *Leuk. Lymphoma* **57**, 21–27 (2016).

172. Baytak, E. *et al.* Whole transcriptome analysis reveals dysregulated oncogenic lncRNAs in natural killer/T-cell lymphoma and establishes MIR155HG as a target of PRDM1. *Tumor Biol.* **39**, 101042831770164 (2017).

173. Chung, I.-H. *et al.* The long noncoding RNA LINC01013 enhances invasion of human anaplastic large-cell lymphoma. *Sci. Rep.* **7**, 295 (2017).

174. Huang, P.-S. *et al.* The long noncoding RNA MIR503HG Enhances Proliferation of Human ALK-Negative Anaplastic Large-Cell Lymphoma. *Int. J. Mol. Sci.* **19**, 1463 (2018).

175. Nobili, L., Ronchetti, D., Taiana, E. & Neri, A. long noncoding RNAs in B-cell malignancies: a comprehensive overview. *Oncotarget* **8**, 60605–60623 (2017).

176. Piva, R. *et al.* Gene Expression Profiling Uncovers Molecular Classifiers for the Recognition of Anaplastic Large-Cell Lymphoma Within Peripheral T-Cell Neoplasms. *J. Clin. Oncol.* **28**, 1583–1590 (2010).

177. Huynh, J., Etemadi, N., Hollande, F., Ernst, M. & Buchert, M. The JAK/STAT3 axis: A comprehensive drug target for solid malignancies. *Semin. Cancer Biol.* **45**, 13–22 (2017).

178. Zamo, A. *et al.* Anaplastic lymphoma kinase (ALK) activates Stat3 and protects hematopoietic cells from cell death. *Oncogene* **21**, 1038–1047 (2002).

179. Inghirami, G. Anaplastic Lymphoma Kinase activating mechanisms, and signaling pathways. *Front. Biosci.* **7**, 283–305 (2015).

180. Küçük, C. *et al.* Activating mutations of STAT5B and STAT3 in lymphomas derived from γδ-T or NK cells. *Nat. Commun.* **6**, 6025 (2015).

181. Hammarén, H. M., Virtanen, A. T., Raivola, J. & Silvennoinen, O. The regulation of JAKs in cytokine signaling and its breakdown in disease. *Cytokine* **118**, 48–63 (2019).

182. Agnelli, L. *et al.* Identification of a 3-gene model as a powerful diagnostic tool for the recognition of ALK-negative anaplastic large-cell lymphoma. *Blood* **120**, 1274–1281 (2012).

183. Fan, C. *et al.* Role of long noncoding RNAs in glucose metabolism in cancer. *Mol. Cancer* **16**, 130 (2017).

184. Aune, T. M., Crooke, P. S. & Spurlock, C. F. Long noncoding RNAs in T lymphocytes. *J. Leukoc. Biol.* **99**, 31–44 (2016).

185. Esteller, M. Non-coding RNAs in human disease. *Nat. Rev. Genet.* **12**, 861–874 (2011).

186. Peng, W.-X., Koirala, P. & Mo, Y.-Y. LncRNA-mediated regulation of cell signaling in cancer. *Oncogene* **36**, 5661–5667 (2017).

187. Saxena, A. & Carninci, P. long noncoding RNA modifies chromatin: Epigenetic silencing by long noncoding RNAs. *BioEssays* **33**, 830–839 (2011).

188. Lungu, C., Muegge, K., Jeltsch, A. & Jurkowska, R. Z. An ATPase-Deficient Variant of the SNF2 Family Member HELLS Shows Altered Dynamics at Pericentromeric Heterochromatin. *J. Mol. Biol.* **427**, 1903–1915 (2015).

189. Zhu, H. *et al.* Lsh is involved in de novo methylation of DNA. *EMBO J.* **25**, 335–345 (2006).

190. Baumann, C. *et al.* Helicase LSH/Hells regulates kinetochore function, histone H3/Thr3 phosphorylation, and centromere transcription during oocyte meiosis. *Nat. Commun.* **11**, 4486 (2020).

191. Law, C. *et al.* HELLS Regulates Chromatin Remodeling and Epigenetic Silencing of Multiple Tumor Suppressor Genes in Human Hepatocellular Carcinoma. *Hepatology* **69**, 2013–2030 (2019).

192. Ren, J., Finney, R., Ni, K., Cam, M. & Muegge, K. The chromatin remodeling protein Lsh alters nucleosome occupancy at putative enhancers and modulates binding of lineage-specific transcription factors. *Epigenetics* **14**, 277–293 (2019).

193. Kollárovič, G., Topping, C. E., Shaw, E. P. & Chambers, A. L. The human HELLS chromatin remodeling protein promotes end resection to facilitate homologous recombination and contributes to DSB repair within heterochromatin. *Nucleic Acids Res.* **48**, 1872–1885 (2020).

194. Xu, X. *et al.* The epigenetic regulator LSH maintains fork protection and genomic stability via MacroH2A deposition and RAD51 filament formation. *Nat. Commun.* **12**, 3520 (2021).

195. Ni, K. & Muegge, K. LSH catalyzes ATP-driven exchange of histone variants macroH2A1 and macroH2A2. *Nucleic Acids Res.* **49**, 8024–8036 (2021).

196. Zhang, G. *et al.* Chromatin remodeler HELLS maintains glioma stem cells through E2F3 and MYC. *JCI Insight* **4**, e126140 (2019).

197. Benavente, C. A. *et al.* Chromatin remodelers HELLS and UHRF1 mediate the epigenetic deregulation of genes that drive retinoblastoma tumor progression. *Oncotarget* **5**, 9594–9608 (2014).

198. Zocchi, L. *et al.* Chromatin remodeling protein HELLS is critical for retinoblastoma tumor initiation and progression. *Oncogenesis* **9**, 25 (2020).

199. Tao, Y., Liu, S., Briones, V., Geiman, T. M. & Muegge, K. Treatment of breast cancer cells with DNA demethylating agents leads to a release of Pol II stalling at genes with DNA-hypermethylated regions upstream of TSS. *Nucleic Acids Res.* **39**, 9508–9520 (2011).

200. He, X. *et al.* Chromatin Remodeling Factor LSH Drives Cancer Progression by Suppressing the Activity of Fumarate Hydratase. *Cancer Res.* **76**, 5743–5755 (2016).

201. Robinson, M. H. *et al.* Upregulation of the chromatin remodeler HELLS is mediated by YAP1 in Sonic Hedgehog Medulloblastoma. *Sci. Rep.* **9**, 13611 (2019).

202. Lee, D. W. *et al.* Proliferation-associated SNF2-like gene (PASG): a SNF2 family member altered in leukemia. *Cancer Res.* **60**, 3612–3622 (2000).

203. Myant, K. *et al.* LSH, and G9a/GLP complex are required for developmentally programmed DNA methylation. *Genome Res.* **21**, 83–94 (2011).

204. Myant, K. & Stancheva, I. LSH Cooperates with DNA Methyltransferases To Repress Transcription. *Mol. Cell. Biol.* **28**, 215–226 (2008).

205. Gordon, S., Akopyan, G., Garban, H. & Bonavida, B. Transcription factor YY1: structure, function, and therapeutic implications in cancer biology. *Oncogene* **25**, 1125–1142 (2006).

206. Kleiman, E., Jia, H., Loguercio, S., Su, A. I. & Feeney, A. J. YY1 plays an essential role at all stages of B-cell differentiation. *Proc. Natl. Acad. Sci.* **113**, E3911–E3920 (2016).

207. Affar, E. B. *et al.* Essential Dosage-Dependent Functions of the Transcription Factor Yin Yang 1 in Late Embryonic Development and Cell Cycle Progression. *Mol. Cell. Biol.* **26**, 3565–3581 (2006).

208. Potluri, V. *et al.* Transcriptional Repression of Bim by a Novel YY1-RelA Complex Is Essential for the Survival and Growth of Multiple Myeloma. *PLoS ONE* **8**, e66121 (2013).

209. Antonio-Andrés, G. *et al.* Role of Yin Yang-1 (YY1) in the transcription regulation of the multi-drug resistance (*MDR1*) gene. *Leuk. Lymphoma* **59**, 2628–2638 (2018).

210. Abate, F. *et al.* Activating mutations and translocations in the guanine exchange factor VAV1 in peripheral T-cell lymphomas. *Proc. Natl. Acad. Sci.* **114**, 764–769 (2017).

211. Bros, Haas, Moll, & Grabbe. RhoA as a Key Regulator of Innate and Adaptive Immunity. *Cells* **8**, 733 (2019).

212. Cools, J. RHOA mutations in peripheral T cell lymphoma. *Nat. Genet.* **46**, 320–321 (2014).

213. Chan, C.-H. *et al.* Deciphering the transcriptional complex critical for RhoA gene expression and cancer metastasis. *Nat. Cell Biol.* **12**, 457–467 (2010).

214. Canovas Nunes, S. *et al.* The small GTPase RhoU lays downstream of JAK/STAT signaling and mediates cell migration in multiple myeloma. *Blood Cancer J.* **8**, 20 (2018).

215. Schiavone, D. *et al.* The RhoU/Wrch1 Rho GTPase gene is a common transcriptional target of both the gp130/STAT3 and Wnt-1 pathways. *Biochem. J.* **421**, 283–292 (2009).

216. Svensmark, J. H. & Brakebusch, C. Rho GTPases in cancer: friend or foe? *Oncogene* **38**, 7447–7456 (2019).

PUBLICATIONS

All described scientific results have been published in the following peer-review international journals:

Abstract: Hells Promotes Transcription in Lymphoma by Resolving Topological Conflicts and By Preventing DNA Damage (ASH Annual Meeting and Exposition 12-12-2021) Winner of ASH Abstract Achievement Award

Cytoskeleton dynamics in Peripheral T Cell Lymphomas: an intricate network sustaining lymphomagenesis, Front. Oncol. | doi: 10.3389/fonc.2021.643620, April 2021

Tameni A. et al. The DNA-helicase HELLS drives ALK- ALCL proliferation by the transcriptional control of a cytokinesis-related program. *Cell Death and Disease*, Article published: 27 January 2021, https://doi.org/10.1038/s41419-021-03425-0.

Fragliasso V. et al. The novel lncRNA BlackMamba controls the neoplastic phenotype of ALK^- anaplastic large cell lymphoma by regulating the DNA helicase HELLS Leukemia (2020)Article Published: 02 March 2020, DOI: 10.1038/s41375-020-0754-8

Abstract: The DNA Helicase Hells Is a New Unconventional Player in ALK- Anaplastic Large Cell Lymphoma Biology November 2019; Blood 134(Supplement_1):1477-1477 DOI: 10.1182/blood-2019-122701

ACKNOWLEDGEMENTS

In this Ph.D. experience I would like to thank in particular the laboratory coordinator, Dr. Alessia Ciarrocchi who allowed me to learn and carry out the research activity. I would like also to thank my scientific tutor, Dr. Valentina Fragliasso, with whom I have published the main scientific works of these three years including 3 important publications in international scientific journals. Thanks to them I have the opportunity to participate in conferences and to present abstracts and posters. I extend my thanks, also to all the colleagues in the laboratory, together with my scientific lab coordinator and tutor, with whom I have exchanged ideas, learned new methods, and who have made me grow personally and professionally. Particularly, I would like to thank Dr. Valentina Mularoni that helped me to technically finish my Ph.D. publication in advance.

I sincerely thank all my family, my partner, and all my friends for supporting me in every choice and situation.

Finally, I would like to thank all the professors who have accompanied us on this path of growth, in particular the coordinator of the doctoral course Professor. Biagini who has always organized courses and Ph.D. days for us, an important moment for the exchange of ideas and knowledge of other medical disciplines.